



TAMPEREEN TEKNILLINEN YLIOPISTO
TAMPERE UNIVERSITY OF TECHNOLOGY

PIRKKA-OLAVI ULMANEN

THE EFFECT OF HIGH POWER ADJUSTABLE RING MODE FI-
BER LASER FOR MATERIAL CUTTING

Master of Science thesis

Examiner: prof. Eric Coatanea
Examiner and topic approved by the
Faculty Council of the Faculty of
Engineering Sciences
on 7.12.2016

ABSTRACT

PIRKKA-OLAVI ULMANEN: The effect of high power adjustable ring mode fiber laser for material cutting

Tampere University of technology

Master of Science Thesis, 114 pages, 0 Appendix pages

May 2017

Master's Degree Programme in Mechanical Engineering, MSc

Major: Design of machines and system

Examiner: Professor Eric Coatanea

Keywords: fiber laser, adjustable ring mode, laser cutting, metal, copper, aluminium, stainless steel

In this Master of Science Thesis is researched Corelase Oy's performance of ARM fiber laser source's in laser cutting with different metals. The cutting quality was measured with surface roughness values and cutting edges angularity.

The theoretical part covers the principles of the fiber laser, CO₂ laser, disk laser and Nd:YAG laser and how they apply to in laser cutting. Also, there is introduction to laser cutting and how the cutting quality can be measured and validate along standard SFS-ISO EN 9013. The test materials were copper, aluminium, mild steel and stainless steel. The copper was tested in 6 mm, 10 mm and 20 mm in thicknesses. The aluminium was tested at 15 mm and 20 mm thick plates. The mild steel had 5 mm, 15 mm and 20 mm plates and the stainless steel had 10 mm and 15 mm thick plates. The experiments were made with one test setup where were used ARM fiber laser source with the output powers of 2+6 kW and cutting head from Precitec. The study focus to find parameters sets which give metals good surface roughness value and to lower the dross formations under the cut edge. Also, the kerf opening angle was measured for 15 mm and 20 mm thick plates which had the best surface roughness.

The most effecting parameters to the surface roughness were the feed rate, the focal plane's position and the nozzle diameter with the assistant gas pressure for all materials. For the mild steel (5 mm and 15 mm), the copper and the stainless steel were achieved the quality class of two for the surface roughness with the ARM laser. For the aluminium and the mild steel (20 mm) achieved the quality class level three. The burr get most effect from the nozzle diameter and the gas pressure.

The tests show that the ARM fiber laser source provide good cutting quality with only one type of cutting head. The ARM laser source is versatile what comes to laser cutting.

TIIVISTELMÄ

PIRKKA-OLAVI ULMANEN: The effect of high power adjustable ring mode fiber laser for material cutting

Tampereen teknillinen yliopisto

Diplomityö, 114 sivua, 0 liitesivua

Toukokuu 2017

Konetekniikan diplomi-insinöörin tutkinto-ohjelma

Pääaine: Koneiden ja järjestelmien suunnittelu

Tarkastaja: professori Eric Coatenea

Avainsanat: kuitulaser, laser, laserleikkaus, metalli, kupari, alumiini, ruostumaton teräs

Tässä diplomityössä tutkitaan Corelase Oy:n ARM valokuitulaser lähteen kykyä leikata metalleja ja millaista leikkauslaatua sillä voidaan saavuttaa. Leikkauslaatua mitattiin pinnankarheuden ja leikkauspinnan kaltevuuden perusteella.

Työn kirjallinen osuus käsittelee erilasereiden toiminta periaatteet (kuitulaser, CO₂-laser, levy laser ja Nd: YAG laser) ja miten ne soveltuvat laser leikkaamiseen. Teoria osuudessa on kerrottu myös laser leikkaamisen perusteista ja miten leikkauksen jälkeä voidaan arvioida SFS-EN 9013 mukaan. Testattavat metallit olivat kupari, alumiini, teräs ja ruostumaton teräs. Kuparista testattiin paksuudet 6 mm, 10 mm ja 15 mm. Alumiinille 15 mm ja 20 mm. Teräkselle 5 mm, 15 mm ja 20 mm sekä ruostumattomalle teräkselle 10 mm ja 15 mm paksuudet. Testaukset tehtiin ainoastaan käyttäen yhtä ARM laser lähdettä, jonka tehot olivat 2+6 kW ja yhtä Precitec:n leikkauspäätä. Työ keskittyy löytämään parametri arvot, joilla voidaan saavuttaa mahdollisimman hyvä pinnankarheus kyseisille metalleille. Myös alapinnan purseen muodostumista seurattiin silmämääräisesti. 15 mm ja 20 mm paksuuksille joilla oli paras pinnanlaatu, tehtiin leikkausuran kulman mittausta.

Merkittävimmiksi parametreiksi jotka vaikuttavat pinnankarheuden muodostumiseen osoittautui leikkausnopeus, fokus korkeus, suuttimen halkaisija suojakaasun paineen kanssa. ARM laser lähteellä saavutettiin pinnankarheudessa luokka kaksi ruostumattomalle teräkselle, kuparille ja raudalle. Alumiinille saavutettiin luokka kolme. Testit osoittivat että, ARM valokuitulaser pystyy tekemään hyvä laatuista leikkausta ja se soveltuu monille eri metalleille.

PREFACE

This thesis is made for Corelase Oy as assignment in 2016-2017.

I want to express my gratitude to Corelase Oy's Jarno Kangastupa and Matti Närhi for this opportunity and to Tampere University of Technology's Professor Eric Coatanea for guidance and supervision. Also, I want to thank TUT Laser Applications Laboratory's Research Manager Jorma Vihinen, Research Engineers Ari Stjerna and Mikko Vainionpää for helping me with the tests and for the guidance with laser cutting.

Also, I want to show my gratitude to my parents and to my brother for the support during my studies and this thesis.

I want also express my gratitude to Tammi Timo for these memorial school years and special thanks to Juuso and Petra for helping me with this Thesis.

Tampere, 17.05.2017

Pirkka-Olavi Ulmanen

CONTENTS

1	INTRODUCTION	1
1.1	Motivation for the Thesis	1
1.2	Research objects	1
1.3	Research methodology	1
1.4	Contents of the Thesis	2
2	PRINCIPLES FOR LASERS.....	3
2.1	Stimulated emission	5
3	LASER TYPES.....	6
3.1	Fiber laser	6
3.1.1	Design and operation principle	6
3.1.2	Power scaling	7
3.1.3	Applications	7
3.2	CO ₂ laser	7
3.2.1	General construction	8
3.2.2	Slow flow CO ₂ laser	9
3.2.3	Fast axial flow CO ₂ laser	9
3.2.4	Diffusion-cooled CO ₂ laser	10
3.3	Disk laser.....	11
3.3.1	Thin disk laser	11
3.4	Nd: YAG lasers	12
3.4.1	Diode pumped Nd: YAG lasers	12
3.4.2	Lamp pumped Nd: YAG lasers.....	13
3.5	Fiber laser vs. CO ₂ laser	13
4	LASER CUTTING	15
4.1	Cutting with reactive gas.....	17
4.2	Inert gas cutting.....	18
4.3	Vaporization	19
4.4	Chemical degradation.....	19
5	LASER CUTTING PARAMETERS	20
5.1	Laser beam's parameter	20
5.1.1	Wavelength	20
5.1.2	Laser power and intensity	21
5.1.3	Laser beam quality	22
5.1.4	Effect of polarization	23
5.2	Process parameters	24
5.2.1	Pulsed vs. continuous-wave mode	24
5.2.2	Focus point, focal length and focal plane position.....	25
5.2.3	Cutting speed.....	26
5.2.4	The process gas	26

5.2.5	Cutting head and the nozzle	27
5.2.6	Nozzle alignment	29
5.2.7	Stand-off distance	30
5.3	Material parameters	30
5.3.1	Physical properties	31
5.3.2	Thermal properties	31
5.4	Laser cutting quality	31
5.4.1	Kerf width	32
5.4.2	Perpendicularity or angularity of the cut edges	32
5.4.3	Surface roughness	33
5.4.4	Dross	36
5.4.5	Heat affected zone width.....	36
6	TAGUCHI METHOD.....	37
6.1	System design.....	37
6.2	Parameter design	38
6.2.1	Signal-noise ratio	39
6.3	Tolerance design	39
6.4	Orthogonal matrix	40
6.5	Forming orthogonal matrix	40
6.6	Modifying orthogonal matrices to own demand	41
6.7	Linear graphs.....	41
6.8	Upper triangular matrix	42
6.9	Analyzing results.....	42
6.9.1	Signal-noise ratio analyzing.....	43
6.9.2	Analyses of variance (ANOVA).....	44
6.10	Studies with Taguchi methods in laser cutting.....	44
7	CASE STUDY	46
7.1	Corelase Oy	46
7.2	Test environment.....	46
7.2.1	Corelase's ARM® fiber laser	46
7.2.2	Precitec Procutter cutting head	47
7.3	The tested metals	48
7.4	The testing parameters for the metals	51
7.5	Cutting the metals and measurements	52
7.6	Test results.....	54
7.7	Mild steel.....	54
7.7.1	5 mm mild steel.....	55
7.7.2	15 mm mild steel.....	60
7.7.3	20 mm mild steel.....	65
7.8	Stainless steel	69
7.8.1	10 mm stainless steel.....	69
7.8.2	15 mm stainless steel.....	73

7.9	Copper	78
7.9.1	6 mm copper.....	78
7.9.2	10 mm copper.....	82
7.9.3	15 mm copper.....	86
7.10	Aluminium	90
7.10.1	15 mm aluminium	90
7.10.2	20 mm aluminium	94
7.11	Cut edges angularity.....	98
8	CONCLUSIONS.....	100
9	DISCUSSION AND FUTURE WORK.....	101
	REFERENCES.....	102

LIST OF SYMBOLS AND ABBREVIATIONS

Al ₂ O ₃	Aluminium oxide
Ar	Argon
ARM™	Adjustable Ring Mode
Bi	Bismuth
CD	Compact Disk
CO ₂	Carbon Dioxide
Cu	Copper
CW	Continuous wave
dB	Decibel
DC	Direct current
DVD	Digital Versatile Disc
Er ³⁺	Erbium-ion
Fe	Iron
FeO	Iron (II) oxide
HAZ	Heat Affected Zone
He	Helium
HeNe	Helium-Neon
Ho ³⁺	Holmium
hν	Photons energy
LAL	Laser Application Laboratory
Laser	Light Amplification by Stimulated Emission of Radiation
Nd	Neodymium
Ne	Neon
O	Oxygen
Pb	Lead
PMMA	Poly (methyl methacrylate)
QFD	Quality Function Deployment
R _a	An integral of the absolute value of roughness profile
RF	Radio frequency
R _z	Mean height of the profile
S/N	Signal-Noise ratio
TEM	Transverse Electric Mode
Ti	Titanium
Tm ³⁺	Thulium-ion
TUT	Tampere University of Technology
YAG	Yttrium aluminum garnet
Yb ³⁺	Ytterbium-ion
<i>a_i</i>	The effect of level
<i>BPP</i>	Beam Parameter Product
<i>E</i>	Energy
<i>D</i>	Raw beams diameter in K-term or with BPP it is diameter of the out coming beam
<i>d_{core}</i>	Fiber diameter
<i>d_{in}</i>	Laser beams diameter
<i>K</i>	K-term in beam quality
<i>M²</i>	M-term in beam quality

n	Number of test repetitions
u	Distance between two parallel lines
Y	General mean value
y_i	One tests results in Signal-Noise ratio
θ	Opening angle in K-term or with BPP it is divergent
θ_{in}	beams opening angle
θ_{max}	Maximum acceptable angle
λ	Wavelength
π	Pi

1 INTRODUCTION

1.1 Motivation for the Thesis

Laser can be found nowadays used in very different environments like consumer electronics, medical application and different fields of industry. In metal industry, the laser is used to cut sheet, plate metals and pipes and welding. The laser cutting is used in the industry, because it offers several advantages over conventional cutting methods like flame or water jet cutting. The advantages for the laser cutting are high cutting speed, low surface roughness, narrow kerf width, cutting edges are straighter and good integration to computer numerically controlled (CNC) machines for cut challenging profiles. These advantages give company an edge to lower their production cost, because there is needed less finishing to the product or semi-manufactured product.

To this demand Corelase Oy has developed the ARM® laser source family to give good cutting quality and high performance with high reflective materials like copper and aluminium. This thesis is assigned by Corelase Oy to study ARM® laser source's performance in challenging laser cutting applications. How it performs with different metals and what kind of surface roughness it could achieve.

1.2 Research objects

The purpose of this study is to investigate and study the ARM® fiber laser sources effect on the cutting quality like surface roughness and burr formation. The tested metals are mild steel, stainless steel, copper and aluminium with different thicknesses. The thesis should determine process parameters which gives good cutting quality for these metals. The tests are made with sheet metals only. The tests are made at Tampere University of Technology's Laser Application Laboratory (LAL) in co-operation with Corelase Oy.

1.3 Research methodology

The research question is; how the high power adjustable ring mode laser effects the cutting quality with different metals and thicknesses. This study's tests are made as an experimental research, where theories and practice are combined into research. The experimental study uses the Taguchi method to find the most effecting parameters and their levels to the surface roughness value.

The needed theory is combined from many different articles, books and writings which gives introductions to this physical phenomena, laser and laser cutting. The study has also student's own observations from the process.

1.4 Contents of the Thesis

This thesis has two parts. The first part is literature review to the subject for familiarize the thesis maker to the laser technology and the different effects of laser cutting parameters to the cutting quality. Chapter two covers laser principles. The third chapter is about different laser types and their usability at cutting. The fourth chapter covers laser cutting with four different modes. Chapter five is about laser cutting parameters and how they affect to the laser cutting quality. There is also an introduction to the standard SFS-EN ISO 9013, which gives instructions how the different cutting quality measurement should be done and the class levels for different quality parameter. The six chapter studies Taguchi method.

The second part of the thesis concentrates mainly on the case study of the thesis, which solves how the tests are made and what results were achieved. Chapter eight is about conclusions and chapter nine answers to future work and discussion.

LITERATURE REVIEW

2 PRINCIPLES FOR LASERS

A laser (**L**ight **A**mplification by **S**timulated **E**mission of **R**adiation) is a device which produces and amplifies an intense beam of highly coherent and highly directional light. This laser light is in infrared or in the almost visible spectrum of light. The lasers wavelength is determined by the used gain medium in the device. [1-3]

The laser device constructs from three main components, which together make an oscillator (Figure 1): a gain medium, a pump source and two mirrors which form a resonator. The gain medium is a component, where the light amplifies by process called stimulated emission (Figure 2). The gain medium can be solid, liquid or gas which activates the physical phenomena. The pump source is a component which provides needed power to create populated inversion in the gain medium. The pump source can be electrical, optical or chemical pumping. The two mirrors act and form the resonator where the light is trapped between the mirrors. The output mirror lets out only the lasers oscillation wavelength light. [1-3]

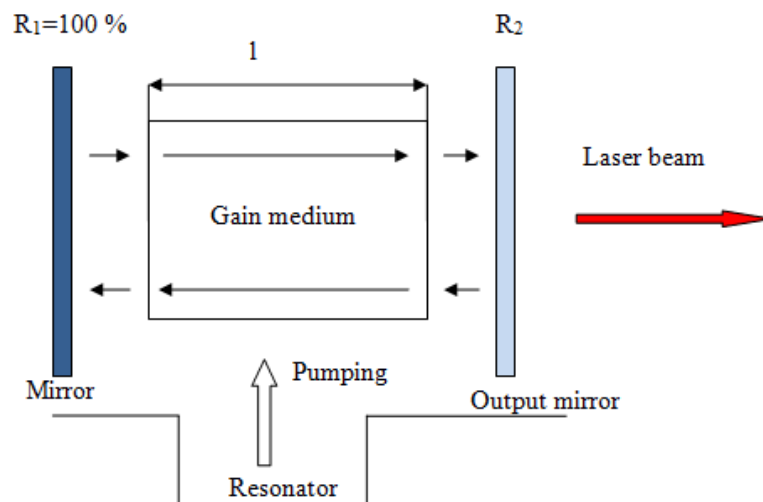


Figure 1: Principle of laser oscillator [2].

From the oscillator, the laser light beam is conducted by optical fiber or with other mirrors to where it is needed to be. The laser's output power ranges from milliwatts to several hundred kilowatts in continuous-wave mode and from tens of kilowatts to petawatt peak power when used in pulsed mode. [1; 2]

The lasers can be divided into two groups: continuous waves (CW) and pulsed lasers. The continuous wave laser produces a constant and steady flow of energy and the output power is steady. The laser beam's power does not oscillate with in time. CW laser are often gas medium lasers like HeNe or Ar-ion and solid-state lasers such as Nd^{3+} and Ti^{3+} . The pulsed laser differs from CW laser by the output power, which is changing over time so it produces short pulses of beam power repeatedly. The pulsed time is ranging from nanoseconds (10^{-9} s) to femtoseconds (10^{-15} s). The pulsed lasers are typically solid-state lasers like: dye lasers, Nd: YAG and Ti: Al_2O_3 . [1; 2]

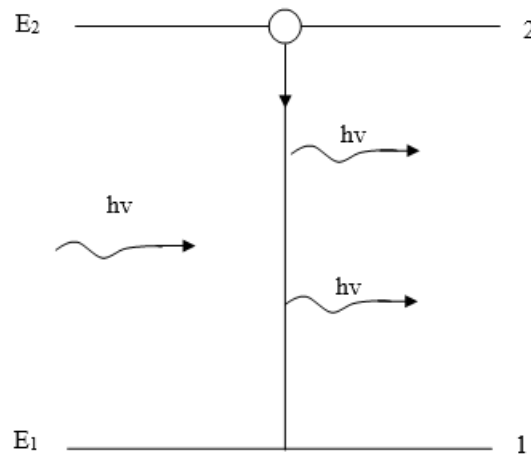


Figure 2: Stimulated emission. E_1 and E_2 are energy states of electron and $h\nu$ photon energy. [2]

The laser beam's intensity is not constant through the beam's crosscut. This power distribution is called mode and it is represented by TEM_{lm} -value (Transverse Electric Magnetic). The subscript of the TEM_{lm} value tells how many power peaks are in the beam's cross section and what shape it has. The best mode is the TEM_{00} , which have highest power density and the best focusing capability. Different kind of TEM_{lm} patterns are shown in Figure 4 and the intensity distribution across the laser beam in two different TEM patterns (TEM_{00} and TEM_{01}) is shown in Figure 3. [1-3]

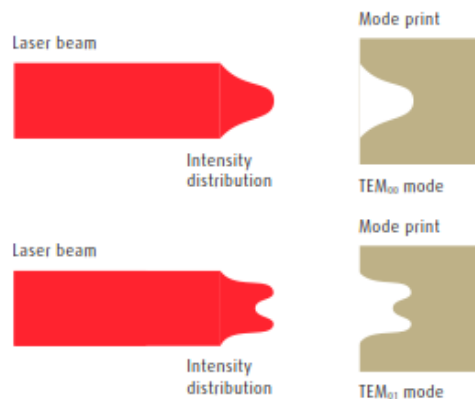


Figure 3: Two different TEM modes intensity distribution adapted from [4].

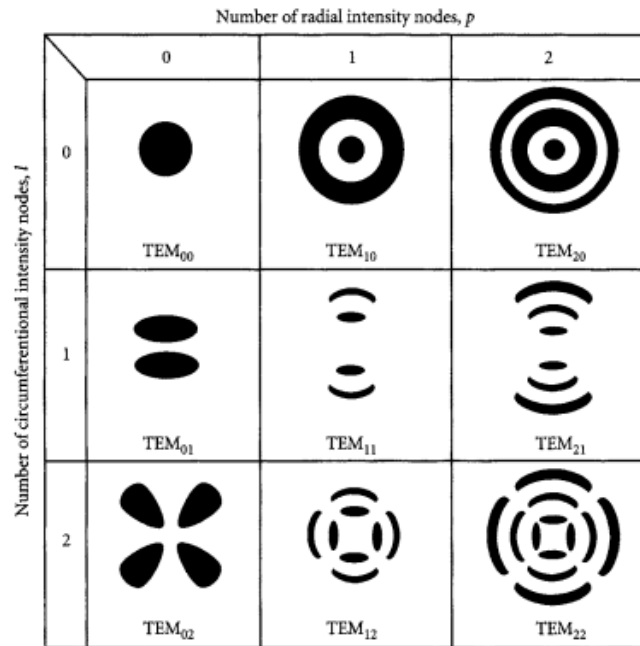


Figure 4: TEM modes adapted from [1].

2.1 Stimulated emission

Stimulated emission is a light amplifying process which makes occurrence of laser light possible. In the stimulated emission, theorized by Albert Einstein (1879-1955) already in the year 1917, an electron is excited with energy from the resonator to energy state E_2 (unstable). Then the electron decays to lower state E_1 (state 1) and emits a photon which has the same phase, propagation direction and polarization state as the stimulating photon. If these photons collide to another excited electron they release another similar photon. This physical phenomenon is repeated in the gain medium if there is outside energy provided into the process. Figures 2 and 5 show the principal of this process. Stimulated emission is forms coherent radiation. [1-3]

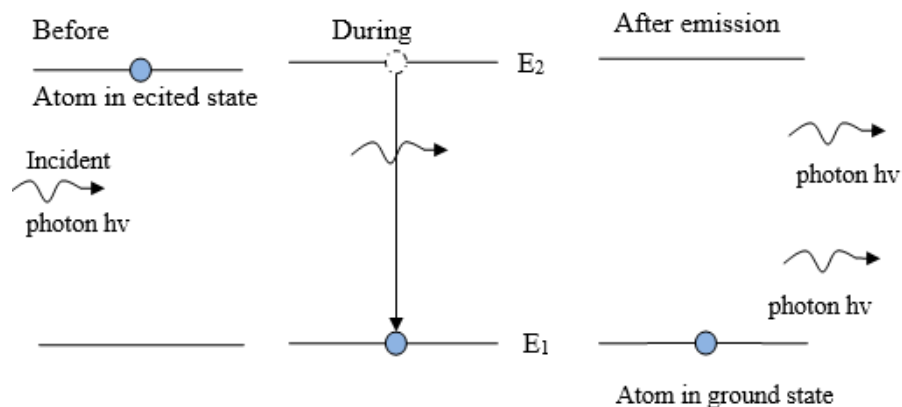


Figure 5: Stimulated emission. [2]

3 LASER TYPES

This chapter introduces lasers which can be used in cutting processes. Capable lasers for this process are fiber laser, CO₂ laser, disk laser, diode laser and Nd: YAG laser. These lasers have high output power (CO₂ up to 20,000 W) and high quality beam for the cutting applications.[3; 5; 6]

3.1 Fiber laser

Before discovering double-clad high power lasers, fiber lasers' primary use was in the telecommunication industry. The high power fiber laser development opened the markets for material cutting, welding, marking and surface finishing. Fiber lasers are rare-earth-doped lasers which are gaining more and more attention by different industrial areas because of their flexibility, high efficiency, low pump threshold and high output powers. These kinds of lasers are diode pumped solid-state lasers and they can operate both continuous-wave and pulsed mode. In continuous-wave mode fiber lasers can achieve several kW output power. Lockheed Martin's introduced 30 kW fiber laser in 2014.[3; 5-9]

The rare-earth materials which are usually used in silicate based fiber laser are neodymium (Nd³⁺), ytterbium (Yb³⁺) and combination of these two (Nd³⁺/Yb³⁺). These materials operate around 1 μm wavelength. Erbium (Er³⁺), Er³⁺/Yb³⁺, thulium (Tm³⁺), Tm³⁺/Yb³⁺, and holmium (Ho³⁺) fibers operate around 1,5-2 μm wavelength.[7; 8]

3.1.1 Design and operation principle

In the fiber laser, the light beam is created inside the optical fiber, which performs as the resonator. The fiber's core is made from rare-earth materials, which are pumped with diodes. The fiber, in which the laser beam is created, is several meters long multi-clad single mode fiber. In this laser, the pumped beam is conducted to the head of fiber and the beam is going through the claddings several times in the fiber without any power losses. The schematics of this kind of laser is shown in Figure 6. Usually the fiber lasers are modular, so when you add many single-mode laser modules together you get more powerful laser source. These are called multimode fiber lasers. The fiber laser's beam is narrow and the quality of the beam is excellent ($M^2 < 1,1$). [3; 5-8]

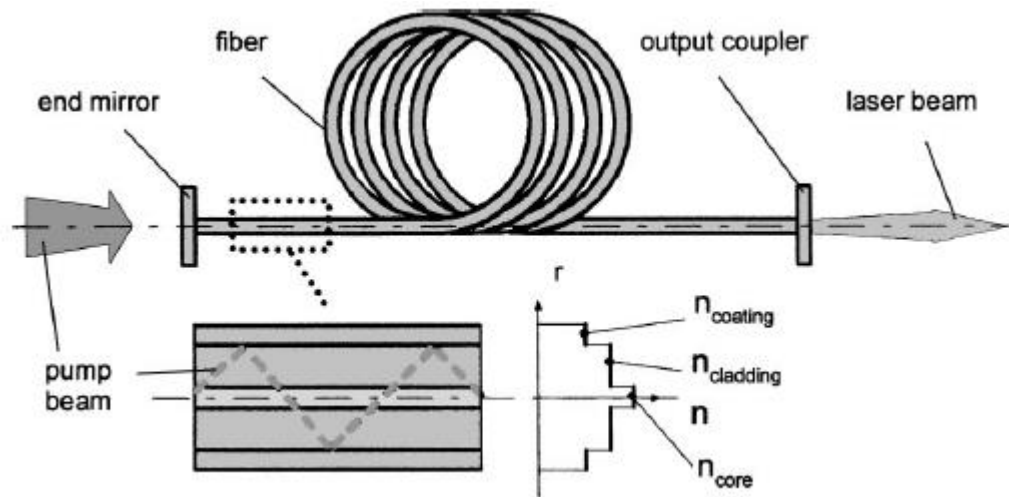


Figure 6: Fiber laser schematic adapted [10]

3.1.2 Power scaling

As mentioned in the last paragraph, the multi kW fiber lasers consist of many smaller modules to achieve the wanted output power and where the powers are combined in a single multimode fiber. The output power can be changed continuously with power supply. In 1 kW laser, the beam delivery fiber's diameter is 100 microns and 10 kW system that is 300 microns. The delivery fiber's diameter also depends from the power of the source and wanted purpose of use. These allow longer working distances. The fiber laser has high reliability, because of the modular construction and there are no consumable parts. [3; 5; 8]

3.1.3 Applications

The fiber lasers are versatile lasers because they have excellent line width and noise performance. The fiber lasers are reliable and have excellent beam quality. For those reasons, the fiber laser has been taken some of the cutting process market from CO₂-laser. The fiber lasers are used in many industries from automotive to airplane and even computer and medical industry to do different things like cutting, welding (spot, normal), surface finishing and marking. [3; 5; 7; 8]

3.2 CO₂ laser

The carbon dioxide (CO₂) laser is the most common used laser source in the metal industry fields. The CO₂ lasers are used for metal cutting, welding and even high precision material processing and even in the medical field tissue coagulation. The CO₂ lasers are commonly operated in continuous-wave mode. In CW mode, the laser's output power range is a few watts from small sealed-off laser modules to more than hundreds

kW for high power the CO₂ lasers with fast gas flow operation. The CO₂ laser systems which are pulsed are based on Q-switching and they can achieve even peak powers of several gigawatts. In theory, the CO₂ lasers plug efficiency is 21% (max value), but with today's machines' the efficiency is only 10-15%. [2; 11]

The carbon dioxide laser uses gas mixtures of helium (He), nitrogen (N₂) and carbon dioxide (CO₂). The mixture works as active medium, which is excited with electrical gas discharge. The common ration of the gas mixture is 1:2:8 (CO₂: N₂: He). The electrical gas discharge is obtained by either direct current (DC) or radio frequency (RF) stimulation. The CO₂ laser provides wavelengths from 9,2 μm to 11 μm and the commonly used wavelength is 10,6 μm. [2; 11]

3.2.1 General construction

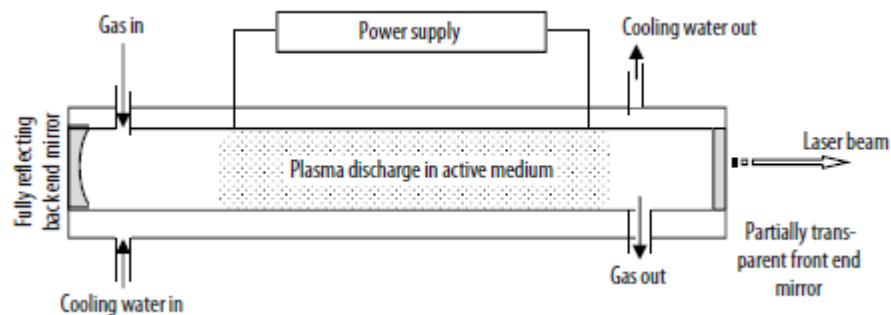


Figure 7: Construction of a slow flow laser adapted from [11].

The CO₂ lasers have many designs which are using different kind of modes of gas flow and cooling (water or air). These designs and modes are combined to achieve the wanted output power. The different designs are: transverse flow laser (cross-flow), fast-axial flow laser, diffusion-cooled slab laser and sealed-off laser. Three of these CO₂ laser designs: fast axial flow, slow flow and diffuse-cooled are mostly used in engineering industry because these laser types can provide the needed output power level for most industry applications. In Figures 7 and 8 is shown two different CO₂ lasers' constructions (slow flow gas lasers in the Figure 7 and fast axial flow laser in the Figure 8). [2; 3; 5; 11]

The CO₂ laser light is in mid-infrared spectrum of light. The mid-infrared emission in carbon dioxide lasers' means it is not possible to use standard glass lenses or glass fiber, because of the high infrared absorption of standard silica-based glasses. The optical lenses and the fibers, which are used to guide the laser beam, is made from zinc selenide, silicon or germanium. [2; 3; 5; 11]

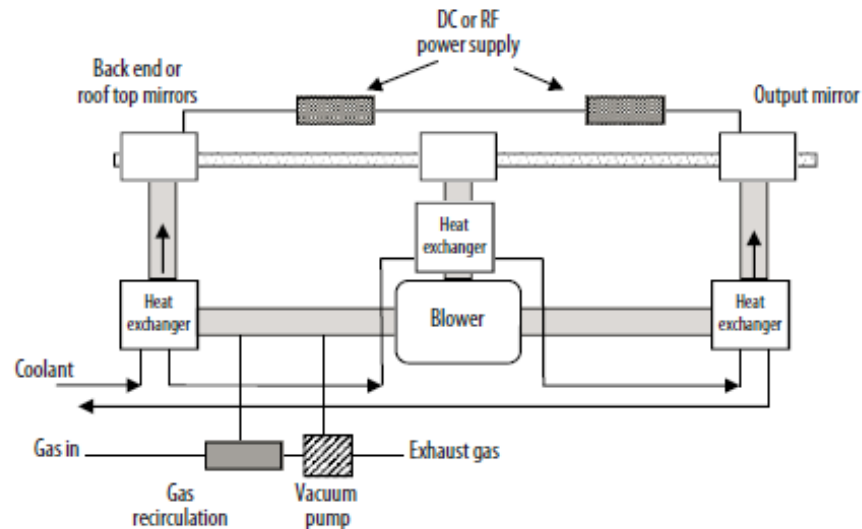


Figure 8: Fast axial flow lasers general construction adapted from [11].

3.2.2 Slow flow CO₂ laser

In the slow flow laser, the gas flows slowly perpendicularly in the resonator's optical axel (Figure 7). The slow flow lasers are cooled through the resonator tube with a convection. The cooling is executed usually with water. The gas flow also helps cooling, although it is minimal. These lasers were the first high power lasers, but because of their general mechanic principal, these lasers were also very big. That's why the slow flow laser has been replaced by another laser types in different fields of industry. [2; 3; 5; 6]

3.2.3 Fast axial flow CO₂ laser

As the name says, the gas mixture is flowing with high velocity perpendicularly in the resonator's optical axel (Figure 8). The high velocity of the medium gas flow helps cooling the device with water. Turbines or high power blowers are used to generate the laser's fast gas flow. These lasers can be connected optically in a series to increase the output power of the resonator shown in Figure 9. With this design is possible achieved output powers from hundreds of watts to more than 20 kW. [2; 3; 5]

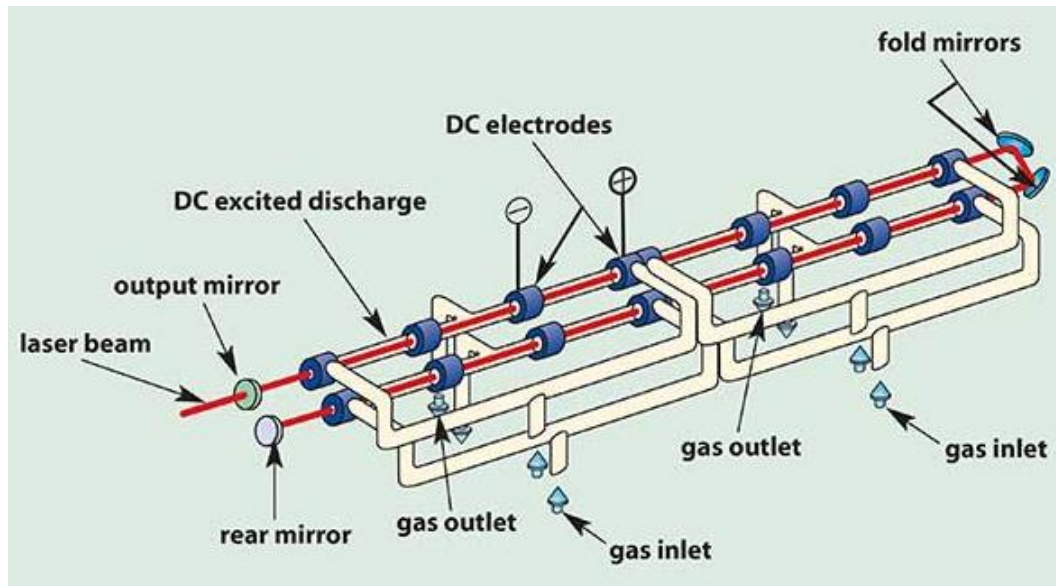


Figure 9: Fast-axial CO₂ laser adapted from [12].

3.2.4 Diffusion-cooled CO₂ laser

In the high power diffusion-cooled CO₂ laser design differs from the other by that they have a gap between a pair of planar RF-electrodes. These RF-electrodes are cooled with water. The discharge of the gas happens between those two RF electrodes, which are made from copper. The small gap between the electrodes, allows high heat dissipation from discharge cavity via the water-cooled electrodes. This produces high power density. This laser type is very compact compared to fast axial flow laser. Figure 10 shows schematics of slab laser. [12; 13]

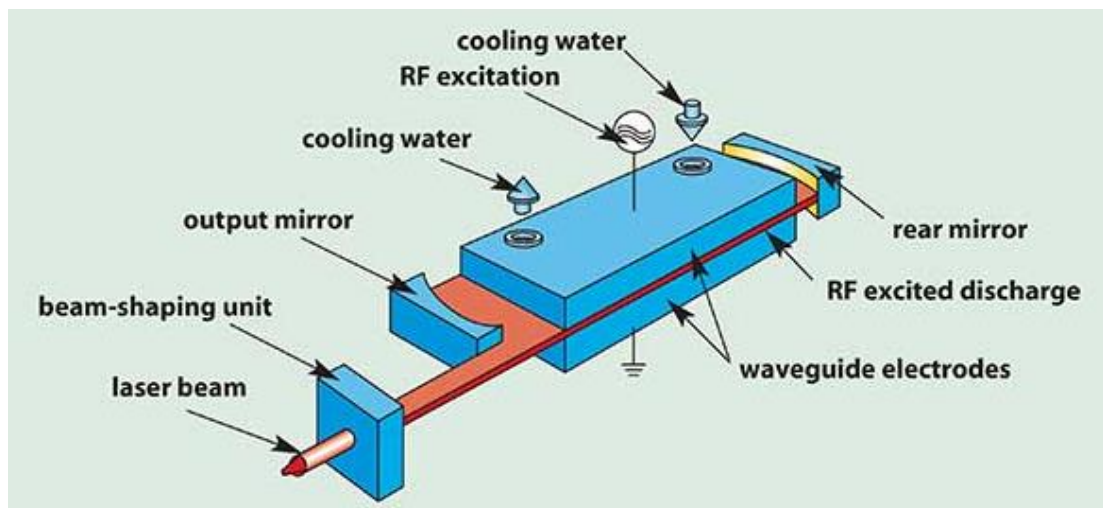


Figure 10: Construction of slab laser adapted from [12]

Advantage, which is notable to mention with this laser, is the very small gas consumption. Because the internal 10-liter cylinder, which is in the laser head, lasts about 1 year

without external gas supply. Another advantage with in this laser is the highly focusable beam.[12]

3.3 Disk laser

The disk laser is a diode pumped (active mirror) solid state laser. These lasers have high output power with good efficiency and very good beam quality. The disk lasers' can be pumped from the end or front or even from the edge of the disk. The principle of the thin disk laser was demonstrated in the year 1993. [10; 14]

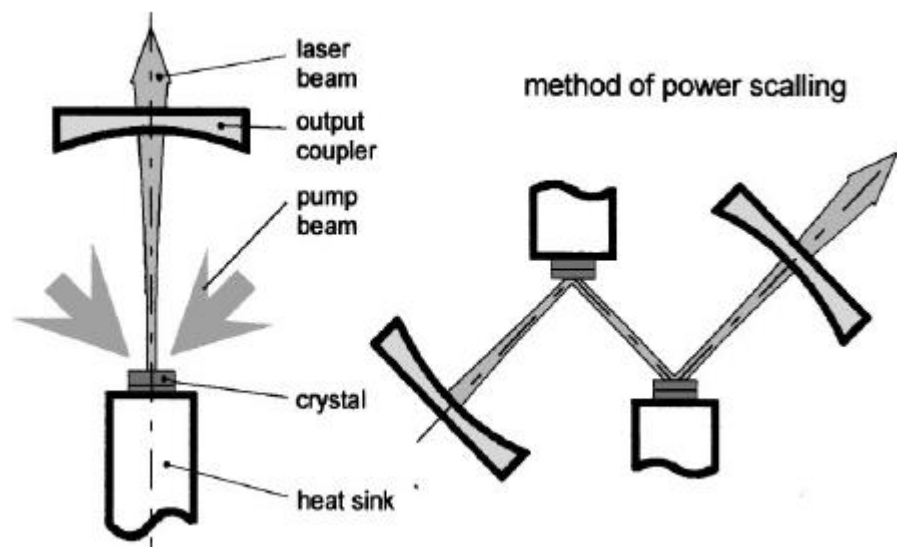


Figure 11: Schematics thin disk laser (left) and method of power scaling with multiple mirrors adapted from [10].

3.3.1 Thin disk laser

The thin disk lasers name comes from a crystal (Yb:YAG), which acts as the active medium and is shaped like a disk, but other shapes have been tested. The disk's diameter is several millimeters, depending on the wanted output power. The disk's thickness is varying from 100 μm to 200 μm depending on, what is used as the active material, pump design or as the doping concentration. The disk's backside has been coated with highly reflective material which is reflective for both, the lasers light and the pumped wavelengths. It is also coated with anti-reflective material from the front for both wavelengths (a pump and laser). The thin disk laser's cooling is achieved with mounting the disk on a water-cooled heat sink, using gold-tin or indium-based solder shown in Figure 11. [10; 14]

The diode pumped beam is reflected with parabolic mirrors to the crystal disk. From there the beam is derived optically back to the crystal several times (see Figure 12). With this method, high pump energy efficiency (90%) is achieved. As fiber laser, these

lasers can be put optically in series to achieve higher output power without losing excellent beam quality. [3; 10; 14]

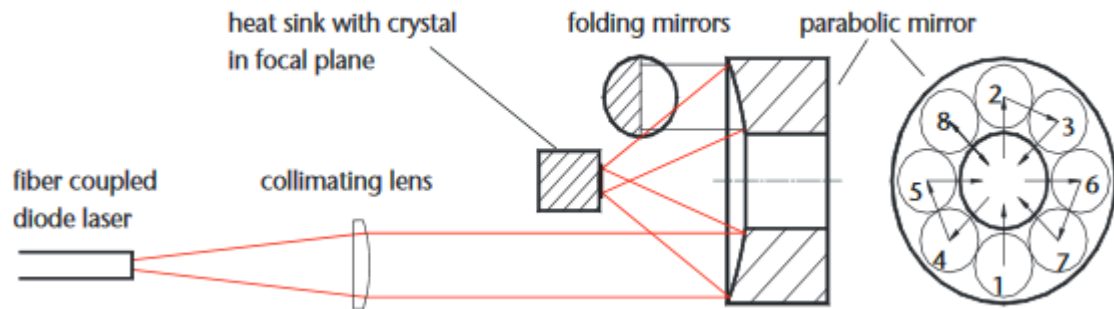


Figure 12: Thin disk laser's operational principal adapted from [14].

3.4 Nd: YAG lasers

These lasers are crystal lasers, where the laser light is generated in yttrium aluminium garnet (YAG) crystal, which are doped with neodymium ion (Nd^{3+}). These lasers provide light wavelength of 1064 nm. The crystal is shaped like a rod and in the device, it is located between two reflective mirrors. The mirrors are water cooled and coated with gold. The mirrors can be constructed from aluminium or ceramics. The excitation in the crystal is made with flash lamps or arc lamps or semiconductor lasers or with diode pumping. The pumping source is placed in the optical perpendicular axis of the mirror. Nd: YAG lasers can be divided into two groups: diode pumped and lamp pumped lasers. Because the laser beam is made in solid rod, there have been problems with cooling so that's why these laser developments have been slow. [1-3; 6]

3.4.1 Diode pumped Nd: YAG lasers

The diode pumped Nd: YAG lasers are solid-state lasers. The diode pumped lasers can be divided in two groups: end-pumped and side pumped systems. In the side-pumped system, array the diodes is arranged along the length of the slab or rod. In the end-pumped system, the pump energy is focused longitudinally on the rod. The diode pumped Nd: YAG lasers are mostly used in continuous-wave mode, but can be used in pulse mode with Q-switching. [1; 2; 15; 16]

The advantages of diode pumped Nd: YAG laser are good efficiency 20-25%, low laser noise, much more compact construction and better lifetime compared to lamp pumped (about 10 000 hours). On the other hand, diodes are much more expensive than lamps. [16]

3.4.2 Lamp pumped Nd: YAG lasers

In the lamp pumped Nd: YAG lasers the excitation is achieved by flash or arc lamps. The arc lamps are used for continuous-wave operations, as the flash lamps are for produce either free-running or Q-switched pump pulses. Both lamps consist of glass tube and they are filled with gas example krypton at couple atmospheres pressure and they have metallic electrode at each end. [1; 2; 15; 17]

In pumping laser crystal, the lamp(s) are arranged alongside with the pumped rod. Usually laser rod and lamp are placed within elliptic pump chamber with reflective walls. With this construction, the generated pumped light has a higher possibility to absorb into the rod. Lamp pumped solid-state lasers are usually face-pumped slab lasers, where array of lamps pumps energy through slabs large face. [1; 2; 15; 17]

Lamp pumped Nd: YAG lasers advantages and disadvantages are listed under [1; 2; 15-17]:

Advantages are:

- Very high pumping power can be generated, especially peak powers
- Lamps are robust
- Much lower price per watt in generated pump energy

Disadvantages are:

- Lamps life time less than 1000 hours
- Wall-plug efficiency very low, mostly 2-3 percent
- High voltages needed for power supplies (safety issue)
- Relatively noisy laser pumping source, leads to higher laser noise

3.5 Fiber laser vs. CO₂ laser

The CO₂ laser has previously been the number one laser in different laser cutting processes, but nowadays fiber laser has been challenging it in cutting industry. The CO₂ laser's benefits are high power with good K value, high cutting speed with thicker (over 5 mm) materials with good cutting edge quality, good efficiency and wavelength of 10,6 μm, which is ideal for heating. Disadvantages for CO₂ laser are gas consumption, weak performance with reflective materials like copper or brass (because of higher wavelength 10,6 μm compared to fiber laser). [18; 19]

The fiber laser provides good efficiency, lower cutting costs (shown in Table 1), because there is no gas consumption inside the laser source like CO₂. The fiber laser cutting provides better cutting quality under 5 mm thick materials compared to CO₂ laser. Fiber laser provides excellent beam parameter product (BPP) value with wavelength of 1065 nm, which is good for processing high reflective materials like brass or copper.

The higher absorption of the fiber lasers light wavelength and higher power density created by the focused beam combine to achieve increase in cutting speed with thin materials when comparing CO₂ laser.[18; 19]

The study “Experimental investigation of fusion cutting stainless steel with fiber and CO₂ laser beams” compares two different laser source fiber and CO₂ by cutting stainless steel sheets 1 mm up to 10 mm thickness. They found out that the fiber has higher cutting speed with thinner sheet, but with 10 mm thick sheet the CO₂ and fiber have identical cutting speed. Same study compared the kerf cross-section area and there were no major differences between these two laser sources. It was also noticed that the surface roughness started growing with fiber in 4 mm to 6 mm thickness and 8 mm to 10 mm with CO₂. [20]

Both lasers have own benefits and disadvantages in cutting. When choosing laser to own process and purpose you should think, what thicknesses and materials you are going to cut, because both lasers are versatile and both deliver good cutting qualities with right cutting parameters. In the table the AL is aluminium, the CRS is cold rolled steel and the SS means stainless steel.

Table 1: Laser cutting cost per 100 feet of material adapted [19].

Material	Thickness (inch)	Cutting gas	CO₂ laser cutting speed and cost to cut 100 ft. of material	Fiber laser cutting speed and cost to cut 100 ft. of material
CRS	0,020	N ₂	992 in./min/\$ 0,26	2362 in./min/\$ 0,05
CRS	0,118	N ₂	189 in./min/\$ 1,35	354 in./min/\$ 0,35
CRS	0,197	N ₂	83 in./min/\$ 3,07	189 in./min/\$ 0,66
SS	0,059	N ₂	378 in./min/\$ 0,67	1654 in./min/\$ 0,09
AL	0,118	N ₂	189 in./min/\$ 1,35	331 in./min/\$ 0,38
CRS	0,250	O ₂	118 in./min/\$ 2,16	113in./min/\$ 1,10
CRS	0,313	O ₂	99 in./min/\$ 2,57	99in./min/\$ 1,26
CRS	0,787	O ₂	26 in./min/\$ 9,79	33 in./min/\$ 3,78
SS	0,236	N ₂	78 in./min/\$ 3,26	154 in./min/\$ 0,81
AL	0,236	N ₂	30 in./min/\$ 4,32	94 in./min/\$ 1,33

4 LASER CUTTING

The laser cutting is thermal operation, where the laser beam, which is focused to the material's surface with optical lenses is vaporizing and melting the material with operational gas (Figure 13). The usual cutting geometry is flat sheet, where the laser cut the programmed shape. The laser cutting process is based on high density of energy (over $10^5 - 10^6 \text{ W/mm}^2$) and small beam diameter on the surface of the material. To apply needed laser beams lights intensity to material's surface, the cutting head focuses the beam to focal point which diameter is 0,1-0,6 mm on the surface. The high intensity of energy melts cylinder through the material whole thickness and surrounding material of the cylinder. The molten material is carried away with the assistant gas flow and pressure. If the assistant gas is reactive like oxygen O_2 , the gas takes part in the cutting process by burning some of the material during the process. If the gas is inactive, like nitrogen N_2 , the gas does not take part to the burning process. The inactive gas flow only pushes the molten material away from the kerf and protects the cut edge from oxidation. The gas is combined with the laser in the cutting head (Figure 14). The main cutting parameters which affects to the quality of the cutting are:

- The intensity of the energy
- Cutting speed (feed rate)
- Focal points place in the material
- Jet's shape (assistant gas shape)
- Nozzle head's distance from the material's surface
- Used assistant gas and its flow rate.

By optimizing these parameters, the best cutting quality can be achieved. [1-3; 5]

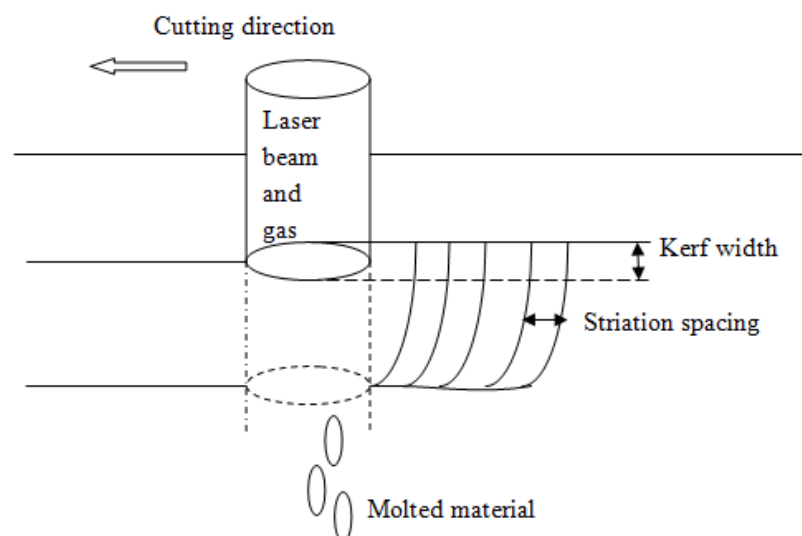


Figure 13. Laser cutting (melt shearing) adapted from[1].

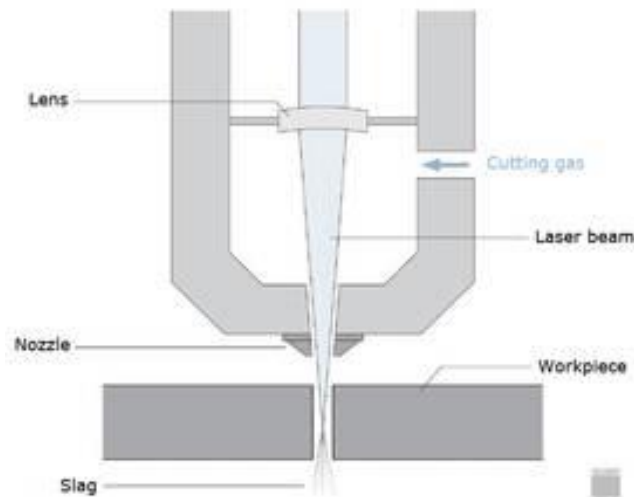


Figure 14: The principle of laser cutting [21].

The laser cutting can be divided in main three cutting methods: oxy-fuel cutting, melting cutting and vaporizing cutting. There are two different methods in addition with previous: chemical degradation and scribing. These different cutting methods differ from each other by little. The difference between the methods is in cutting or assistant gas and by the chemical process in how the cutting gas and the laser effects on the material and smelt it. Table 2 shows, which method is used with different materials normally.[1-3; 5]

Table 2:The laser cutting methods for various materials (suitable method is show by x) adapted from [1]

Material	Reactive gas				
	Inert gas melt shearing	melt shear- ing	Vaporization	Chemical degradation	Scribing
Ferrous alloys	x	x	-	-	-
Non-ferrous alloys	x	x (Ti)	-	-	-
Polymers	x (Thermoplas- tics)	x (Thermo- sets)	x (PMMA)	(Thermosets)	-
Ceramics	x	-	-	-	x
Glasses	x	-	-	-	x
Elastomers	-	-	-	x	-
Composites	x	-	-	x	x

The laser cutting system contains assistant gas delivery system, laser source, cutting head where the optical lenses and gas nozzle are and robotic table or arm to move the cutting head or to move cut work piece. Figure 15 shows the schematics for cutting system.

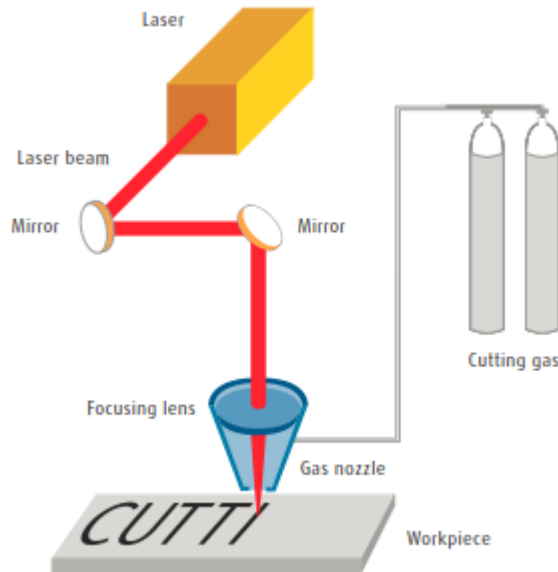


Figure 15: Principle for cutting system adapted from [4] .

4.1 Cutting with reactive gas

The oxy-fuel laser cutting (reactive gas melt shearing) is cutting method, where oxygen or air is used as active assistant gas (Figure 16). Here the laser's focused beam heats the material and with the support of the oxygen active exothermic reaction with the material. The principal of exothermic reaction is shown in equation 1. Where the Fe is iron and the O is oxygen. When they are combined, they form iron(II) oxide (Fe(II)O). This exothermic reaction brings more energy to the process and increases the temperature of the cutting kerf. Sometimes this oxygen iron reaction is the main dominant energy source in this cutting process. [1; 2; 5]



The front edge's oxidation helps the laser beams light to absorb more easily to the metal's surface. This oxidation of the metal helps the cutting by lowering the molted material's viscosity and the surface tension. With those effects, the smelt flows away from the kerf more easily. In the oxygen cutting, the assistant gas pressure is low (0,5 - 1 bar) and the pressure depends from what material is cut and how thick it is. The assistant gas also blows the molten material away from the kerf and protects the laser optics overheating and splashes. This method is used with copper, carbon steels and low alloy steels. [1; 2; 5]

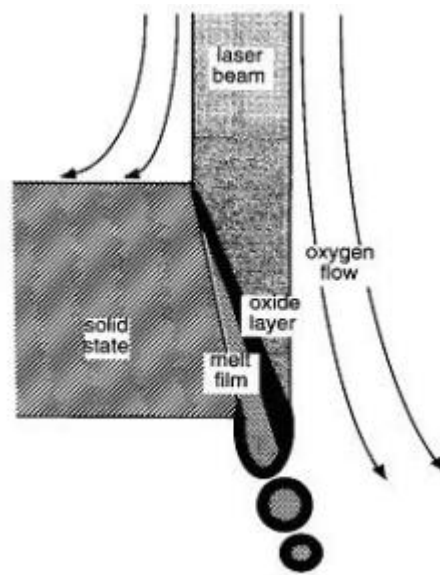


Figure 16: The principal sketch of reactive gas melt shearing [5].

4.2 Inert gas cutting

In the inert gas laser cutting, the laser beam heats the material and the high pressured (even 20 bar or more) inert gas blows the molten material away from the kerf shown Figure 17. This method has slower cutting speeds, when compared to the reactive gas cutting. In this cutting process, the laser is the only energy source and the assistant gas is cooling the cutting area. The inert gas melt shearing differs from the oxy-fuel cutting method by the assistant gas which is used. This gas is inactive gas which means that the gas does not take part the chemical process and it also shields the heated material from surrounding air. The gas also protects the laser optics. [1-3; 5]

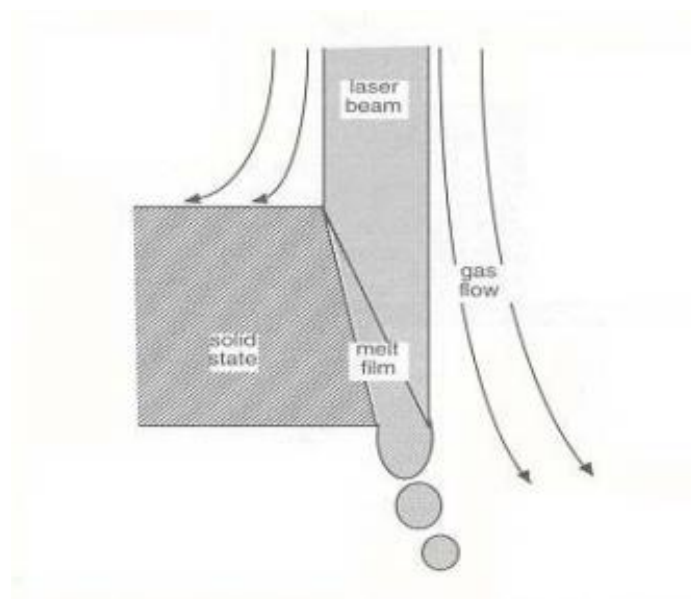


Figure 17: The principal of inert gas cutting [5]

The used inert gas in the cutting process is usually nitrogen (N₂) when oxidation in the material is not allowed. Pressured air can also be used for example with plastics but in this case burning of the cutting edge may occur. With titanium, the used gas is usually argon (Ar) or helium (He) because those gases do not react with titanium. The gas has high pressure (above 10 bar) because the liquid smelt can stick under the material and solidify as a dross underside of the cutting edge. With this method, the same materials can be cut as with oxygen cutting but it is mainly used with high-alloy steel, stainless steel, aluminum, titanium, polymers and ceramics. [1-3; 5]

4.3 Vaporization

The vaporizing cutting method (Figure 18) is used with acrylic, plastics, rubber, paper, wood, leather and with some ceramics. The cut material is vaporized with high intensity and high power of the laser. In vaporization cutting, the laser beam heats instantly the material beyond its melting point and vaporized it. The assistant gas is used to push away the vaporizing gases and at the same prevents the formed gases to take part to the cutting process. This method is used with very thin metals or materials with very slow speeds. This gives very high accuracy to the cutting and the cutting quality is higher. [1-3; 5]

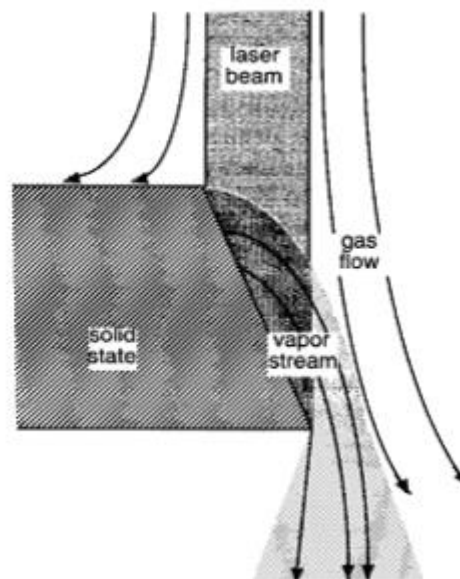


Figure 18: A sketch of laser vaporizing cutting method [8]

4.4 Chemical degradation

In this mechanism, the laser beam is breaking chemical bonds and forms new compounds. This mechanic is important when cutting of thermoset polymers, wood, elastomers and some composites. The cutting rate in this method is slower than melt shearing and the quality is better in the cutting edges. [1]

5 LASER CUTTING PARAMETERS

The lasers cutting parameters are depending on which material is going to be cut, from its thickness, laser beam characteristics, the wanted cutting rate and the wanted edge quality. The laser cutting is multi parametric problem. The parameters can be grouped to laser beam's parameters, process parameters and material parameters. In the literature, the smelt shearing cut mechanism and carbon-manganese steel are used for the baseline for these parameters. [1; 11]

5.1 Laser beam's parameter

The laser beam's parameters are mostly parameters, which the user or the operator cannot change or effect during cutting. The beam parameters are wavelength, laser beam quality and polarization. The other parameters are laser power and its intensity, but the operator can change these parameters. In the next paragraphs, is told how they effect on the cutting process and quality.

5.1.1 Wavelength

The laser beam has a wavelength (λ) (Figure 19) and the wavelength depends on what kind of laser is used and its active medium. Example CO₂ laser provides wavelength of 10,6 μm , fiber laser 1,07 μm and Nd: YAG 1,06 μm . These wavelengths are in infrared light spectrum. In Figure 20. is shown different lights wavelengths. Shorter wavelength's absorption will be higher into the material. This is important when cutting high reflective materials like copper, silver or aluminium even gold. With shorter wavelength, finer focus point for a given mode (TEM₀₀) structure can be achieved. and optics train which effects directly to the cutting accuracy, with it can be achieved a narrower kerf width and a lower edge roughness. In Figure 21 is shown some commercial lasers characterized by wavelength and average power. [1; 2; 6; 11]

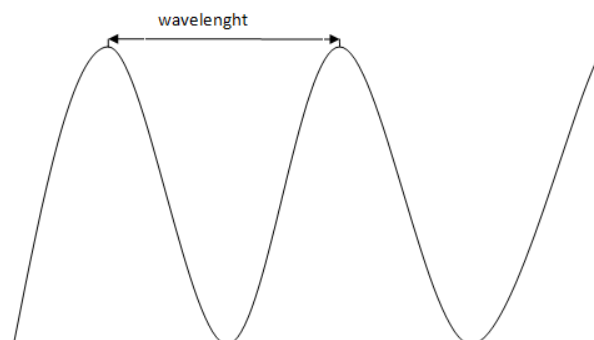


Figure 19: How the wavelength is measured.

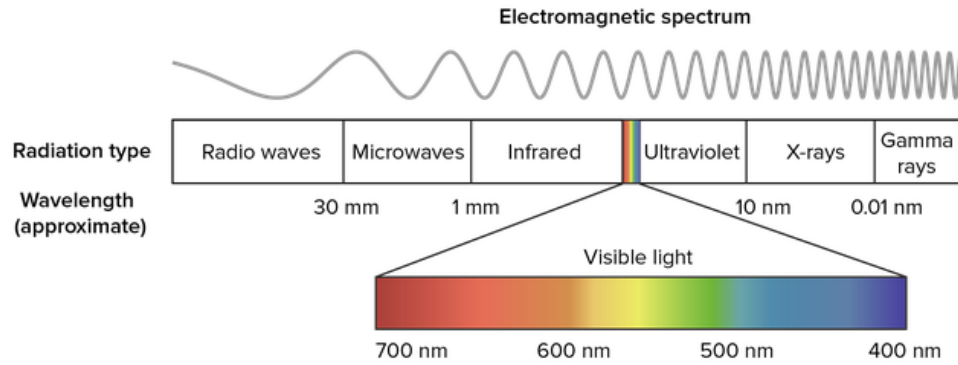


Figure 20: Light's wavelengths spectrum adapted from [22].

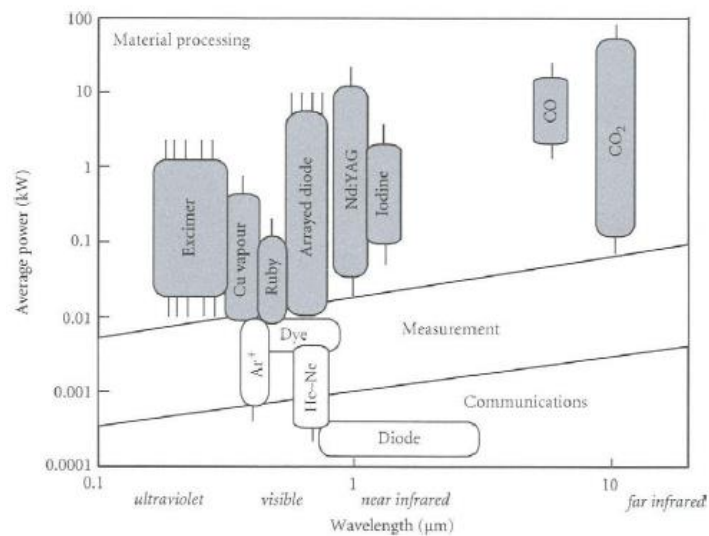


Figure 21: Commercial lasers characterized by wavelength and power and background is showed ground applications adapted from [1].

5.1.2 Laser power and intensity

The laser's output power is the energy which is emitted through the laser light in a second. The intensity is the laser beam's power divided by the area which it is concentrated (Formula 2). Higher intensity can be achieved by focusing the laser beam to smaller spot area or increasing the output power. This is better for cutting applications, because with smaller spot the material heats quicker which effects on the cutting speed and cutting quality. [1; 11]

$$Intensity = \frac{Laser\ Power}{Irradiated\ area} = \frac{W}{mm^2} \quad (2)$$

The power and intensity effects on the overall cutting performance, it allows cut faster speed and/or cut thicker material with slower speed. If the cutting has too much power

to compared speed, the cut kerf width can increase, the cut quality drops, thicker recast layer appears, an increase in dross forming and sharp corners become rounded. But if there is not enough output power the cutting process cannot even start. [1; 11]

5.1.3 Laser beam quality

The beam quality is important effecting factor in laser machining in overall. The laser beam has better focus ability than normal light, because of its coherent (the beam does not expand very much over distance) and it have only one wavelength (monochromatic). The laser beam has little dispersion in practice. This means that the cross-section area of the beam is growing only by little as the distance from resonator to measurement point is increasing. The laser beam's dispersion is called as divergent, which is beam's spreading angle. Good quality beams divergent is only 1-1,5 mrad. [1-3; 5; 6]

The beam quality is described with K , M^2 and BPP (Beam Parameter Product) terms. With the laser is used different measurement quality terms, example CO₂ laser's quality is described with K or M^2 term and fiber laser is using BPP. K - and M^2 -terms are determined by next the formulas:[1-3; 5; 6]

$$K = \frac{4 * \lambda}{\pi * \theta * D} \quad (3)$$

where K is calculated term, λ is the beams wavelength, θ the beams opening angle (two times the divergent) and D is the raw beam diameter. K - and M^2 -terms connection between each other is determined by the formula 4.: [1-3; 5]

$$K = \frac{1}{M^2} \quad (4)$$

The closer these terms are to value one (1), the closer is the ideal beam. This means good focus ability and smaller focus spot can be achieved with it.[1-3; 5]

With the optical fiber, the term BPP is used to show the beam's quality. Formula 5. determines BPP -value: [1-3; 5]

$$BPP = \frac{D * \theta}{4} = mm \cdot mrad \quad (5)$$

where BPP is the calculated term, D is the out coming beam's diameter from the fiber and the θ is the divergent. The K -, M^2 - and BPP terms have a relation between each other and it is shown in formula 6. [1-3; 5]

$$K = \frac{1}{M^2} = \frac{\lambda}{\pi * BPP} \quad (6)$$

The BPP term determines, how thin optical fiber can be used to carry the beam. The focusable beam must be smaller than the fibers diameter and the beam's divergent must be smaller than the overall reflection angle (Figure 22). In Figure 22 d_{core} is fiber diameter, d_{in} beam's diameter, θ_{in} beam's opening angle and θ_{max} is acceptable maximum angle. [1-3; 5]

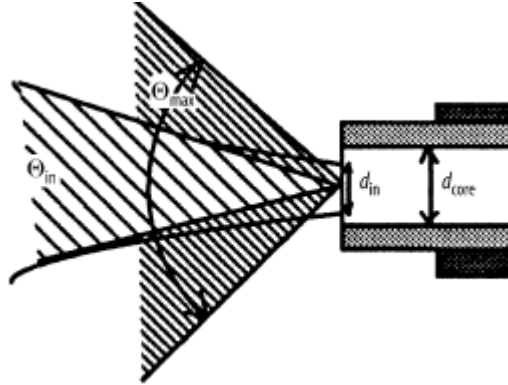


Figure 22: Fiber coupling geometry adapted from [11].

The BPP is better when the laser light beams are entering to the fiber than the out coming beam's BPP. The optical fiber's curvature and the small flaws in the fiber affects to the beam when it is carried in the optical fiber. Bad quality of the beam effects directly focus point's diameter by increasing it and this affects to cutting speed and penetration to the material. [1-3; 5]

When the beam quality is excellent (K- and M^2 - terms are near 1), the focus point is small. With small focus point, small kerf, higher cutting speed and better penetration can be achieved because higher beam intensity in material surface. Then it is possible to use bigger focal length which makes it possible to cut thicker material. [1-3; 5]

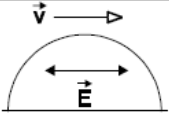
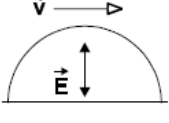
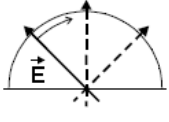
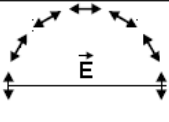
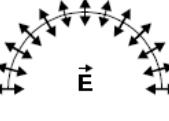
5.1.4 Effect of polarization

The stimulation emission phenomena produce trains of light waves; these waves' have electrical vectors which are lined up. This is called polarization. Different kinds of polarization are shown in Table 3. This phenomenon must be taken into consideration with cutting CO₂ laser, because the CO₂ laser produces light which is linear polarized. With Nd: YAG lasers this light is randomly polarized. Polarization have effect on cutting performance and it is cutting direction dependent. [1; 11]

When cutting metals with the p-polarized laser beam, light is absorbed significantly at grazing angles of incident. When beam is polarized to the same direction as the cut, the p-polarized light is absorbed to the front edge of the cut. If the light is s-polarized the absorption happens in the sides of the kerf. With these polarizations, narrow kerf with high perpendicularity can be achieved and the cut can be made with the highest speed. If

the polarization is in angle to the cut, the absorption happens more in the sides of the cut and this leads to wider kerf with tapered sides which are depending of the angel of cutting direction and the plane of polarization. [1; 11]

Table 3: Different types polarizations adapted from [23].

Laser beam polarization type	Schematic view	Designation in the text
Plane polarization, an electrical vector is parallel to the beam velocity vector		P
Plane polarization, an electrical vector is perpendicular to the beam velocity vector		S
Circular polarization		C
Azimuthal polarization		A
Radial polarization		R

To the polarization can be effected with optical devices to uniform circularly polarized beam from linear polarized beam. With this linear polarized beam, compromised uniformed kerf width can be achieved at expense of cutting speed. [1; 11]

5.2 Process parameters

The process parameters are changeable by the user/operator before starting the process or during the cutting process. These process parameters are feed rate, used assistant gas and pressure, place of the focus point and continuous wave or pulsed mode for the delivered output power. With alteration of these parameters the cutting quality can be improved the cutting and the wanted results can be achieved. [1; 24]

5.2.1 Pulsed vs. continuous-wave mode

The laser beam can be delivered to the material surface by either pulsed or continuous-wave (CW) mode. The laser is in continuous-wave mode, when the beam's power is continuous and even through time. The pulsed laser's beam is in pulses which are high powered and the pulses are extremely short in time. The CW laser can be used like the

pulsed laser, but the pulsed laser cannot use like the CW laser. With both types, high intensity of the beam can be achieved. [1; 11]

The CW beam is preferred for smooth, high cutting rate applications, particularly with thicker sections. The lower energy pulsed beam is typically used for precision cutting of fine components. Beam with higher pulsed peak energy is used to cut materials which have high thermal conductivity and with complex and narrow geometries. Also, pulsed laser is suitable to make small holes. When using optimized pulse laser, reduced dross formation can be achieved which is suitable feature to some metals like aluminium. Also, optimized pulse laser minimizes the burning effect when cutting mild steels and improves the edge quality. [1; 11]

5.2.2 Focus point, focal length and focal plane position

The focus point is the point where the laser beam is focused with the cutting head's optical lenses (focus optics). The size of the spot is determined by the optical lenses' focal length and it determines the depth of field of the laser beam. Also, smaller spot size is favoring good mode and a shorter wavelength of the beam. [1; 2; 4]

Smaller focus point can be achieved by changing the focal length of the focus optics. For example, with CO₂ laser in TEM₀₀ mode, the laser beam's diameter is 15 mm. Optics with 127 mm focal length produces a spot diameter about 0,15 mm with depth of focus 1 mm. Smaller spot is used with thinner material to achieve good surface quality and smaller kerf. The focal length is usually 80-120 mm with thin material. With thicker material is it recommended to use longer focal length to achieve necessary depth of field around half the plate thickness. Higher power laser machines produce bigger focus point and that how helps to cut thicker materials. [1; 2]

Focal plane position is the focus point's depth into the material. It can be inside, surface or upside of the material's surface. For oxygen cutting, the maximum cutting speed is achieved when the focal plane of the beam is positioned at the plate surface for thin sheets. When cutting thick plates, the focus point should be about one third of the plate thickness below the surface. With the mild steel, the focal plane can also be up from the metal's surface 1 mm to 4 mm depending from the steel's thickness.

For fusion cutting (inert gas), the optimum position to the focal plane is closer to the lower surface on the plate. With this position, wider kerf is achieved allowing larger part of the gas flow to penetrate the kerf and press the molten material away from it. If the focal plane is too high or positioned too far below work piece's surface, the kerf width and recast layer thickness increases to the point where the power intensity falls below to the level required for cutting. [2]

5.2.3 Cutting speed

The cutting speed is the speed which the laser head or the cut piece is moved during the cutting process. The cutting speed (feed rate) is depending from the output power of laser and the assistant gas flow. These parameters must be balanced together. When the cutting speed is increasing, the striation on the cut edge becomes more markable, also the dross is forming more likely on the underside of the plate and the penetration of the laser beam is going to be weaker. On the contrary, when cutting too slow speed, to the edge of the cut is going to get more excessive burning which effect on the edge's quality and increases the width of the heat affected zone (HAZ). In general, the cutting speed for a material is inversely proportional on its thickness. [1; 2]

5.2.4 The process gas

The used gas has five functions during laser cutting. To move molten material away with pressure from the kerf without allowing drops to solidify on the underside. With inert gas like argon (Ar) or nitrogen (N₂) to protect the molten material from oxidation. In active gas cutting (cutting with oxygen) to start the exothermic reaction and maintain it through the cutting process. The process gas protects the cutting optical lenses from spatters, which can harm or destroy the optical lenses. Also, the cutting gas cool the cutting edge with forced convection. This affects to the width of HAZ. The importance of process gas increases with the material thickness. [1; 2]

The gas flow to the cutting place can be changed with increasing or decreasing pressure, changing cutting heads nozzle's diameter or nozzle's type or by moving the cutting head's nozzle further away or nearer the cutting surface. The gas pressure has an effect on the cutting quality. With excess active (oxygen) gas pressure results burning, oxidation and it increases the kerf width. If the gas pressure is too low the molten material is not ejected efficiently through the kerf, it creates dross and eventually a loss of the cutting front. [1]

The oxygen is used in cutting mild steels and stainless steels when high cutting speed is important and secondary important is edge quality and pigmentation of the cut kerf by oxidation and burning. With cutting oxygen, the gas purity is important. Example when cutting 1 mm mild steel it can be cut more quickly by using 99,9 or 99,99% purity oxygen in comparison to the standard oxygen purity of 99,7%. In Figure 23 the purity effects on the cutting speed can be seen. In Figure's 23 diagram is used 800 W laser output power is used with assistant gas pressure 3 bar when cutting 1 mm mild steel. [1; 4]

The nitrogen is commonly used inert gas in cutting because it is relatively inexpensive gas. Nitrogen gas is used to produce high quality cutting edges in such materials like stainless steels and nickel-base alloys. Argon is used when cutting titanium, because it prevents the formation of oxides or brittle titanium nitrides. Pressured air is used in cut-

methods as assistant gas with aluminium, polymers, wood, composites, glass and quartz. [1]

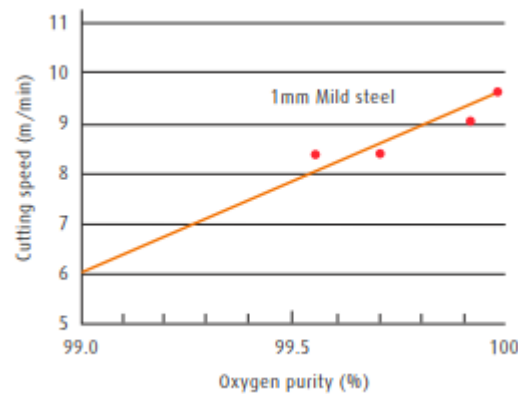


Figure 23: The assistant gas (oxygen) purity effect to the cutting speed adapted from [4].

5.2.5 Cutting head and the nozzle

The cutting head combines the focusing optical lenses and the gas nozzle in to one device, shown in figures 24 and 25. The cutting head also includes mounting points, adjustment screws for the lenses, cooling inlets for water and inlets for assistant gases. Also, the cutting head can be equipped with mechanical or capacitive distance sensor for closed loop control of height to keep the wanted distance from the cut surface. [1; 2; 25]

The cutting head's nozzle primary functions are to ensure, that the process gas flow is coaxial with the laser beam and to stabilize the pressure on the work piece surface. The shape, orientation, alignment and standoff distance of the nozzle effects on the auxiliary gas jet. When the nozzle is correctly chosen, the cutting process quality is increased, because nozzle effects on maximum cutting speed, and dross forming underside the cut edge. The nozzles' have several geometries which can be used for the used application (shown in Figure 26). The nozzles are typically made from copper, because it has low absorption to laser light and high thermal conductivity.[1; 2; 25]

The gas pressure is build up in a chamber below the optical focusing lens. The pressure gauge is installed to measure the stagnation pressure in the chamber. The gas pressure is defined by the stagnation chamber, it is often higher than 0,09 MPa (0,9 bar), which is critical value for air, oxygen and nitrogen. Above this pressure the under expanded gas jet is leaving the nozzle at sonic speed. [1; 2; 25]

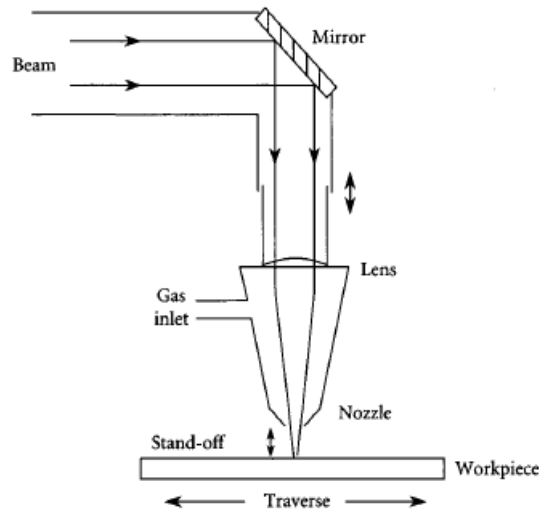


Figure 24: Schematic's of cutting head adapted from [1].



Figure 25: Precitec's Procutter cutting head adapted from [26].

In standard (conical) nozzle the gas is expanding through a circular, narrowing bore which leads to cylindrical exit aperture. The nozzle's orifice ranges between 1 mm and 3 mm and it is chosen according to the material and plate's thickness. If the nozzle is too small, it creates problems to alignment and localizes the gas jet which results rough edge. The nozzle which is too big, do not provide enough gas flow to eject molten material and effects on gas consumption. [1; 2; 25]

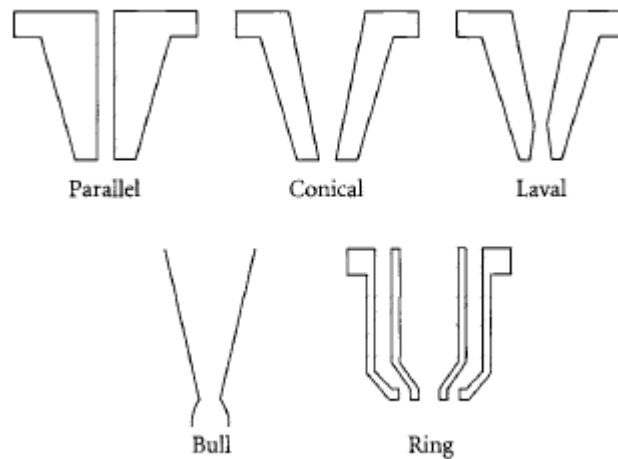


Figure 26: Different kinds of nozzle geometries adapted from [1].

Mostly used cutting head nozzle types in industrial when cutting flat sheets applications have covering profile and cylindrical shape. These nozzles are easy to manufacture and give good results for cut edge. Laval design nozzle delivers higher pressure over larger distances, involving supersonic flow through whole material thickness. With laval nozzle higher cutting speed can be used. Disadvantage to this nozzle type is the smallest cross-section must be adapted to converging beam and so bigger nozzle diameter must be used and this results in higher gas consumption.[1; 2; 25]

The ring nozzle type is used with reactive gas like oxygen to be delivered on to the cutting point to enhance cutting speed or control burr formation, while an inert gas can be introduced at a different pressure on the outer annulus. [1; 2; 25]

5.2.6 Nozzle alignment

The nozzle alignment with the laser beam is effecting on the quality of the cut. The alignment effects on the surface roughness and the eject of the molten material from the kerf (formats dross). If the laser beam and the nozzle are not in alignment, the gas does not flow symmetrically across the top of the cut zone. This may lead undesirable burning and poor edge quality. In Figure 27 is shown effects of misalignment and correctly alignment nozzle. [24]

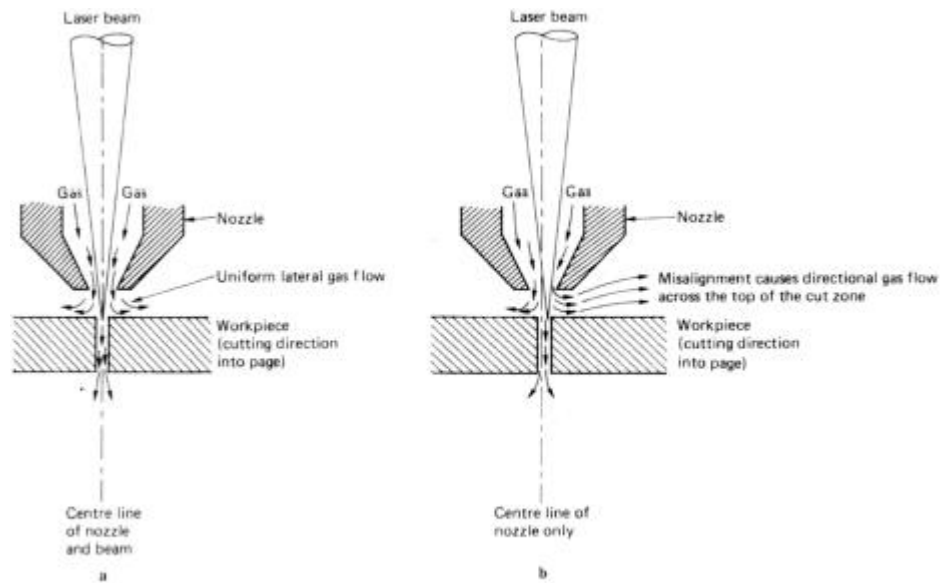


Figure 27: Nozzle alignment effect adapted from[24].

5.2.7 Stand-off distance

The stand-off distance is the distance between the nozzle and the work piece's surface. This is important practical parameter, because this distance effects gas flow patterns which effect directly cutting performance and cut edge quality. The stand-off distance is ranged from 0,5 mm to 2 mm order to minimize turbulence and it also depends from design of the nozzle. Typically, when the nozzle diameter is 0,8 - 3 mm the standoff distance is in range of 0,5 mm to 1,5 mm for the best cutting quality. With short stand-off distance, stable cutting conditions can be achieved, but the risk to damage optical lenses increases, because of the splatters. [1; 4; 24]

5.3 Material parameters

The materials have own properties, which effect on the cutting process. The mechanical properties like tensile and yield strength, hardness, fatigue resistance and ductility do not influence on laser cutting process. As we know the laser cutting is thermal process so the material's thermal properties like melting and vaporizing point, thermal conductivity and specific heat capacity effects on the process. Also, material's optical properties like light absorption and reflection effects on the heating process. Physical properties influence to the process, if there is grease or paint on the surface. The material's thickness effects on the feed rate and the focal points place which effect directly to the surface roughness. [1; 2; 27]

5.3.1 Physical properties

The surface tension and viscosity of the molten material have high influence to the quality of the cut edge and the cutting speed. Molten materials with low viscosity and high surface tension are more difficult to remove from cutting front by the process gas and this leads to formation of the dross underside the cut. [1; 27]

The thickness of the plate determines the relation between the feed rate which cutting can be made and the incident beam power, for given set of processing parameters. Also, if the material has grease or paint on its surface, it may lead to unpredictable performance. For cutting a scale-free surface is desirable, since changes in scale thickness or the presence of rolled-in defects and grooves are detrimental to edge quality. Metal with presence of oxide layer which is thin and uniform can help the laser light to absorb better to the surface and improve the cutting performance. [1; 27]

5.3.2 Thermal properties

The materials with high reflectivity to infrared laser light, such as copper can lead to difficulties with initiation and maintenance of the cutting process. To start cutting process a higher power density is needed, but once the process is started and stabilized the power can be reduced. With high reflectivity of the material, the laser light cannot absorb so well to the material as low reflectivity materials and heats up the material faster. [1]

To maintain the cutting front in the cutting process, either high power levels or slow cutting speed is required, because the heat of the beam is rapidly transported through cutting front with high thermal conductivity. The thermal conductivity is property how fast or slow the heat is conduct across material. This influences how fast is the material is cooling. Materials which have high heat capacity are requiring greater amount of energy to raise their temperature to which is needed to melt the material. [1]

5.4 Laser cutting quality

The laser cutting quality is containing many factors which can be measured, like kerf width, surface roughness, perpendicularity or angularity of the cut edge, accuracy of the cut piece and dross. To standardize measuring and tolerances for cutting quality, European Committee for Standardization has given a standard SFS-EN ISO 9013 to guide these quality parameters for oxyfuel flame cutting, plasma cutting and laser cutting. This standard is applicable to flame cuts from 3 mm to 300 mm, plasma cuts from 1 mm to 150 mm and laser cutting from 0,5 mm to 40 mm. It also includes geometrical product specifications and quality tolerances. In next sections, different standards specification and quality tolerances for laser cutting will be demonstrated. [2; 28]

5.4.1 Kerf width

The kerf width is the width which the beam or flame makes into the material when it is removing molten material from it. The kerf width in laser cutting is depending on laser beam's focus point diameter and position of focal plane. Typically, the kerf width is 0,5 - 1,0 mm in laser cutting. The kerf width is normally narrower at the bottom surface of the cut plate than the top surface. The kerf width is dependent on the plate's thick-ness, so that kerf increases when the plate is getting thicker. With thin material cutting the minimized kerf width is typically preferred. With thick plates the molten material is harder to eject from small kerf, so the larger kerf is preferred. In Figure 28 is shown characteristic properties to cutting. [2; 28]

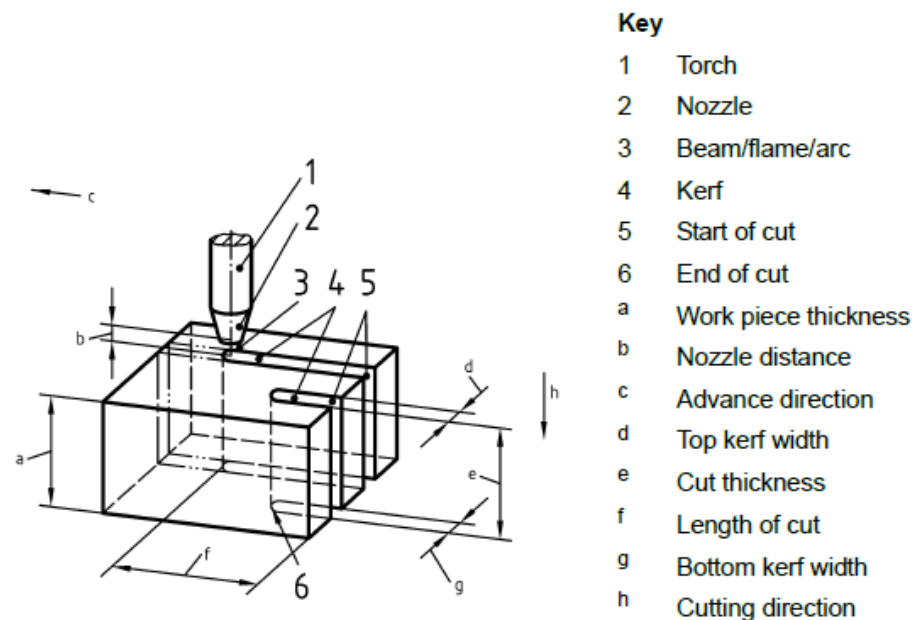


Figure 28: Laser cut terms adapted from[28].

5.4.2 Perpendicularity or angularity of the cut edges

The perpendicularity of the cutting edge result from that the cutting kerf is narrowing to the bottom of the cut. The cutting kerf's edges perpendicularity or angularity u is measured with two straight parallel lines distance each other which the cut surface profile is inscribed and within the set angle. The distance is measured from the actual surface to intended sur-face as Figure 29 shows. Quality classes are defined from in a limited area of the cut surface. From the surface area, the dimension Δa shall be reduced. This area depends on work pieces' thickness allowing at the same time some melting of top edge. [28]

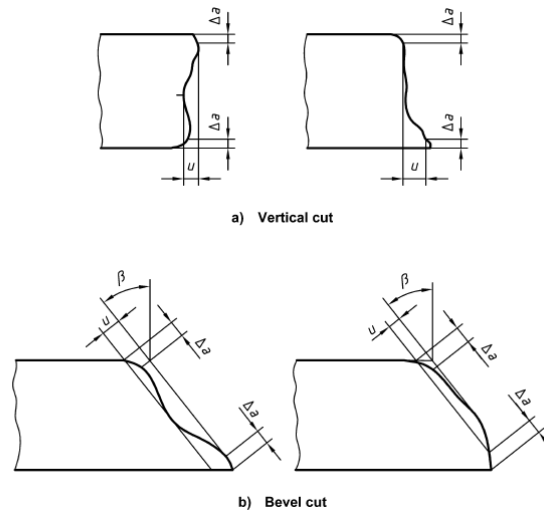


Figure 29: How to measure cut edges perpendicularity or angularity adapted from [28].

5.4.3 Surface roughness

The surface roughness is formed during the laser cutting. The beam cuts to the material parallel ripples from top to bottom of the cut edge and forms the surface roughness. These ripples are technically known as striations and are produced by the beam in its unpulsed mode of operation. The burning cycle which takes place when laser cutting is shown in Figure 30. When striations are closer together the smoother is the surface and if they are apart from each other the surface is rougher. [24; 27]

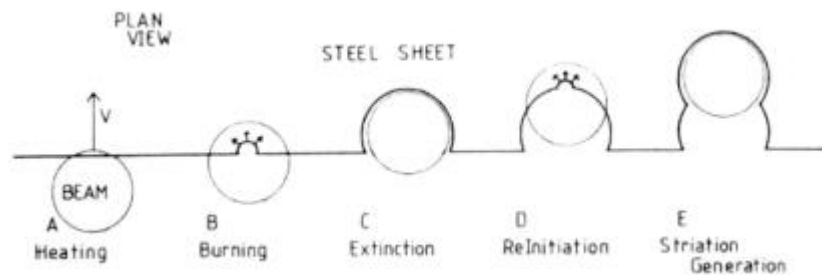
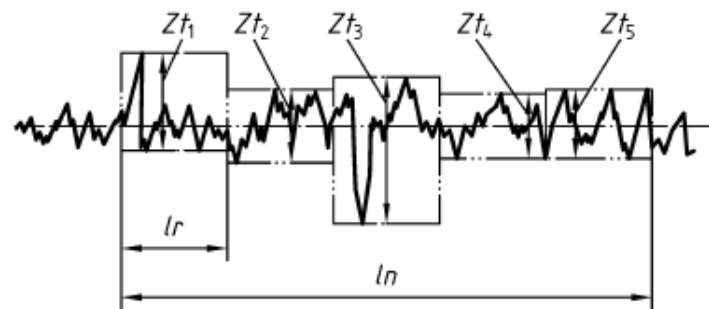


Figure 30: The formatting of striation adapted from [24].

The surface roughness is the irregularity of the surface profile and it can be measured as an integral of the absolute value of roughness profile R_a or as the mean height of the profile R_z . The standard SFS-EN ISO 9013 uses R_{z5} value to measure surface roughness. The R_{z5} value is mean of five sampling length l_r from measurement length (shown in Figure 31). The measurements length is 15 mm, which is divided to five partial measuring lengths (shown in Figure 31). The distance the between highest peak and the lowest valley is determined for each partial measuring length. The R_{z5} value is in micrometers. [1; 27]



where

Zt_1 to Zt_5 represent single profile elements;

ln is the evaluation length;

lr is the single sampling length (1/5 of ln).

Figure 31: Mean height of the profile adapted from [28]

The measurement for the laser cutting is taken from below one third of the top surface and if the work piece thickness is 2 mm or less then it is taken from the center. After measurement, the value is compared to standard diagram (Figures 32 and 33). The diagram shows limits for different roughness quality classes. Standard provides two different graphs for the mean height of the profile one for work piece thickness up to 30 mm and another work piece thickness up to 150 mm. The limit areas can be calculated with standards given formulas which are shown in the Table 4, where a is plates thickness in mm. The standard also gives graph of achievable cutting qualities for different cutting process shown Figure 34. [28]

Table 4: Mean height of the profile Rz 5, adapted from [28].

Range	Mean height of the profile, $Rz5 \mu m$
1	$10 + (0,6a \text{ mm})$
2	$40 + (0,8a \text{ mm})$
3	$70 + (1,2a \text{ mm})$
4	$110 + (1,8a \text{ mm})$

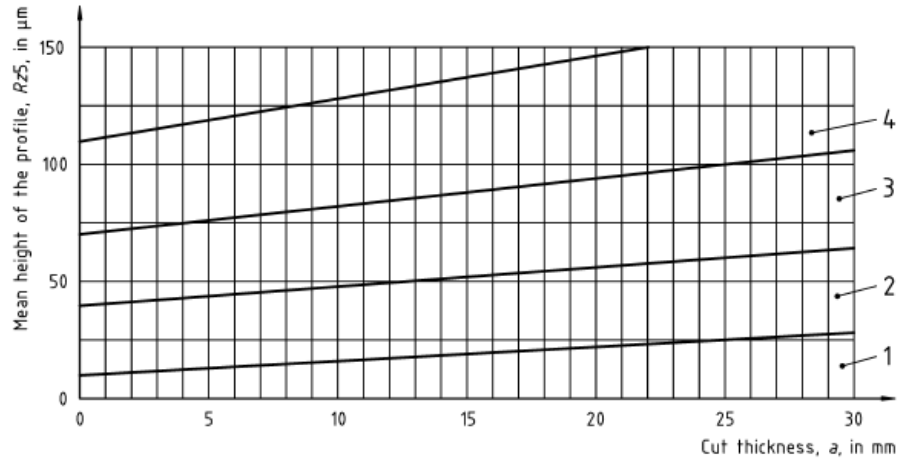


Figure 32: Mean height of the profile, graph for work piece up to 30 mm adapted from [28].

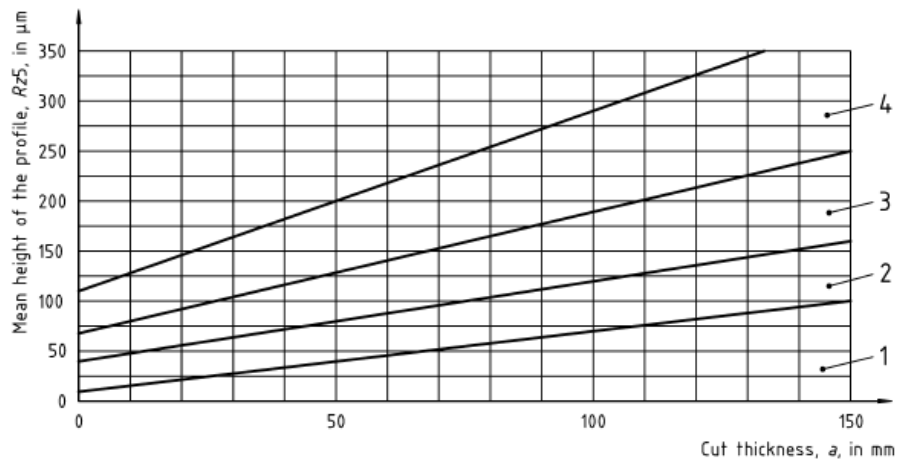


Figure 33: Mean height of the profile, graph for work piece up to 150 mm adapted from [28].

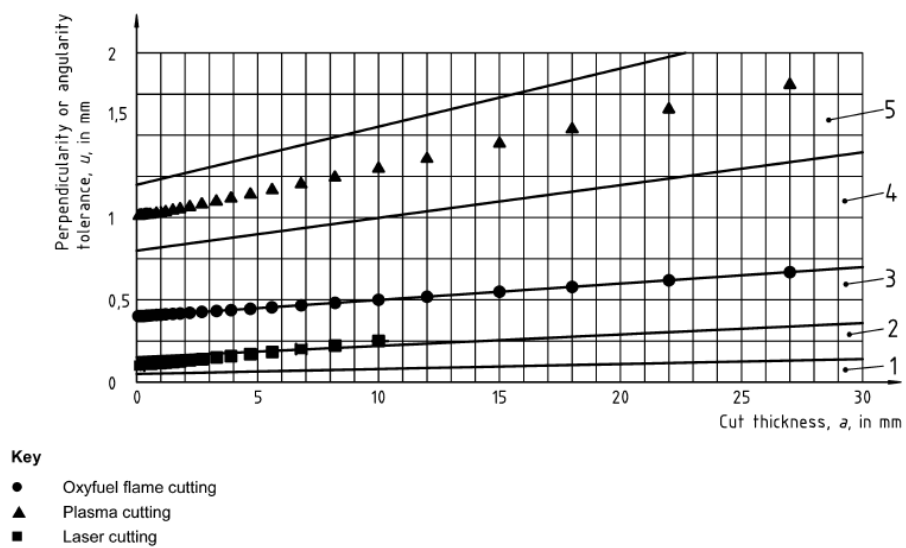


Figure 34: Achievable qualities for different process adapted [28].

5.4.4 Dross

The dross is molten material which is cooled underside on the cut edge. The burr is highly adherent dross (solidified material) or solidified oxides (slag) which forms on underside the cut. The dross is formed if the gas pressure is not enough to eject whole molten material through the kerf or the kerf is not width enough to molten material to flow through it, because of excessive power or slow cutting speed. Molten materials with high values of surface tension and low viscosity are difficult to remove from the cutting front by the used process gas and this can result to dross underside. The dross formation can be blocked or decrease with correctly chosen cutting parameters. The standard does not give any specific limits or values to dross, but mentions that it could be also used as a quality character, because less dross means less after machining. [1; 27; 28]

5.4.5 Heat affected zone width

The heat affected zone (HAZ) is the area of base materials, either metal or thermoplastics, which is not melted during cutting process and has had its microstructure and properties altered by the heat intensive process. The HAZ is shown in Figure 35. The HAZ width is increased as the energy input per unit length and cut thickness increases. The HAZ width is important when the cutting is made near heat sensitive components. Standard does not give any limits to the HAZ, but it is important to recognize during process, because HAZ is often associated with undesirable effects like distortion, surface cracking, embrittlement, decrease in weld ability, decrease in corrosion and fatigue resistance. HAZ width can be affected by the output power and the cutting speed. [1; 28; 29]

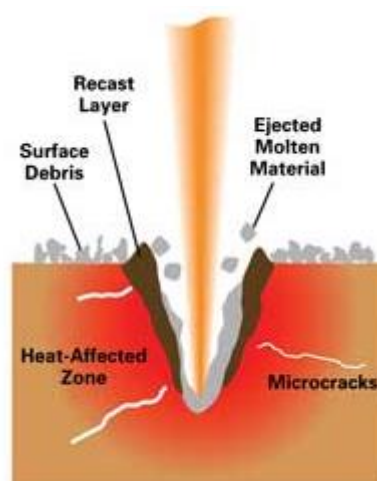


Figure 35: Heat affected zone adapted from [30].

6 TAGUCHI METHOD

Doctor Genichi Taguchi did develop the Taguchi method, which is statistical or robust design method to improve the quality of manufactured goods. These methods have been applied to engineering, biotechnology, marketing and advertising fields. The Taguchi method is divided into three main parts: 1. system design, 2. parameter design and 3. tolerance design. Dr. Taguchi considers the parametric design to be the most important part in this method. This parametric design allows the parameters to be chosen to minimize the effects on performance arising from variation in manufacture, environment and cumulative damage. Taguchi method's primary used tools are orthogonal arrays and methods connect factors to arrays. Interaction between different factors is solved with linear graphs or with Taguchi upper triangular matrix. To analyze the results, is used simple response table or graphical show. With these analyzes, the signal noise ratio (S/N-ratio) or analysis of variance table (ANOVA) can be used to make deeper analyzes. [31]

Taguchi method have been judged by statistician, because the examples which are shown in this method's literature, are fallacious, but even this the method is shown that it works many times and with it can be achieve markable advantages. There are suppositions that the half of the achievements of quality improvement in 1980 Japan are because of the Taguchi method.[31; 32]

6.1 System design

The system design (primary design) is designing, which considers the customer's requirements for the product. For the primary design, it is hard to develop a mathematical equation, because it tries to solve which are the right products for the customers' requirements and the product concepts. The system design tries to combine science from the newest technologies and the innovation of the designers (creativity). [33; 34]

To help designers to take into consideration the needs of the customers and to guide the choices what the designers make. There is used Quality Function Deployment (QFD) as an aid to make these decisions. In QFD (Figure 36) is used different matrices and tables to chance the customer's needs to product specifications. The QFD can be used with or without Taguchi method.[33; 34]

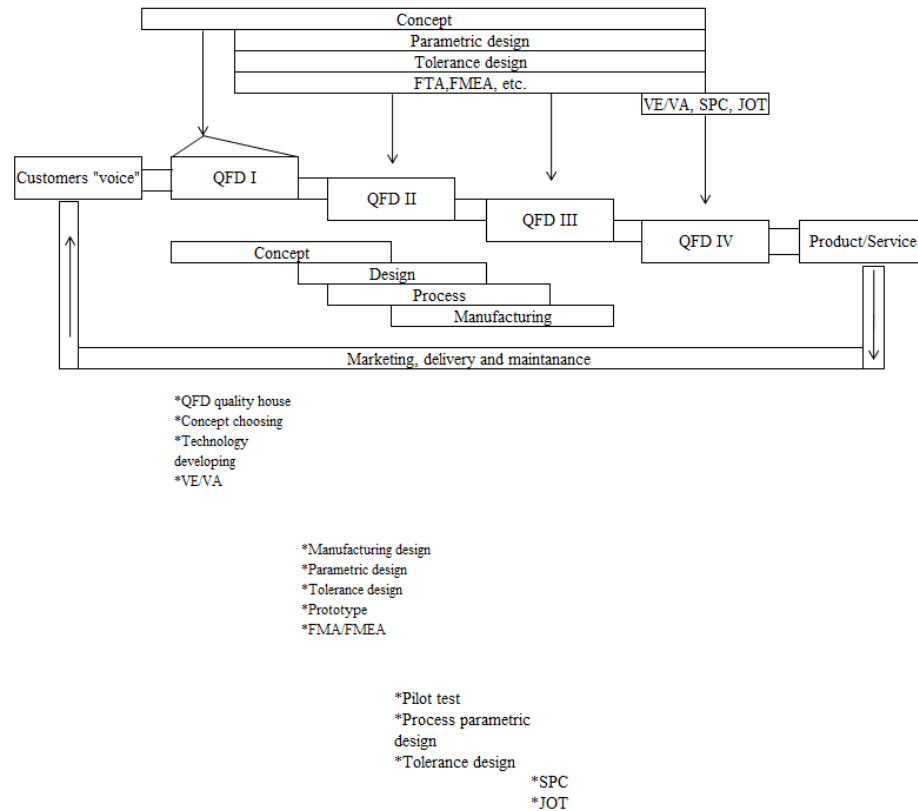


Figure 36: QFD and parametric design adapted from [33]

6.2 Parameter design

The parametric design is essential and the most important part of the Taguchi method. In this part is determined the factor (example materials, measurements which the engineer have been chosen,) values so that it can be achieved with maximal performance (optimizing) and minimizing the distraction from environment (robust design). Also, the achievement should reach with minimum cost for the product. [31]

The aim for the parameter design is:[33]

- Design product or service that it is durable for the interference by choosing optimal parameters.
- The design starts from cheapest and coarse components and materials.
- Variation is minimized without moving out the cause of the variation, because the moving out the fault is costly and in parametric design changing parameters' value does not increase costs.

The parameters are factors which inflict or cause actions or fault. Taguchi divides these parameters into four parts: [35]

- the signal factor, the factor which the operator put into process to get certain output from machine or process
- the control factors are factors which the operator can determine freely like number of registers, insulation, size of air conditioning unit etc.
- the scaling factors are control factors which can be easily controlled to get wanted connection between signal and attribute
- the noise factors are factors/parameters that are beyond the control of the designer like outside temperature, moisture etc.

Orthogonal matrix, linear graphs and upper triangular matrix, analysis of variance and signal-noise ratio are the tools which are used in parametric design. Taguchi mentions that in the parametric design the factor should be chosen so that they are cheap to use and their levels are easy to change during testing. [35]

6.2.1 Signal-noise ratio

During the parameter design, (when making the tests) signal factors are tested by changing noise factor. These combinations are tried to systematically increase the results of measurements variation. By this can be tested signal factors sensitivity to noise factors and find the optimal value for it. [33; 34]

Outside noise factors, which can be changed during test can be one or more factors. Example tolerances +T %, 0%, - T % or different environment conditions like humidity, temperature, reflection, wind, heat, etc. In the Taguchi method is not tried to direct the disturbances reasons, but to find the signal factor parameters which lowers the effect. It is important that during the test is get variation a condition, where the process or product will work. [33; 34]

6.3 Tolerance design

This phase is unnecessary if the needed results are achieved during the system and parametric design. If the needed goals are not achieved, then the tolerance design can be used. The factors used in tolerance design may have been abandoned during parametric design because of high costs. In the tolerance design it is researched, whether these new factors can achieve the needed quality. If this concludes the wanted results, the examination of minimizing the quality response of the factor levels tolerances can be started. [35]

6.4 Orthogonal matrix

In mathematics, an orthogonal matrix is a square matrix with real entries whose columns and rows are orthogonal unit vectors.

$$Q^T Q = Q Q^T = I, \quad (7)$$

where I is the identity matrix. This leads to the equivalent characterization: a matrix Q is orthogonal if its transpose is equal to its inverse:

$$Q^T = Q^{-1}. \quad (8)$$

The orthogonal matrix is used until this day to determine game order in team games. This is used for that the all teams are in equal position. This matrix property is used also in design of experiment. With orthogonal arrays in design of experiments, varied data which is not wanted to blend with each other is collected. [33; 34]

Benefits of using orthogonal matrix in design of experiment are:

- the needed test quantity is lower,
- the factors are in equal state between each other,
- the main factors are distinguishable
- the result is reliable and it can be repeat.[33; 34]

Array's benefit comes more distinguished when using multiple factors in the testing and when they have interdependence with each other. For example, if it is tested thirteen factors in three different state, it means in full factorial testing $13^3=1594322$ test, when using orthogonal matrix there is only 27 test. [33; 34]

6.5 Forming orthogonal matrix

In this method used orthogonal matrices are formed from Roman squares, which are $M \times M$ form and there is not two same number in same column or row. First is same size square connected into Greek-Roman square, after this the number pairs are combined into matrix so that they are orthogonal between each other. In Figure 37. is shown how to combine two 3×3 - square into L9- orthogonal matrix. The name Greek-Roman square comes from that another Roman square is marked with Greek alphabets to separate from each other. After this Greek-Roman squares number pairs are sort that in L9-orthogonal matrix two first column comes in numerical order and column three and four get the number pairs from the Greek-Roman square in the same column. [31]

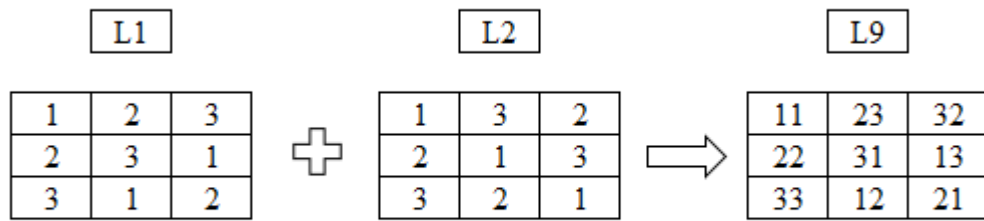


Figure 37: Greek-Roman square formed from two Roman square

The Taguchi methods most used orthogonal matrices are shown most literature in appendix, so deeper matrix forming knowledge is not important and in mathematically their forming are difficult. [31]

6.6 Modifying orthogonal matrices to own demand

Modifying of the matrices are made with under strict orders. The columns can be combined, when a factor is getting more states to research or the columns are deleted if there is not enough factors and interdependence is not wanted to research or there is not interdependence. The deleting of states (dummy technique) is used when some factor has less states than others factors, like if factor have two states and others have three states which are researched. In combination planning two factor which have two states are combined to one three states matrix. Pseudo-parametric planning some parameters are linked together; this is used if some combinations cannot be used. If experiment have factor which have more states than others, so the above-mentioned techniques are cannot be used, then is best to use partly filled planning. [31; 33; 34]

6.7 Linear graphs

The linear graphs tell which column gets the main factors of the experiment. The linear graphs also tell which columns is the interdependence of the factors. For big matrices, there is many linear graphs available. The circles are presenting the main factors and their columns and the lines presents the interaction between them. In Figure 38. is shown two linear graph for L8- orthogonal matrix. [33; 34; 36]



Figure 38: Two linear graphs for L8 matrix adapted from [37]

6.8 Upper triangular matrix

Dr. Taguchi also mentions upper triangular matrix for solving the interaction between different factors. In upper triangular matrix, the column or columns where the interactions are shown are in the same numerical part in upper triangular columns and rows intersections. Example L8 matrix upper triangular matrix shows that the columns two and four, factors interactions are shown in column six (Figure 39). [33; 34]

1	2	3	4	5	6	7
1	3	2	5	4	7	6
	2	1	6	7	4	5
		3	7	6	5	4
			4	1	2	3
				5	3	2
					6	1
						7

Figure 39: L8 orthogonal matrix upper triangular matrix. [35]

6.9 Analyzing results

There are many statistical ways to analyze results. Depending on the situation, can be used perception technique, ranking, column technique, ANOVA, signal-noise ratio (S/N-ratio), arithmetic mean graphs, interaction graphs and response tables. Here is concentrated to response tables, because they are easy to use and make conclusions.[32-34]

A specific factor’s effect on the experiment results is easily shown by calculating response for it. After calculation, the responses values for different factors is marked to the table and then is calculated difference for the same factors different states response values. This way is the most effecting factors states showed for the experiment. The

responses can be mean values or signal-noise ratio values. In Figure 40 is example for imaginary L4- orthogonal matrix experiment calculation for response table. [32-34]

	Factor 1	Factor 2	Factor 3	Result
Test 1	1	1	1	A
Test 2	1	2	2	B
Test 3	2	1	2	C
Test 4	2	2	1	D

State	Factor 1	Factor 2	Factor 3
1	0,5*(A+B)	0,5*(A+C)	0,5*(A+D)
2	0,5*(C+D)	0,5*(B+D)	0,5*(B+C)

Figure 40: L4 experiment plan and response table for it[34]

6.9.1 Signal-noise ratio analyzing

The tests are analyzed with calculating signal-noise ratio for all the tests in the matrices. This S/N ratios formula depends from the studied quality is and what we want with it. There are three different formulas which can be used to analyze signal-noise. [33; 38]

Larger is better is a characteristic value which does not take on negative value and the most wanted value is infinity. The larger is better formula is calculated with formula 9:

$$S/N = -10 \cdot \log \left[\frac{1}{n \cdot \sum_i \left(\frac{1}{y_i^2} \right)} \right] \quad (9),$$

where y_i is one tests results and n is number of test repetitions. In smaller is better the target value is zero and it does not take on negative values. For the smaller is better the formula is:

$$S/N = -10 \cdot \log \left[\frac{1}{n \cdot \sum_i (y_i^2)} \right] \quad (10),$$

where also y_i is one tests results and n is number of test repetitions. The third formula to analyze signal-noise ratio is desired value is the best and it is calculated with formula 11:

$$S/N = 10 \cdot \log [Y_{av}^2 / s^2 - 1/n] \quad (11),$$

where Y_{av} is average value from measurement values, s is standard deviation and n is number of test repetitions. When used, this desired value is best for optimization, there is needed to use either one or two sum statistics value. S/N ratio is quadratic and it is easy to notice. Signal-noise ratio's unit is decibel (dB). You can also make to S/N ratio its own response table. [34; 38]

6.9.2 Analyses of variance (ANOVA)

If analyzing result with response table is not meeting the requirement, then can be used ANOVA (analyses of variance). ANOVA is needed especially when different factors error variance and when is determining the estimated values error variance. In tolerance design the ANOVA is necessary. ANOVA has five states:[32-34]

- First make response table,
- Calculate correction value (means sum of squares) S_m
- Calculate total sum of squares where is subtract correction value
- Calculate factors sum of squares
- Form variance table

For meaningless factors, F- multiplier can be calculated which is then compared to the Fischer distribution tables values. [32-34]

6.10 Studies with Taguchi methods in laser cutting

In “Application of the Taguchi method for optimization of laser cutting” review Madić Miloš and Radovanović Miroslav are studying how the Taguchi method is used in optimization of laser cutting during 2008-2012. In the study, they selected ten different studies for inspection (shown in Table 5). They noticed that in these studies the Taguchi method was used for primarily to identify the robust cutting process parameters and what are mostly effecting parameters to the quality and noise. [39]

Also, they noticed that in most cases multi-objective optimization with the Taguchi method were made. With this method, they were combining the Taguchi method with different techniques like grey relational analysis and weighted sum method to get near optimal solution. In studies were studied kerf width, taper, kerf deviation and surface quality (surface roughness). Also, they noticed that with laser cutting the usability of Taguchi method is limited when studying heat affected zone, burr inclusion or material removal rate. [39]

Taguchi method can be used to study laser cutting, but with some limitations as we can see from the study of Madić Miloš and Radovanović Miroslav. [39]

Table 5: Summary of Taguchi method used studies adapted from [39].

Reference	Laser system	Parameters *	OA	Assist gas	Process performance **	Workpiece material	Multi-response
Pandey and Dubey [21]	Nd:YAG	v, p, p _w , p _f	L ₂₇	O ₂	K _w , K _d	duralumin	yes
Sharma and Yadava [22]	Nd:YAG	v, p, p _w , p _f	L ₉	O ₂	K _t , R _a	aluminium alloy	yes
Dubey and Yadava [23]	Nd:YAG	v, p, p _w , p _f	L ₉	O ₂	K _w , MRR	high silicon-alloy steel	yes
Dubey and Yadava [24]	Nd:YAG	v, p, p _w , p _f	L ₉	O ₂	K _w , K _t , K _d	superni 718	yes
Dubey and Yadava [25]	Nd:YAG	v, p, p _w , p _f	L ₉	O ₂	K _w , K _d	8011 aluminium alloy	yes
Dubey and Yadava [26]	Nd:YAG	v, p, p _w , p _f	L ₉	O ₂	K _t , MRR	8011 aluminium	yes
Rao and Yadava [27]	Nd:YAG	v, p, p _w , p _f	L ₂₇	O ₂	K _w , K _t , K _d	superni 718	yes
Caydaş and Haşçalık [28]	CO ₂	v, P	L ₁₆	O ₂	K _w , R _a , HAZ	St-37	yes
Chen et al. [29]	CO ₂	v, p _f , f, q	L ₉	compressed air	R _a , r	PMMA	yes
El Taweel et al. [30]	CO ₂	v, P, p, d, TEM	L ₁₆	N ₂	K _w , K _t , b	Kevlar-49	no
<p>* v: cutting speed, p: assist gas pressure, p_w: pulse width, p_f: pulse frequency, P: laser power, f: focus position, q: assist gas flow, d: material thickness</p> <p>** K_w: kerf width, K_t: kerf taper, K_d: kerf deviation, R_a: surface roughness, HAZ: heat affected zone, MRR: material removal rate, r: optical transmittance ratio, b: burr height</p>							

7 CASE STUDY

This paragraph solves what and how the testing of the thesis was done and what were the test results. Here is also introduced the laser source and the testing facility. Also in this part is the introduction of Corelase Oy.

7.1 Corelase Oy

Corelase Oy is midrange company which provides wide range solutions for laser industry. Their lasers are used in annealing, cutting, drilling, welding and surface coating. The wide range of products of fiber and diode pumped lasers are sold directly to end users and integrators. Corelase Oy has wide range of experience and know-how from the field of various laser processing applications so it can provide good service to their customers in their problems. Company is located at Tampere, Finland at Rusko's industry area. Corelase Oy was found 2003 and it became part of Rofin Group by an acquisition at 2007. In 2016, it became part of Coherent-group. Corelase has 53 employees at their service [40; 41]

7.2 Test environment

The tests are made in Tampere University of Technology's Laser Application Laboratory (LAL), which provides needed premises, robots and needed process gases for this thesis work. The test environment contains Fanuc robot which operates the cutting table and it can be driven in all three axels by programming. There is also another robot from KUKA to hold the Precitec's cutting head. This robot can be programmed and moved, but it was used only little in this work. Also, the environment included water cooling system for the laser source and the cutting head.

7.2.1 Corelase's ARM® fiber laser

ARM® (Adjustable Ring Mode) fiber laser is Corelase's new fiber laser source which was released at 2015. The fiber laser does not have any moving parts, because it is based on all-fiber design and up to 2 kW single oscillator. The patented technology of ARM® creates dynamic ring mode which can be adjusted on-the-fly. The ARM® is designed for processing highly reflective material. Applications for this fiber laser are welding, cutting, drilling, heat treatment, cladding and many more. [42]

The ARM® laser provides two different laser beams through one fiber cable. The shape of the outer laser beam is circle and the inners shape is a spot. These beams output power can be changed individually from 0 to maximum power shown in Figure 41. The la-

ser used in these tests had output power 6 kW to outer ring and 2 kW to the inner spot. Benefits which can be achieved with this kind of laser, are piercing power, high cutting quality, thickness up to 30 mm and ability to cut any metal even high reflective metals. In welding the benefits are reduced hardening effect, melting of filler wire with ring beam combined with key hole welding with center beam and relaxed mechanical tolerances with butt welding. [42]

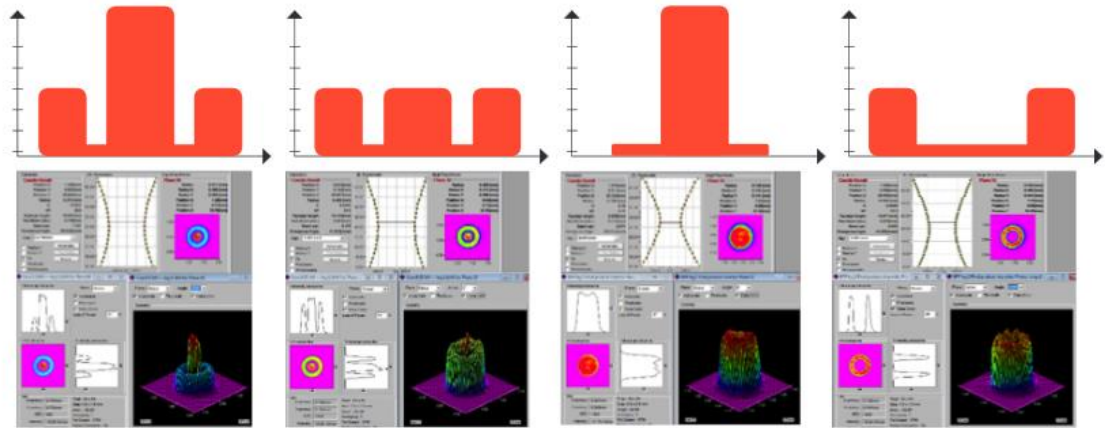


Figure 41: ARM laser's beam shapes adapted from [42].

The tested laser source's technical specifications are shown in Table 6.

Table 6: Tested ARM lasers specifications

ARM Specifications			
	Center	Ring	
Maximum output power	2000	6000	W
Center wavelength	1070±5		nm

7.2.2 Precitec Procutter cutting head

Precitec's Procutter (shown in Figure 42) what is made for solid-state laser cutting. For the monitoring the cutting head's parameters (temperature, pressures for cutting gas and inside cutting head, optics and errors) Precitec provides Procutter app for android. Cutting head's technical data is listed under: [26]

- max. laser power 6 kW with wave lengths of 1030-1090 nm
- focal length collimation FC: 100 mm
- Focal lengths FF: 125 mm, 150 mm, 175 mm, and 200 mm (in this cutting head it was 175 mm)
- N_Amax: 0,13 at FC100

- Vertical adjustment range: FC100/FF125: +6 mm/ -9 mm; FC100/FF150: +9 mm/ - 13 mm; FC100/FF175: +12 mm / -18 mm; FC100/FF200: +15 mm / -20 mm
- Dimensions (WxD): 92x115 mm
- weight 4,2 kg (straight version. FF 12 mm)

The used focal length of the collimation lens was 100 mm and the focusing length was 175 mm. With these lenses, the focus position could be move between +12 mm to -18 mm. To adjust the vertical position of the focal plane manual adjustable power supply was used and the pulsed beams were made with two different manual pulse generators.



Figure 42: Precitec's Procutter cutting head adapted from[26].

7.3 The tested metals

The metals which were selected for the tests was mild steel, stainless steel, aluminium and copper. These materials were selected because they are commonly used in different area of industry where the laser cutting is used. The mild steel was structural steel S355K2G3. The tested thicknesses were 5 mm, 15 mm and 20 mm. The chemical composition and mechanical properties for S355K2G3 mild steel are shown in the Tables 7 and 8.

Table 7:Chemical composition for S355K2G3 mild steel adapted from [43]

Chemical composition

Grade	C %	Si %	Mn %	P %	S %	N%	Cu %
S355K2G3	0,23-0,24	0,550	1,600	0,025	0,025	-	0,550

Table 8: Mechanical properties for S355K2G3 adapted from [43]**Mechanical properties in typical room temperature:**

	Rm (MPa)	Re (MPa)
S355K2G3	510-680	355

The stainless steel was AK Steel type 304, which is their variation from basic 18-8 grade, (type 302) with a higher chromium and lower carbon content. The tested thicknesses were 10mm and 15 mm. AK steel type 304 is covered by these specifications: AMS 5513, ASTM A 240 and ASTM A 666. The mechanical and physical properties are shown in the Table 9.:

Table 9: Type 304 stainless steel's mechanical and physical properties adapted from [44].**Mechanical properties in typical room temperature:**

	Rm (MPa)	Re (MPa)	Hardness Rockwell
Type 304	586	241	B80

Physical properties:

Density	8,03	g/cm ³
Specific heat capacity (0-100 °C)	0,5	kJ/kg*K
Thermal conductivity 100 °C	16,2	W/m*K
Thermal conductivity 500 °C	12,4	W/m*K
Modulus of Elasticity in torsion	78*10 ³	MPa
Modulus of Elasticity in tension	193*10 ³	MPa

The aluminium was Klöckner & Co AW-6082 grade aluminium. The properties are shown in the Tables 10. and 11. The tested thickness were 15 mm and 20 mm.

Table 10: *Aluminium's mechanical and physical properties adapted from [45].***Mechanical properties in typical room temperature:**

	Rm (MPa)	Re (MPa)	Hardness Brinell
AW-6082	275	244	84

Physical properties:

Density	2,07	g/cm ³
Thermal conductivity	150-170	W/m*K

Table 11: *Chemical composition from the aluminium.***Aluminium EN AW-6082 Chemical composition**

Element	Si	Fe	Cu	Mn	Mg	Cr	Ni	Zn	Ti
min. wt. %	0,7			0,4	0,6				
max. wt. %	1,3	0,5	0,1	1	1,2	0,25	0,25	0,2	0,1

The copper was MKM Manfelder Kupfer und Messing GmbH CU-OF (EN 1652 1997) copper and it was tested in thicknesses 6 mm, 10 mm and 15 mm. These kinds of coppers have typically properties of hydrogen-resistance, very high conductivity and easy to weld. The copper's chemical composition and mechanical properties are shown in Table 12.

Table 12: *Copper's chemical composition and mechanical properties adapted [46].***Chemical composition:**

Cu	Pb	Bi
99,99478 %	0,00015%	0,00003%

Mechanical properties in typical room temperature:

	Rm (MPa)	Rp0,2 (MPa)
Cu-OF	255	220

7.4 The testing parameters for the metals

The testing parameters to Taguchi orthogonal matrix were chosen in co-operation with Corelase Oy. The chosen parameters were assistant gas pressure, feed rate, focus position, nozzle diameter, nozzle's distance from the surface, center and ring beams' output powers and center and ring beams' frequency. These parameters have an influence on the surface quality. There were also fixed parameters: nozzle's distance from the test pieces' surface (specific materials), duty cycle (if the modulation of the beam was used), and the assistant gas type. The fixed parameters did change over by the thickness and the material which were cut. The used parameters are varying by the tested specimens thickness and material, because the same parameter combination which cuts 15 mm stainless steel won't cut 15 mm mild steel. The parameter's value ranges for different metals are shown in the Tables 13-16. The precise test parameters are shown in conclusions for each metal.

Table 13: Mild steel's testing parameters

Mild steel S355K2G3		
Assistant gas	Oxygen, Nitrogen (5 mm)	
Assistant gas pressure	0.5-1 (18-22 for 5 mm)	bar
Feed rate	5 - 25	mm/s
Nozzle diameter	1 - 3	mm
Focal planes position	depends on the thickness	
Center beam output power	0 - 2	kW
Ring beam output power	0 - 6	kW
Center beams frequency	CW,2000,5000	Hz
Ring beams frequency	CW,2000,5000	Hz
Duty cycle (fixed)	50%	%
Nozzles distance from surface	0,5 - 1	mm

Table 14:Stainless steel's testing parameters

Stainless steel type 304 from AK Steel		
Assistant gas	Nitrogen	
Assistant gas pressure	18 -22	bar
Feed rate	9 – 17	mm/s
Nozzle diameter	2 -3	mm
Focus position	depends on the thickness	
Center beam output power	1,25 – 2	kW
Ring beam output power	3,5 – 6	kW
Center beams frequency	CW	Hz
Ring beams frequency	CW	Hz
Duty cycle (fixed)	-	%
Nozzles distance from surface	0,4;0,5;0,6;0,75;1	mm

*Table 15: Copper's testing parameters***Copper CU-OF**

Assistant gas	Oxygen	
Assistant gas pressure	16 - 20	bar
Feed rate	2 -35	mm/s
Nozzle diameter	1,5 -3	mm
Focus position	depends on the thickness	mm
Center beam output power	1,6 – 2	kW
Ring beam output power	5,2 – 6	kW
Center beams frequency	CW, 1000, 5000	Hz
Ring beams frequency	CW, 1000, 5000	Hz
Duty cycle (fixed)	75	%
Nozzles distance from surface (fixed)	1	mm

*Table 16: Aluminium's testing parameters***Aluminium AW-6082**

Assistant gas	Nitrogen	
Assistant gas pressure	16 - 22	bar
Feed rate	2-9	mm/s
Nozzle diameter	1,5-3	mm
Focus position	-17 - -9	mm
Center beam output power	2	kW
Ring beam output power	6	kW
Center beams frequency	CW,1000, 2000	Hz
Ring beams frequency (fixed)	CW	Hz
Duty cycle (fixed)	75	%
Nozzles distance from surface (fixed)	1, 2	mm

The Taguchi orthogonal matrices were based on these parameters and their combinations. For the different parameters three different parametric levels were chosen which were tested in the Taguchi orthogonal matrix. The three levels were selected depending on the levels combination which would cut the metal and so provide different kind of results which could be seen in the tests.

7.5 Cutting the metals and measurements

The tests were made with only one laser source and one cutting head. The focus optics or laser source components were not changed during the tests. The cutting was made from right to left and the cutting length was approximately 50 mm. The cut started always outside of the material and it finished outside of the material. This was done be-

cause was wanted to ensure, that the laser was on before entering the material itself and to ensure that all other testing parameters were correct before the cut started (example gas pressure). The nozzle's distance from the surface of the piece was measured with calipers to ensure that it is constant through all tests. The focal plane's position was adjusted with manual power supply. With Precitec's Procutter application was used to measure the correct focal plane position.

The Laser Application Laboratory provided the measurement instruments and needed programs to measure studied parameters for this master thesis. For measuring the surface roughness there were used the Taylor- Hobson Surtronic 3+ measurement tool (Figure 43) and the Digital Surf's MountainsMap® Premium 5.1 Surface imaging & analysis program. The raw data from the surface roughness measurement tool was imported via RS232 cable to the program where the needed analysis were made. The measurement tools technical data is shown in the Table 15. The stylus which was used in the measurements was 112/1502: diamond tip with radius 5 μm .



Figure 43: Taylor - Hobson Surtronic 3+ surface roughness measurement tool. [47]

Table 17: Taylor-Hobson Surtronic 3+ technical data [48].

Technical Data

Gauge range	$\pm 150 \mu\text{m}$
Resolution	$0,01 \mu\text{m}$
Transverse length	min. 0,25 mm; max. 25,4 mm
Pick up type	Variable reluctance
Stylus	112/1502: Diamond tip radius $5\mu\text{m}$ 112/1503: Diamond tip radius $10\mu\text{m}$
Parameters	Ra, Rz, Rz (DIN), Ry, Sm, Rt
Traverse speed	1 mm/s
Accuracy of Parameters	2 % of reading + LSD μm

The surface roughness was measured three times using three points near surface (about 1 mm from the surface), middle of the piece and near bottom (about 1 mm from the bottom surface). The tests were made with standard SFS-EN ISO 9013 instructions; the method is described in chapter 5.4.3. Before measurements, the instruments were calibrated by the instructions with the reference specimen type 112/1534 which have $R_a = 6$.

The kerf opening angle was measured from all tested materials (for thicknesses 15 mm and 20 mm). This was measured by using Mahr coordinate measuring machine from the cut side of the test piece.

7.6 Test results

This chapter introduces the test result for surface roughness and their effect. The test result does not include the Taguchi noise factors and are only based on the average response tables. The dross formation result is based on observations only. The cut edges angularity was also measured for three best surface roughness result for each 15 mm and 20 mm thick test piece. The test result graphs for all materials are from average response tables and the smaller the value the better. The calculation formula (Formula 12). for these values is:

$$a_i = \frac{\sum_{j=1}^n Y_j}{n} - Y \quad (12)$$

where a_i is calculated difference between general mean value and parameters' one level's mean value (effect), n is number of values and Y is general mean value for parameter values. These values are shown in the figures as roughness and its unit is micrometer (μm).

Because the test results parameter levels were limited to only in three levels, it cannot be said how the parameters effect on the result in between the levels or before or after the level.

7.7 Mild steel

The mild steel was tested with thicknesses 5 mm, 15 mm and 20 mm to show that the test setup could cut different thicknesses with different operation gas without changing any parts of the cutting system. The test was made by using Taguchi table L27. The mild steel cutting with oxygen is a very sensitive process which was noticed during testing. You need to find the correct combination of laser parameters to achieve even the penetration through the whole thickness. This is easier with thinner materials and the cutting window narrows when going to thicker plates. The tests show that which parameters are the most effecting to the cutting edge's surface roughness. Nitrogen cutting

was not as sensitive to the fluctuation of parameters, but these cuts were made only with one thickness (5 mm), so with thicker plates the effect can be seen differently.

7.7.1 5 mm mild steel

Overall the cutting processes were clean and there was no fluctuation of the process during the change of the test parameters. 5 mm was cut with high pressure nitrogen. There was clean and bright cut surface and oxidation did not appear like in oxygen cutting. The tested parameters and their values are show in the Table 18.

Table 18: 5 mm mild steel's test parameters.

Test parameters

	1	2	3
Assistant gas pressure (bar)	18	20	22
Feed rate (mm/s)	15	20	25
Nozzle diameter (mm)	1,5	2	2,5
Focus spot's position (mm)	2	3	4
Power of the spot (kW)	1,5	1,75	2
Power of the ring (kW)	2	2,25	2,5
Modulus of the ring (Hz)	CW	2000	5000
Nozzle's distance from the surface (mm)	0,5	0,75	1

The assistant gas pressure (Figure 44) shows that the higher pressure is better for the middle and lower part of the piece. Lower pressure was better for the upper edge. This shows that, the gas diameter which comes from the nozzle grows on the surface when increasing the pressure and gives worse surface to upper edge, but better roughness to lower edges, because the molten material flow out more easily.

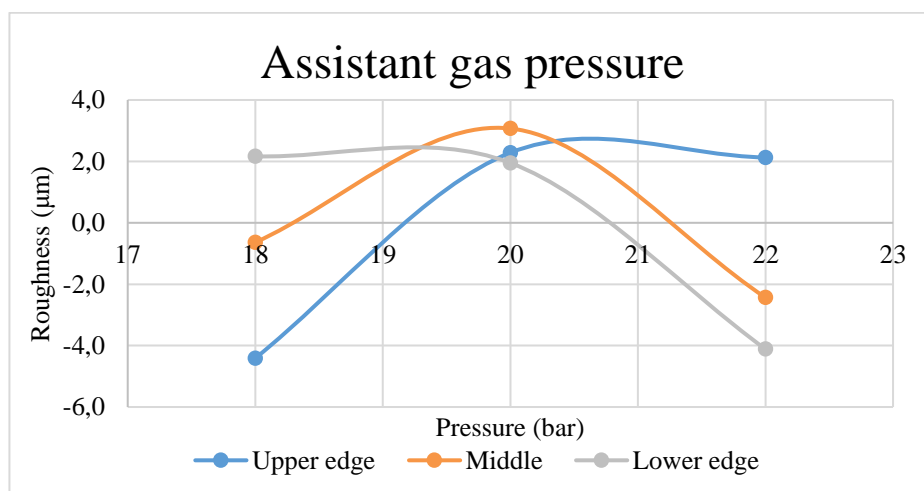


Figure 44: Assistant gas pressure's impact to the surface roughness.

The feed rate values were 15 mm/s, 20 mm/s and 25 mm/s and the test shows that the highest feed rate performs the best when observing the roughness of the cut edge's (shown in the Figure 45). The graphs lines are almost linear, so with these output powers there might be enough power to increase the feed rate or could drop some overall output power down instead.

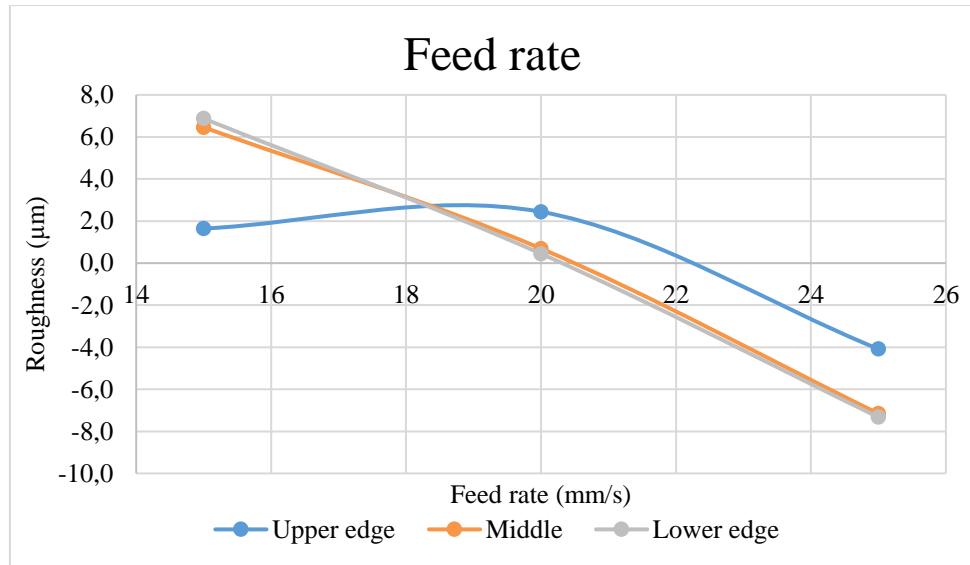


Figure 45: Feed rate's impact to roughness.

The output powers of spot and ring (the figures 46 and 47) show the same as the feed rate indicates: that the process can be driven with less energy from the laser source to achieve good quality of cutting or instead the feed rate could be risen from 25 mm/s (1,5 m/min). There is a suggestion that the ring's output power could be higher (2 kW → 2,25 kW) to achieve this. The overall output power is ranged from 3,5 kW (1,5+2 kW) to 3,75 kW (1,5+2,25 kW). The optimal value is near these output powers for the feed rate of 25 mm/s.

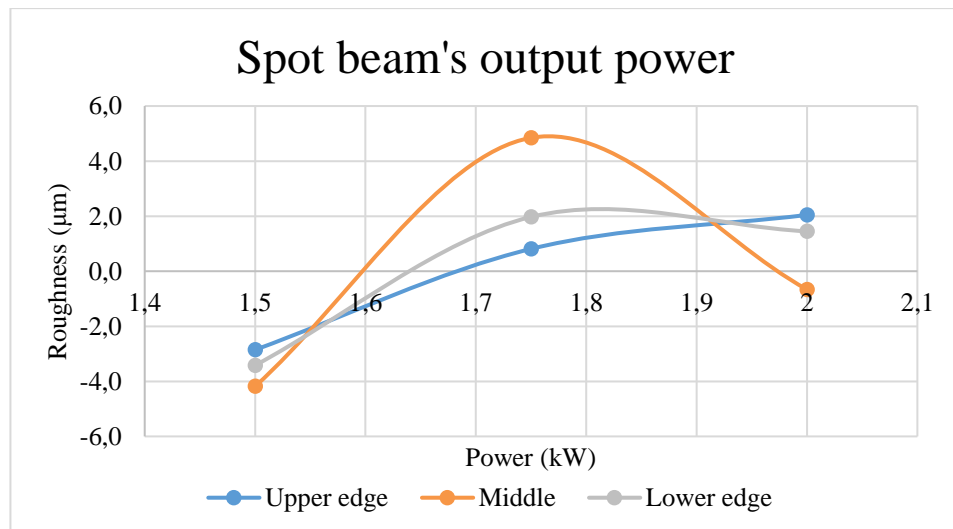


Figure 46: Spot beam's output powers effect.

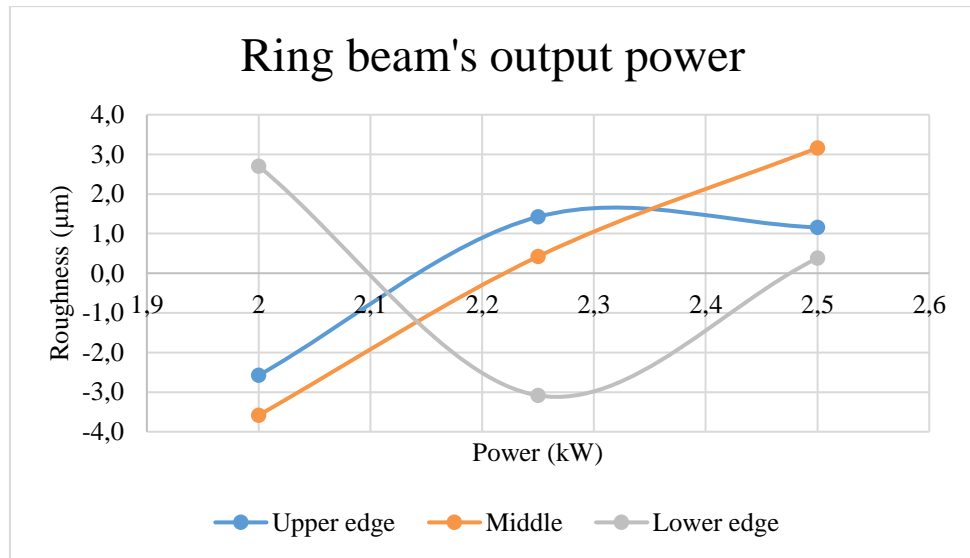


Figure 47: Ring beam's powers effect to different parts.

The modulation's effect on the surface roughness is not very big, except for the lower part of the piece. Figure 48 shows that the higher modulation frequency gives better roughness than the continuous wave mode. This tells the same as the feed rate and the output powers: the process could use less energy or the cutting speed could increase with CW mode.

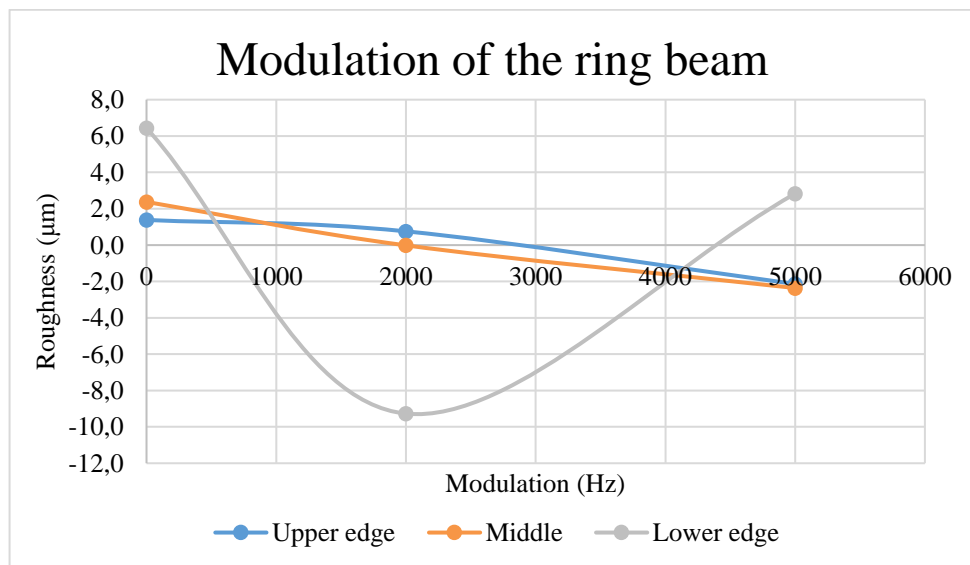


Figure 48: Ring beam's modulation. Value 0 means CW mode in this figure.

The optimal value for the focal plane's position was +3 mm which was shown by tests calculations (Figure 49). The +2 mm and +4 mm values were worse than the optimal value. The graph from the test shows that the value could be a little smaller than +3, but to confirm that, more testing is required.

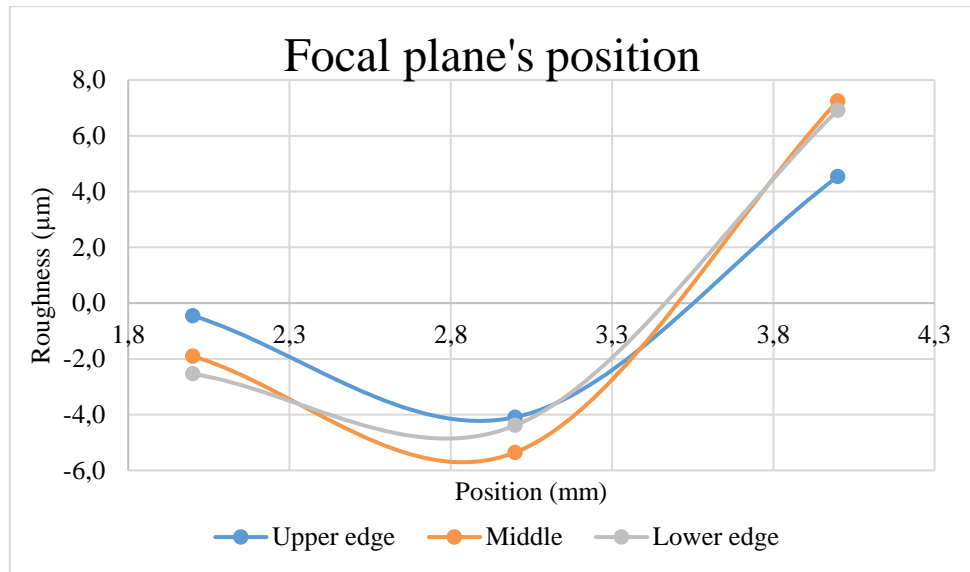


Figure 49: Focal plane's position effect.

The nozzle diameter tests show that the biggest (2,5 mm) nozzle gives the best performance for the surface roughness (Figure 50). This tells that there is need for higher gas flow to the molten material to remove it from the kerf and to achieve good quality. Also, the lines' shape indicates that larger diameter could be used with these pressures and this assistant gas to achieve better surface roughness.

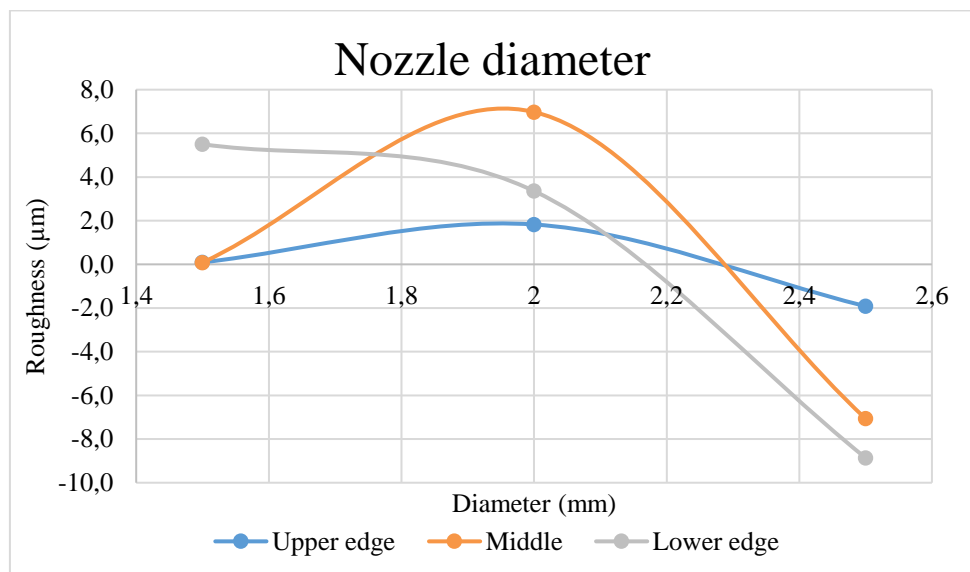


Figure 50: Nozzle diameter's impact to the surface roughness with 5 mm mild steel.

The nozzle should be near the surface. The test shows (Figure 51) that distance of 0,5 mm gives the best value and when going higher the roughness rises. This is due the gas flow's diameter, which increases when going higher and then it removes bigger diameter the molten material from the kerf.

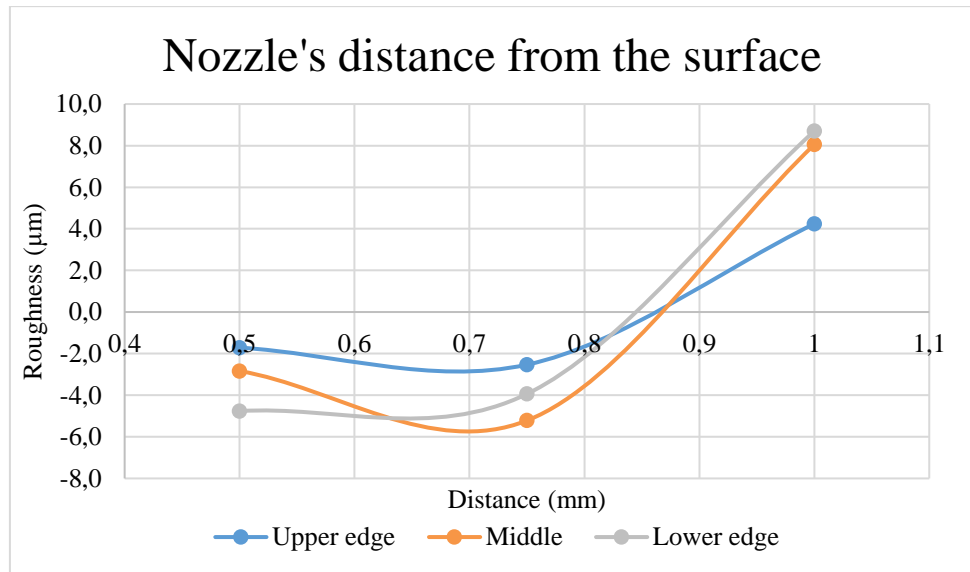


Figure 51: Nozzle's distance from the surface.

The Taguchi table and the calculations resulted in almost identical cutting parameters for all surfaces (upper, middle and lower). Only the gas pressure increased from 18 bar to 22 bar and the modulation of the ring changed from 5000 Hz to 2000 Hz and the distance of the nozzle from the surface from 0,75 mm to 0,5 mm. The suggested parameters are shown in the Table 18. The Taguchi response table's parameter groups performed identically with the test groups. The Taguchi parameters performed better in their own area as they should. Figure 52 shows the Taguchi tables parameters groups different cutting edges. In the figure, the order of the tables parameter sets is from left to right upper, middle and lower edge (lower edge has two parameters sets). For the lower edge the Taguchi table resulted in two parameters sets where the only change was the ring's output power modification from 2 kW to 2,25 kW.

Table 19: Taguchi tables recommended parameters.

	Assistant gas pressure (bar)	Feed rate (mm/s)	Nozzle diameter (mm)	Focus spot (mm)	Power of the spot (kW)	Power of the ring (kW)	Modulus of the ring (Hz)	Nozzle distance (mm)
Upper edge	18	25	2,5	3	1,5	2	5000	0,75
Middle	22	25	2,5	3	1,5	2	5000	0,75
Lower edge	22	25	2,5	3	1,5	2 or 2,25	2000	0,5

As we can see from the selected parameters (Table 19.) the cutting window is quite narrow which gives smooth roughness for the surface. From these three parameters groups the overall best surface roughness was achieved with the middle part's parameters, but

all were very near each other and even better in own area. With the best parameter set was achieved the surface roughness quality class of 2. The achieved overall surface roughness average values were for:

- the upper edge set 36,5 μm
- the middle part set 34,2 μm
- the lower edge with output power of 2 kW set 36 μm
- the lower edge with output power of 2,25 kW set 35,7 μm

To the dross formation to the underside of the cut edge was noticed that the correlation of nozzle diameter, the nozzles distance from the surface and the assistant gas pressure are affecting it. With the nozzle and high pressure near, the surface the dross formation was less than if the pressure was lower and the nozzle smaller.

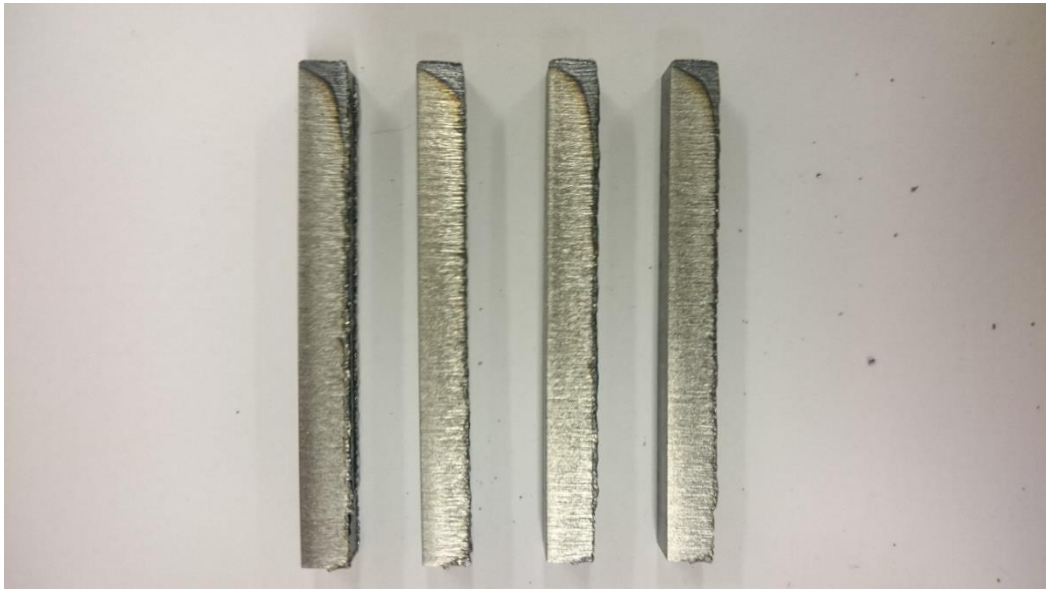


Figure 52: Taguchi response table's cut edges.

7.7.2 15 mm mild steel

The actual process was clean and stable, but some tested parameter groups were unstable due excess energy which comes for too high oxygen pressure or too much energy from the laser beam. This affected the formation of the striation of the surface. There were deep and wide lines throughout the cut surface in some cases. The 15 mm mild steel was cut by using oxygen gas with low pressure. The test parameters are shown in the Table 20.

Table 20: 15 mm mild steel's test parameters.**Test parameters**

	1	2	3
Assistant gas pressure (bar)	0,6	0,8	1
Feed rate (mm/s)	8	10	12
Nozzle's diameter (mm)	2	2,5	3
Focus spot's position (mm)	3	4	5
Power of the spot (W)	0	200	400
Power of the ring (W)	2700	3000	3300
Modulus of the spot (Hz)	CW	2000	5000
Nozzle's distance from the surface (mm)	0,8	1	1,2

The gas pressure (Figure 53) did show similar effect on all the cut edge's parts. That the higher the pressure, the roughness rose. This is due that the excess oxygen burns during the process and brings more energy and heat into the process. So, there were deeper and wider lines on the surface.

The feed rate showed that with these output powers (2700→3700 W), the fastest feed rate gives the best results in the lower and middle parts, but the upper edges roughness rose. The upper edge is better when the feed rate is 10 mm/s (0,6 m/min), but the surface roughness changes when the feed rate increasing to 12 mm/s (Figure 54). There might be room to increase the feed rate with these output powers.

The output power of the ring shows difference in different parts of the cut edge, like that the lower and middle parts need more power to achieve better roughness. But the upper part needs 10% less power to achieve better roughness. When observing the output power of the spot, the effect is opposite to the ring's output power. The lower part does not need power from it, the middle part needs there to be a little more power (200 W) at the spot. The upper part's surface roughness shows that there must be more output power from the spot (Figure 55). The modulation of the spot beam helped to achieve better surface roughness with the lower and middle parts, but the upper edge preferred CW mode. The frequency of 2000 Hz gave better surface roughness quality than the 5000 Hz to the middle part. The lower part did benefit from the frequency of 5000 Hz. Both frequencies gave the upper edge higher roughness value than the CW mode.

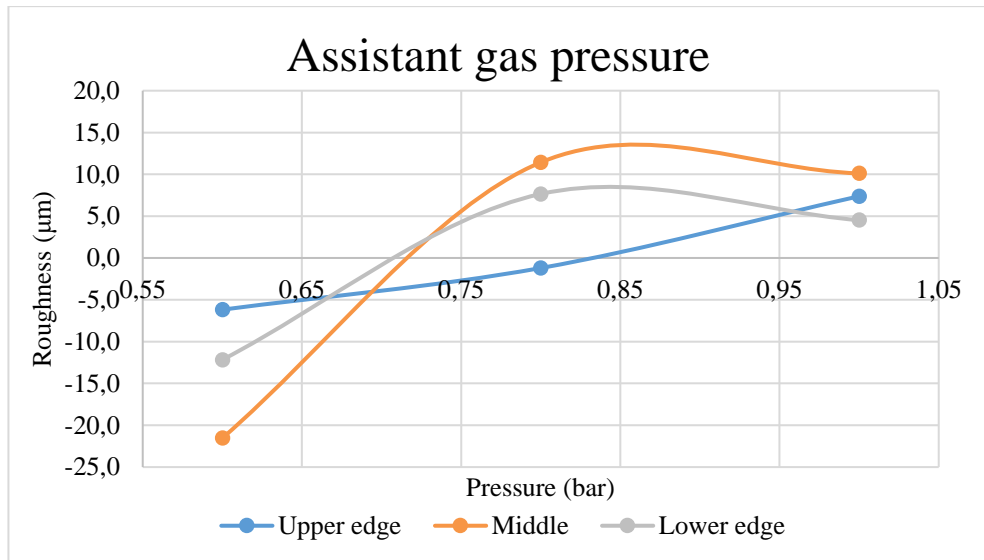


Figure 53: Assistant gas pressure.

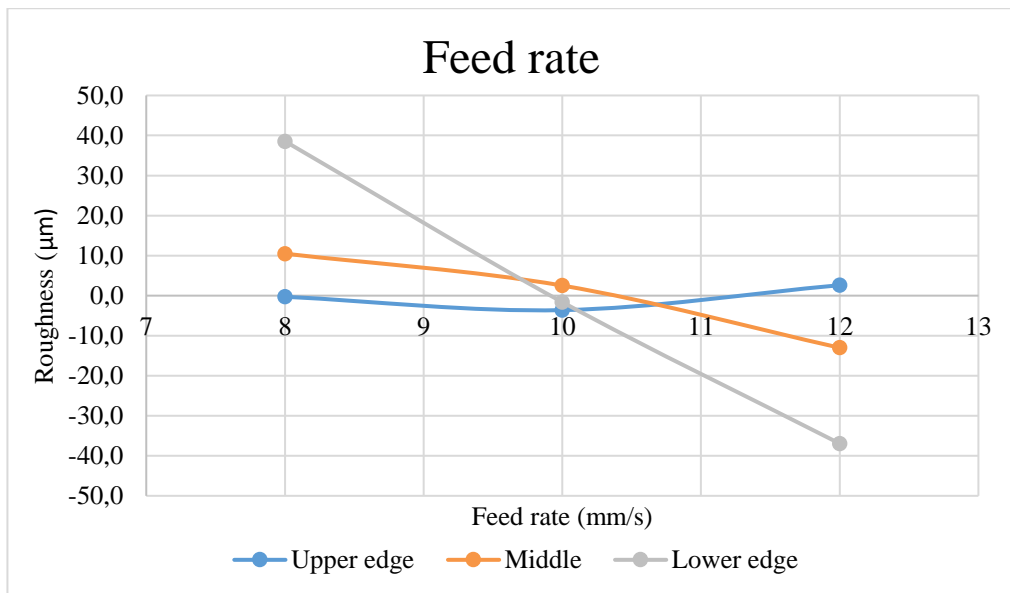


Figure 54: Feed rate.

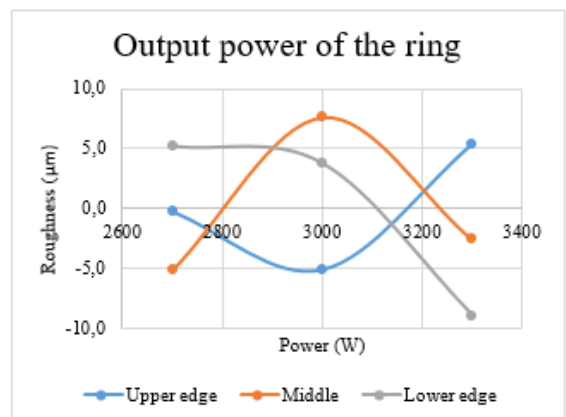
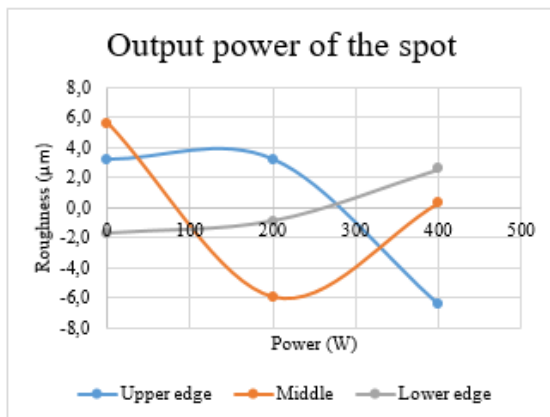


Figure 55: Spot and ring beams' ouput powers impact.

The focal plane position was tested +3, +4 and +5 mm for this thickness. Test showed that the optimal value is between the values of +3 mm and +4 mm. The lower edge did benefit from the bigger value (Figure 56). This might be due the molten materials diameter which is bigger and the molten material flows out more easily from the wider kerf than from smaller kerf.

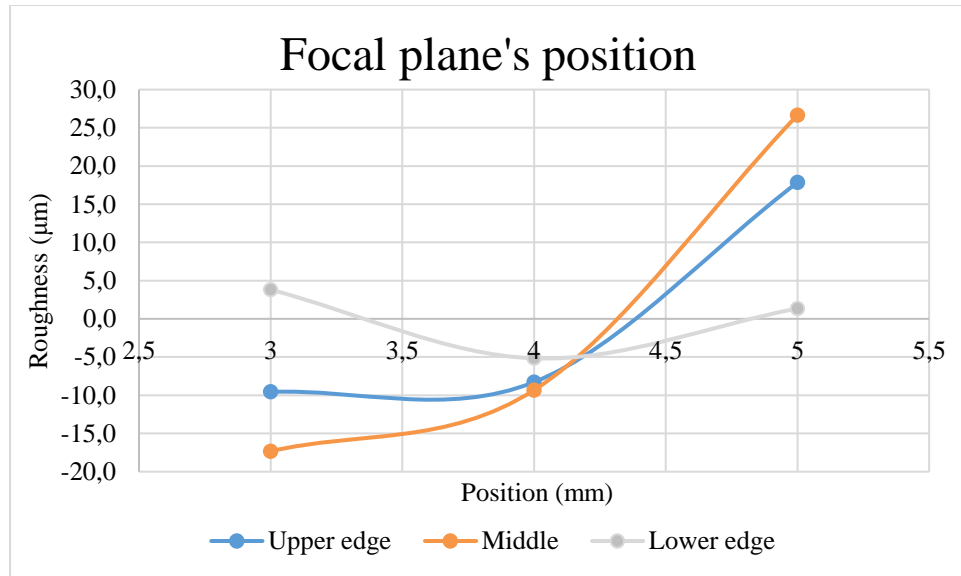


Figure 56: Focal plane's positions.

The nozzle diameter for the upper edge should be smaller (2 mm) than for the middle and lower parts (2,5 mm) of the cut edge (shown in Figure 57). But the 3 mm nozzle gives almost equal surface roughness value for the upper part like 2 mm nozzle. The 3 mm nozzle increases the surface roughness value for the lower and middle part. The nozzle should be near the surface (Figure 57), because of the low gas pressure. This is because the oxygen can help better that way to take part into the burning process and help the molten material flow away from the kerf.

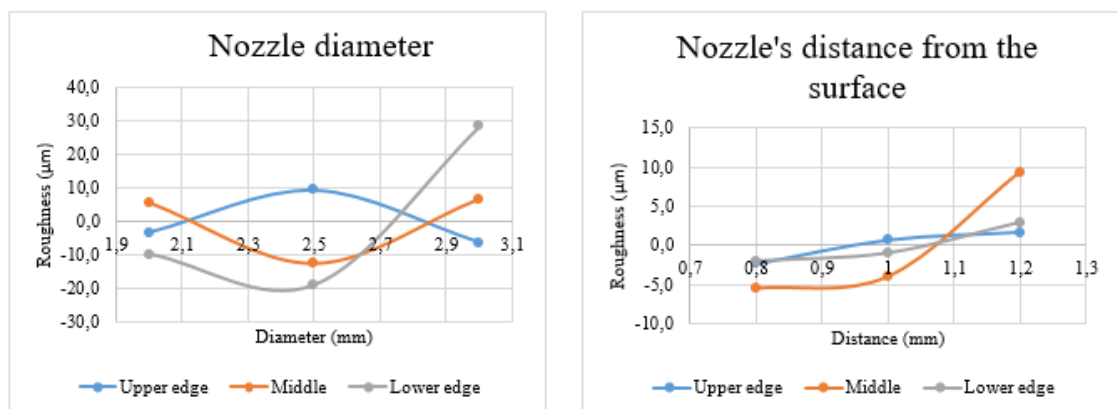


Figure 57: Nozzle's diameter and distances from the surface.

Table 21 shows calculated values for different parts of surface from Taguchi. The best overall average surface roughness of the table's parameter groups was the lower edges surface parameter group, but other two were better in their own areas. With the best parameters set, the surface roughness quality class of 2 was achieved. The Taguchi table's cutting edge are shown in Figure 58.

Table 21: Calculated parameter values for different areas.

	Assistant gas pressure (bar)	Feed rate (mm/s)	Nozzle diameter (mm)	Focus spot (mm)	Power of the spot (W)	Power of the ring (W)	Modulus of the spot (Hz)	Modulus of the ring (Hz)	Spot duty cycle	Nozzle distance (mm)
Upper edge	0,6	10	3	3	400	3000	CW	CW	50 %	0,8
Middle part	0,6	12	2,5	3	200	2700	2000	CW	50 %	0,8
Lower edge	0,6	12	2,5	4	0	3300	5000	CW	50 %	0,8

With the Taguchi table's parameter sets overall surface roughness average values were achieved with:

- the upper edge set 85,76 μm
- the middle part set 65,61 μm
- the lower edge set 52,72 μm

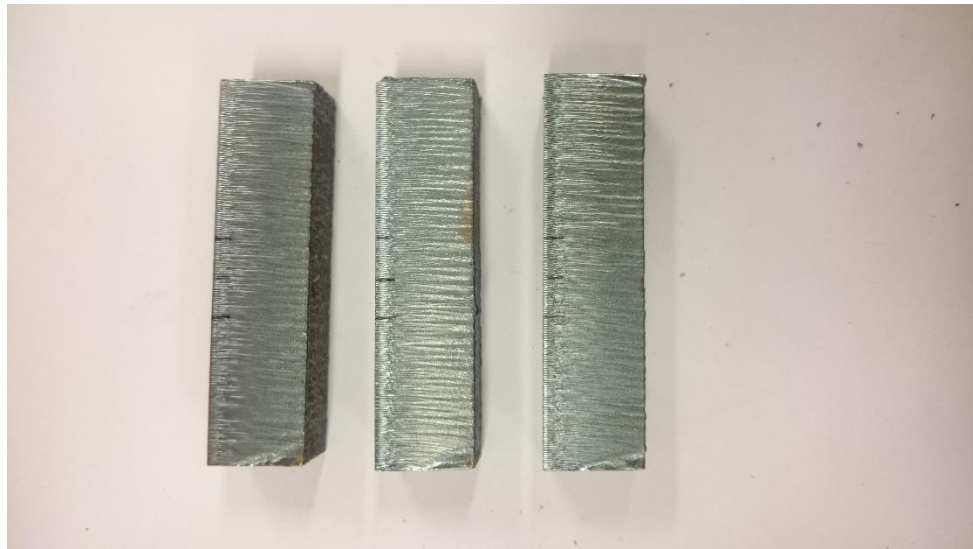


Figure 58: The Taguchi table's cut edges. From left to right: upper edge, middle edge and lower edge.

7.7.3 20 mm mild steel

When, cutting the 20 mm mild steel with this setup the limitation of the cutting head's focus lenses was almost reached. We could not achieve enough big focus spot on the surface and it did lead to that the some of the parameters group did not even penetrate the whole thickness, so they had to twist loose with pliers from the other side. But we also get some results which penetrate through the hole thickness. The test parameters and their values are shown in the Table 22.

Table 22: 20 mm mild steel's test parameters.

Test parameters

	1	2	3
Assistant gas pressure (bar)	0,5	0,6	0,7
Feed rate (mm/s)	8	10	12
Nozzle's diameter (mm)	2	2,5	3
Focus spot's position (mm)	4,5	5	5,5
Power of the spot (kW)	800	900	1000
Power of the ring (kW)	1800	2000	2200
Modulus of the spot (Hz)	CW	1000	5000
Modulus of the ring (Hz)	CW	1000	5000
Nozzle's distance from the surface (mm)	1,3	1,5	1,7

The assistant gas pressure change between the test values made little change, but not very significant. The optimal value is around 0,5 bar to 0,6 bars. The pressure with correct the nozzle had bigger impact on the surface roughness, because too small a diameter did not give enough oxygen to the burning area and the piece did stick together lower part of cut edge. The biggest nozzle give too much oxygen to the surface to burn and format striation which were wide and deep. The optimal for this thickness was 2,5 mm diameter nozzle (Figure 58) which gave all parts good surface quality. Also, the nozzle distance change did effect the surface roughness (Figure 59). The optimal value was up 1,5 mm from the surface. The 1,3 mm and 1,7 mm increased the surface roughness upper and lower part, but the 1,7 mm gave better results to the middle part.

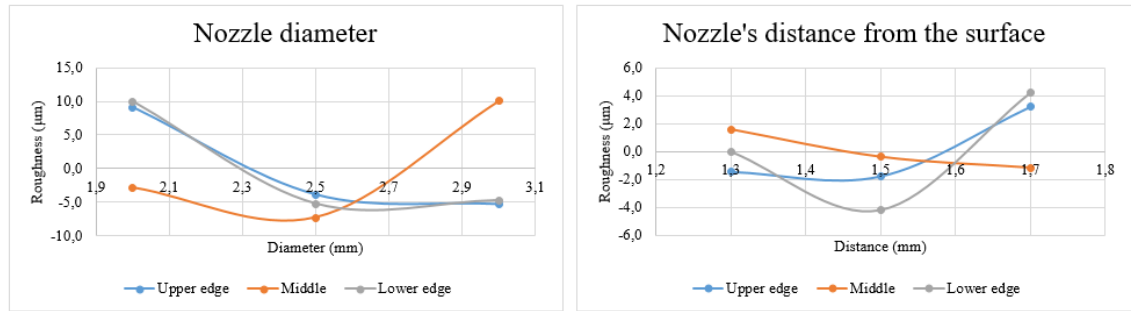


Figure 59: Nozzle diameter and its distance from surface and their effect on the roughness.

The focal plane's position optimal value was + 4,5 mm from the surface for the upper and middle part. +5,5 mm perform little bit better in the lower edge than + 4,5 mm, but the change was minor between those values (Figure 60). It could be explained through measurement inaccuracy. The change was more significant with the lower and middle parts roughness when the values changed.

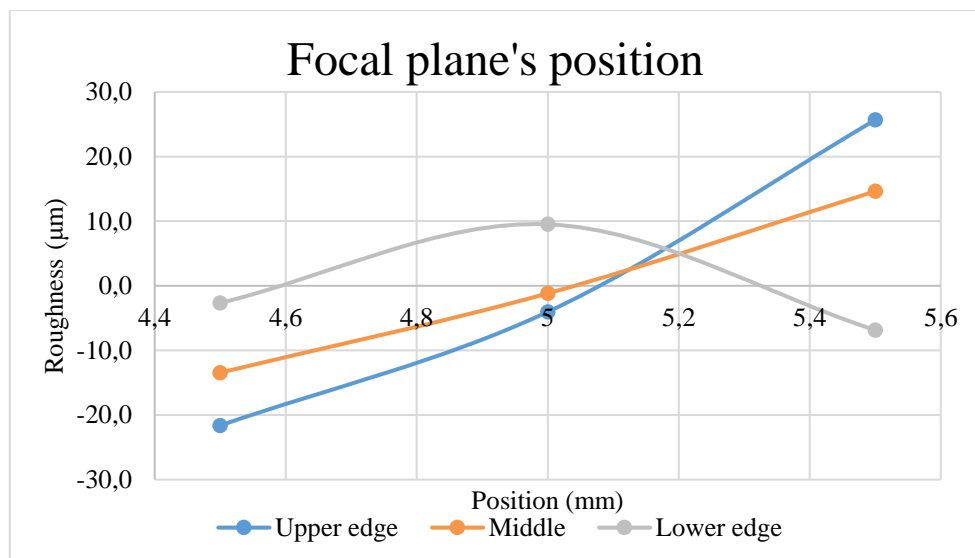


Figure 60: Focal plane's positions effect.

The feed rate's optimal value was 12 mm/s. The graph was almost linear throughout all the cut edge parts (Figure 61). The output power of the ring beam shows that the lowest value (1800 W) is optimal for this thickness for all parts (shown in the Figure 62). The ring beam's modulation showed that a 1000 Hz and 5000 Hz has a lowering effect on the surface roughness with the lower edge, but 5000 Hz gives almost the same or higher value than the CW for the upper and middle parts (Figure 62).

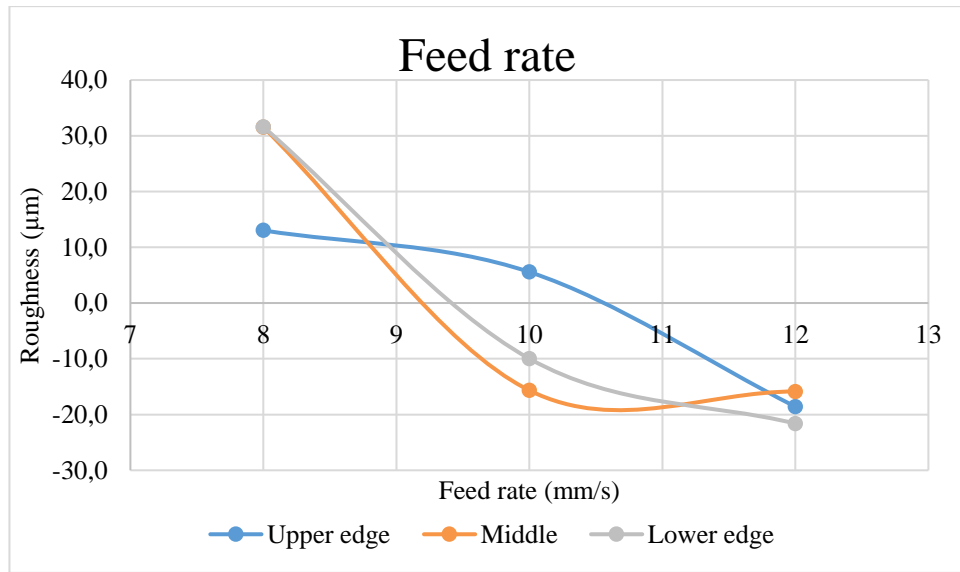


Figure 61: Feed rate's effect to 20 mm cut edge.

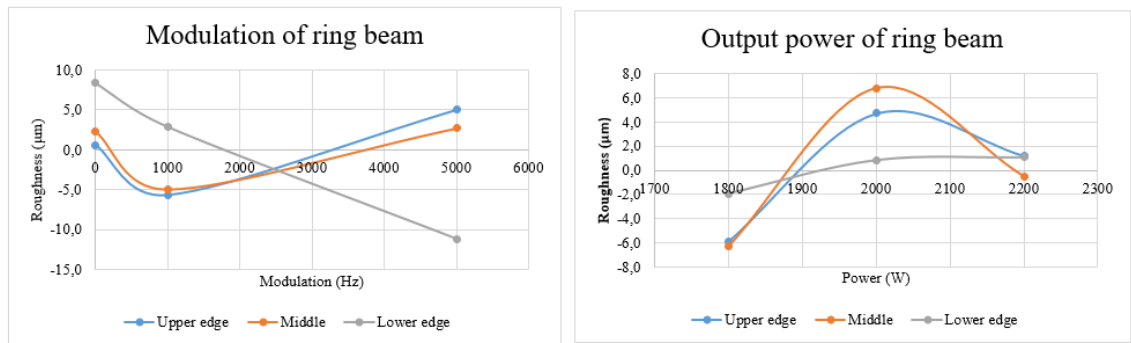


Figure 62: Ring beam's output power and the modulation's effect.

The spot beam's output power graph showed that it is better to have less power in the spot beam to achieve better surface roughness. Also, the modulation of ring beams gave benefit for the surface roughness. But opposite to the ring beam's modulation. 5000 Hz did give better quality to lower and middle part and the 1000 Hz to the upper part.

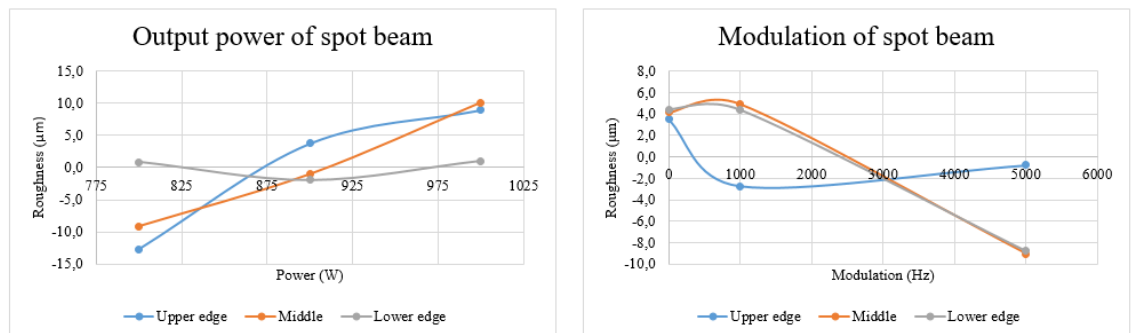


Figure 63: Spot beam's output power and modulation's effect.

Table 23: Taguchi tables suggested cutting parameters.

	Assistant gas pressure (bar)	Feed rate (mm)	Nozzle diameter (mm)	Focus spot (mm)	Power of the spot (W)	Power of the ring (W)	Modulus of the spot (Hz)	Modulus of the ring (Hz)	Nozzle distance (mm)
Upper edge	0,5	12	2,5	4,5	800	1800	1000	1000	1,5
Middle	0,5	12	2,5	4,5	800	1800	5000	1000	1,7
Lower edge	0,6	12	2,5	5,5	900	1800	5000	5000	1,5

The Taguchi tables suggested cutting parameters (Table 23) did not give wanted result, because our Taguchi table did not take full penetration to consideration. So, we did go back to test table and did choose three best overall and fully penetrated cutting parameter groups for this thickness (they are shown in Table 24). The chosen one showed that the feed rate should be slower and pressure of the assistant gas should be 0,1 bar higher, nozzle diameter should be the biggest and overall power (spot + ring) should be approximately 100-200 watts higher when comparing the Taguchi table (Table 23) and the chosen three cutting parameter table (Table 24) These parameters in Table 24 did not format dress on the underside of the cut edge. The table 24 cut edges are shown in Figure 64. With the best parameters set, we achieved surface roughness quality class of 3. With the better cutting parameter sets were achieved overall surface average values for:

- the first set 57,6 μm
- the second set 60,9 μm
- the third set 65,2 μm

Table 24: Three best overall surface roughness cutting parameter groups.

	Assistant gas pressure (bar)	Feed rate (mm)	Nozzle diameter (mm)	Focus spot (mm)	Power of the spot (W)	Power of the ring (W)	Modulus of the spot (Hz)	Modulus of the ring (Hz)	Nozzle distance (mm)
First	0,6	10	3	4,5	800	2000	5000	1000	1,7
Second	0,6	10	3	4,5	900	2200	CW	5000	1,3
Third	0,6	10	3	4,5	1000	1800	1000	CW	1,5



Figure 64: Picture from the best results (from left to right 1-3).

7.8 Stainless steel

The test was made by using Taguchi table L18. The test setup was the same as the mild steel cutting. The stainless steel cutting process with correct values was clean and stable (stable splatter) and the cutting edge was clear and flat. The process was not so unstable and as delicate the oxygen cutting.

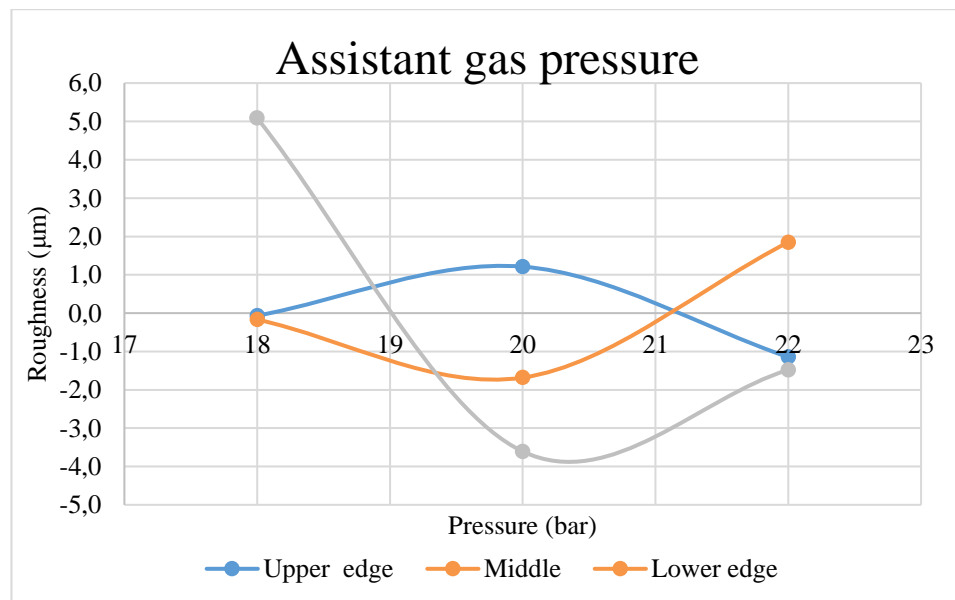
7.8.1 10 mm stainless steel

The whole test range from the Taguchi table parameters gave good surface roughness and flat surface to do measurements. Full penetration of the laser beams (spot and ring) was achieved with all parameter groups. The formation of dross had small changes with the parameter groups. That's why it is hard to say what kind of effect has each parameter change. The measured surface roughness values were very near each other with some tested parameter. It is hard to say which is better, because of the measurement inaccuracy is need to be taken into consideration. The test parameters and their values are shown in the Table 25.

Table 25: 10 mm stainless steel's test parameters.**Test parameters**

	1	2	3
Assistant gas pressure (bar)	18	20	22
Feed rate (mm/s)	13	15	17
Nozzle's diameter (mm)	2	2,5	3
Focus spot's position (mm)	-7	-7,5	-8
Power of the spot (W)	1250	1500	1750
Power of the ring (W)	3500	3750	4000
Nozzle's distance from the surface (mm)	0,5	0,75	1

The assistant gas pressure's test results show that the higher pressure gave better result for the surface roughness (Figure 65). The upper edge did benefit from the 2 mm nozzle, the middle from the 2,5 mm and the lower part from the 3 mm nozzle (Figure 66). Because when using larger nozzle, the kerf size gets bigger and makes then the surface rougher at the upper edge, but smoother in the lower part and opposite with the smaller nozzle. The nozzle's distance from the surface showed in tests that the nozzle should be near the surface to achieve smoother cut edge (Figure 66). This is due that the nitrogen is shielding the surface from the air (burning/oxidation) and it has higher and stable flow to drive molten material through the kerf.

**Figure 65:** Assistant gas pressure's impact.

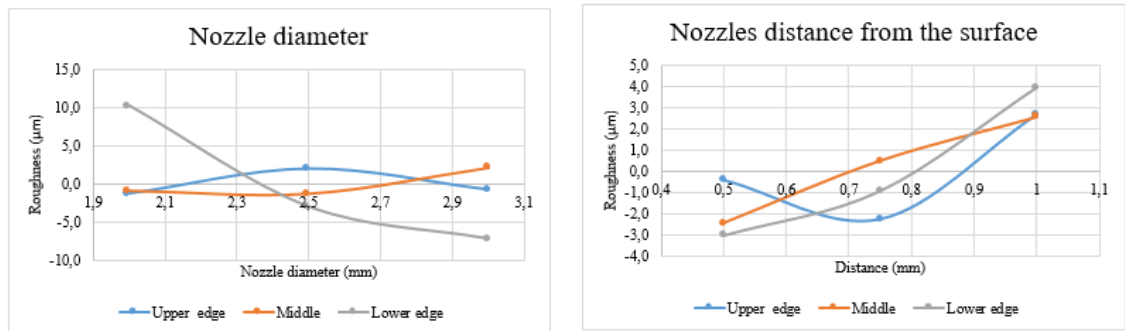


Figure 66: Nozzle diameter's and its distance from the surface

The focal plane's position place got one optimal value, but every cut edge get its own value. The upper edge benefit from the highest value; the middle part did benefit when the focal plane was in the deepest position and the lower did get its best values when the focal position was in the middle value. The achieved values are so near each other that it is nearly impossible to say which parameter value is the best. The parameter values should have larger gap between them that better result could be achieved.

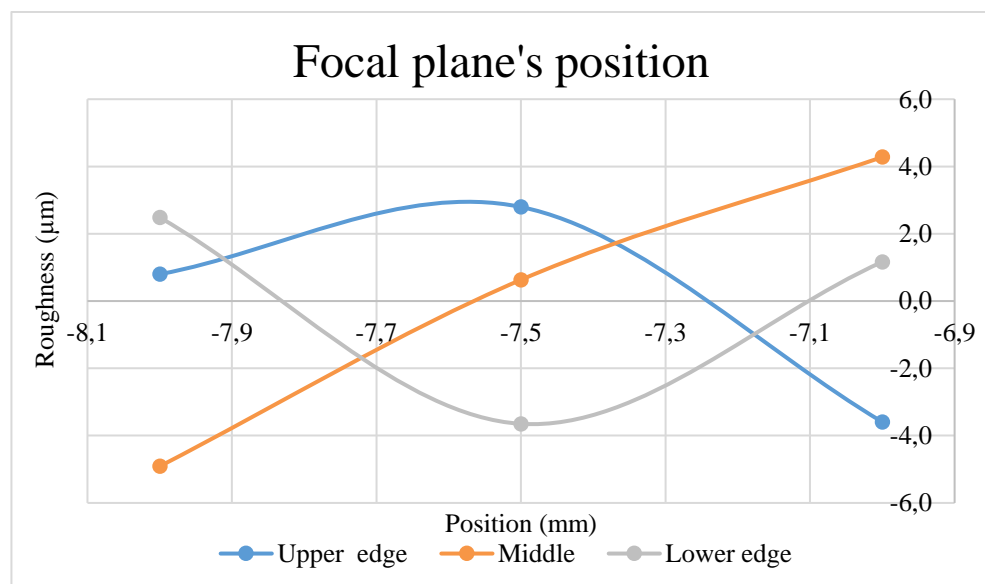


Figure 67: Focal plane's positions results.

The feed rates result shows that with these powers could use feed rate of 15 mm/s. But there was also fluctuation between different cut edge parts (Figure 68). The ring beam's output power optimal value is near the 4000 W quality (Figure 69). The output power of spot indicated that it needs more output power to help penetrating the material and start the process. The optimal value was 1500 W and when decreasing or increasing the value the surface roughness did change (Figure 69).

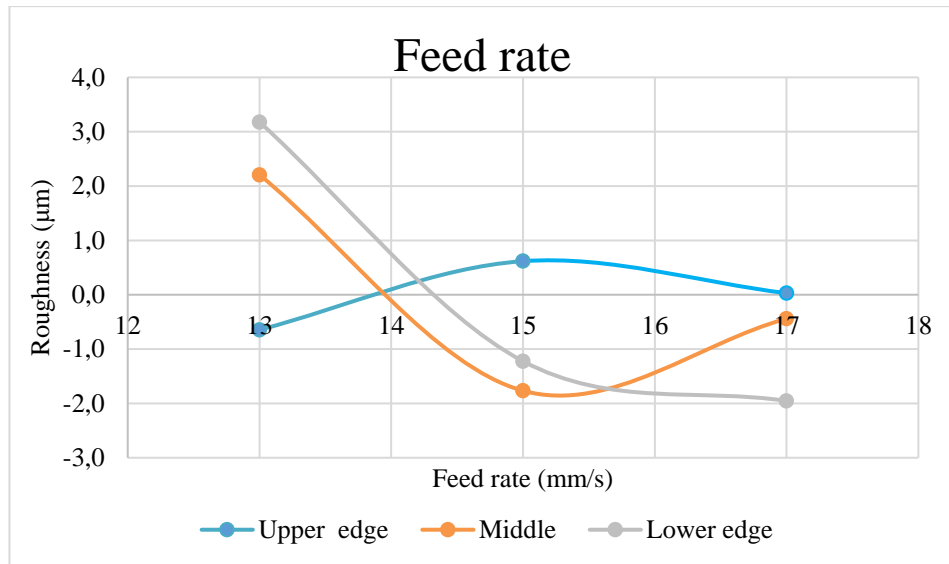


Figure 68: Feed rate's effect.

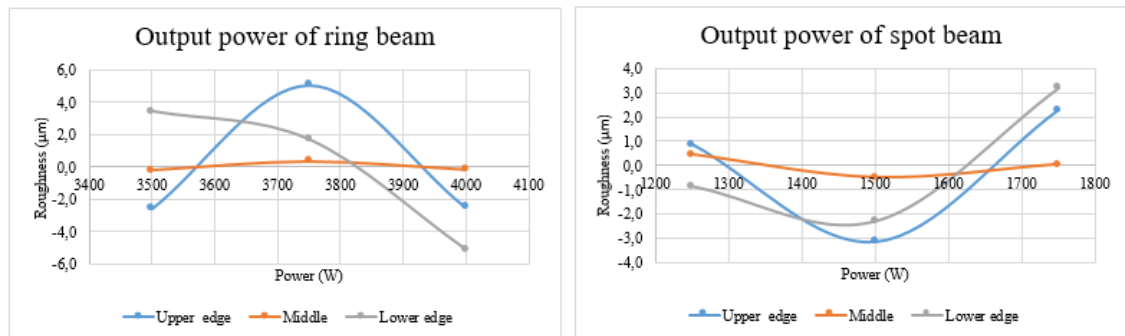


Figure 69: The output powers impact to the surface.

Table 26: Taguchi table's suggested cutting parameters to different areas.

	Modulus of the ring (Hz)	Assistant gas pressure (bar)	Feed rate (mm/s)	Nozzle diameter (mm)	Focal planes distance (mm)	Spot power (W)	Ring power (W)	Distance of the nozzle (mm)
Upper edge	CW	22	13	2	-7	1500	3500	0,75
Middle	CW	20	15	2,5	-8	1500	3500	0,5
Lower edge	CW	20	17	3	-7,5	1500	4000	0,5

The Taguchi table almost give all edges identical cutting parameters shown in Table 26. Only the speed, the nozzle diameter and the focal plane are changing in all. This might be due from that some of the parameters values where too near each other and there was not so big effect on the surface roughness. The Taguchi table's parameter groups did not give any better overall surface roughness average values as the tested groups. We had

too small a gap between the values. With rougher values, could be achieve a better result and see better where the optimal point is. With the best parameters set was achieved the surface roughness quality class of 2. The Taguchi table's cut edges are shown in Figure 70. In the figure the order is from left to right upper edge, middle and lower edge parameters set cut edge. The Taguchi table's overall surface roughness values for the sets were with:

- the upper edge set 50,1 μm
- the middle set 47,12 μm
- the lower edge set 51,06 μm

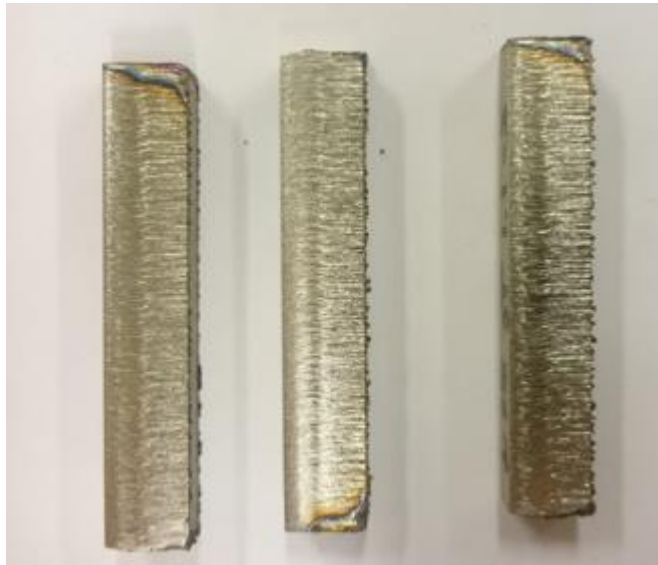


Figure 70: The Taguchi table's parameters cut edges for 10 mm stainless steel.

7.8.2 15 mm stainless steel

The 15 mm stainless steel cutting was similar like 10 mm, but with increased output powers for the spot and ring beam. There were some parameter groups which did format rough surface in the middle of the cut piece (Figure 71). This was very interesting, because there was not only one parameter change which did affect this behavior. In this cutting, we were at the upper limit of the overall output power from the laser source. It shows in the test. The tested parameters and their values are shown in the Table 27.



Figure 71: Stainless steel rough surface.

27: 15 mm stainless steel's test parameters.

Test parameters

	1	2	3
Assistant gas pressure (bar)	18	20	22
Feed rate (mm/s)	9	10	11
Nozzle's diameter (mm)	2	2,5	3
Focus spot's position (mm)	-12	-13	-14
Power of the spot (kW)	1800	1900	2000
Power of the ring (kW)	5800	5900	6000
Nozzle's distance from the surface (mm)	0,4	0,5	0,6

The assistant gas pressure test result indicates here like in 10 mm, that the higher pressure is better, but here it was clearer (Figure 72). Also, the nozzle diameter result show that the optimal diameter is between 2,5 mm and 3 mm preferring the bigger nozzle. The nozzle's distance from the surface did get optimal value. The optimal value was 0,5 mm from the surface. With the 0,4 mm and 0,6 mm distances the surface roughness value rose. Figure 73 shows the nozzle's diameters and distances impact to the surface roughness.

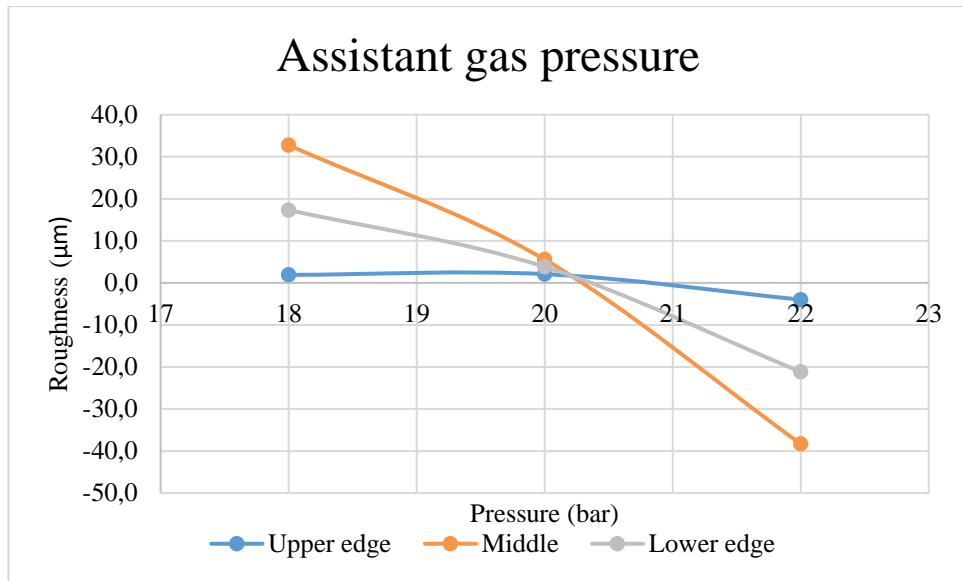


Figure 72: Assistant gas pressure.

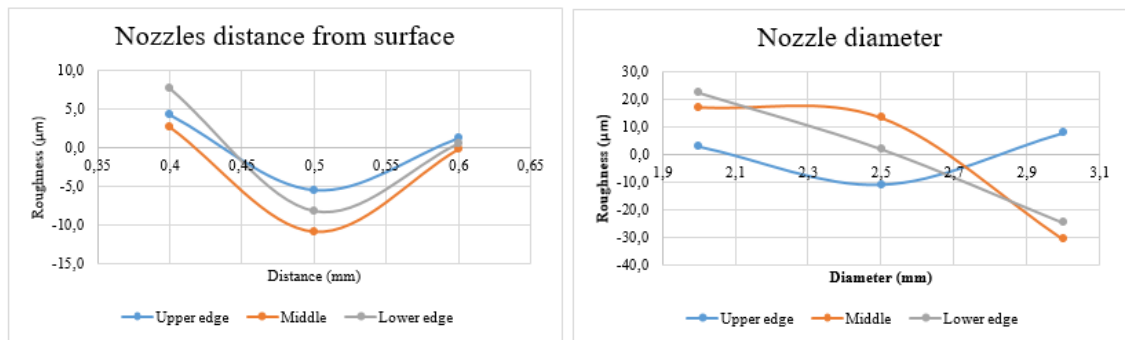


Figure 73: Nozzle parameters impact to the surface.

Both output powers' results indicate that the process needs more output power to achieve a good surface (Figure 74). The source should drive at its maximum capacity with this feed rate. The feed rate (Figure 75) should be with these output powers 10 mm/s (0,6 m/min). Here the tests show that when we increase the feed rate to 11 m/s the roughness rises. This could mean that we are near the maximum thickness, but lowering the feed rate a thicker plate could be driven.

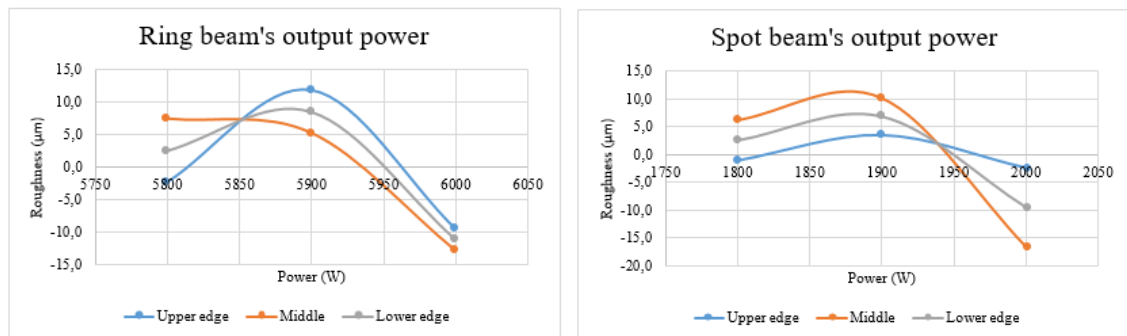


Figure 74: Output powers effect graphs.

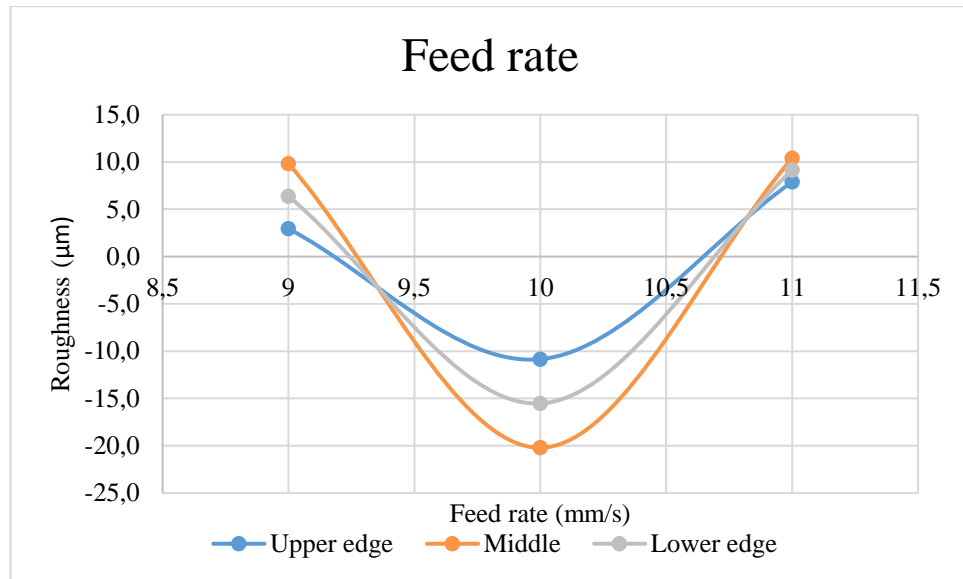


Figure 75: Feed rate impact to surface.

The focal plane position had the most impact on the surface roughness with this thickness. The -12 mm give the best result for all cut edges and when we did go deeper the surface roughness rise (Figure 76). Because of the graphs lines (Figure 76) are almost linear, the focal planes position – 11 mm could be tested if it gives better value than the – 12 mm.

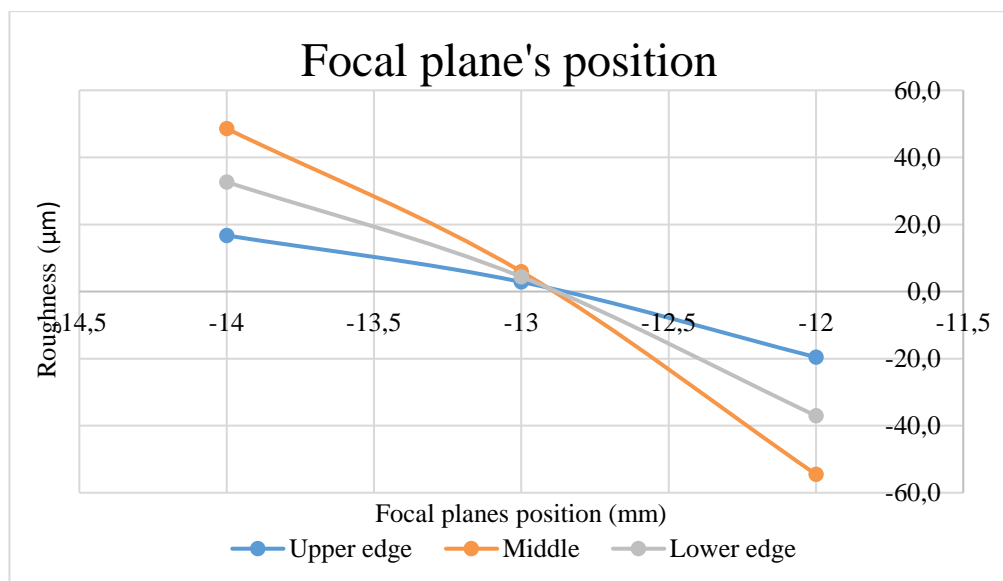


Figure 76: Focal plane's positions effect on the roughness.

The Taguchi table's calculation (Table 28) gave only one parameter group for all these areas, which was a surprising result. This can be caused by that we were at the limit of the output powers or there was not enough gap between certain parameter values like nozzle's distances from the surface. The achieved cutting edge of the Taguchi table's parameter set is shown in Figure 77. When we cut with the Taguchi table's suggested

parameters, the results were not overall so good as when we cut some parameter groups in Taguchi table. With the Taguchi table sets were achieved overall surface roughness values for the set was 50,18 μm . In the Table 29 is shown three better overall parameter groups. They are almost identical, but there are changes in the output powers, the focal planes position and the speed fluctuates more. With the best parameters set surface the roughness quality class of 2 was achieved. The difference between these tables' surface roughness values ranges from 12 μm to 14 μm .

Table 28: Taguchi's optimal parameters for 15 mm stainless steel.

	Modulus of the ring (Hz)	Assistant gas pressure (bar)	Feed rate (mm/s)	Nozzle diameter (mm)	Focal planes distance (mm)	Spot power (W)	Ring power (W)	Distance of the nozzle (mm)
Upper edge	CW	22	10	3	-12	2000	6000	0,5
Middle	CW	22	10	3	-12	2000	6000	0,5
Lower edge	CW	22	10	3	-12	2000	6000	0,5

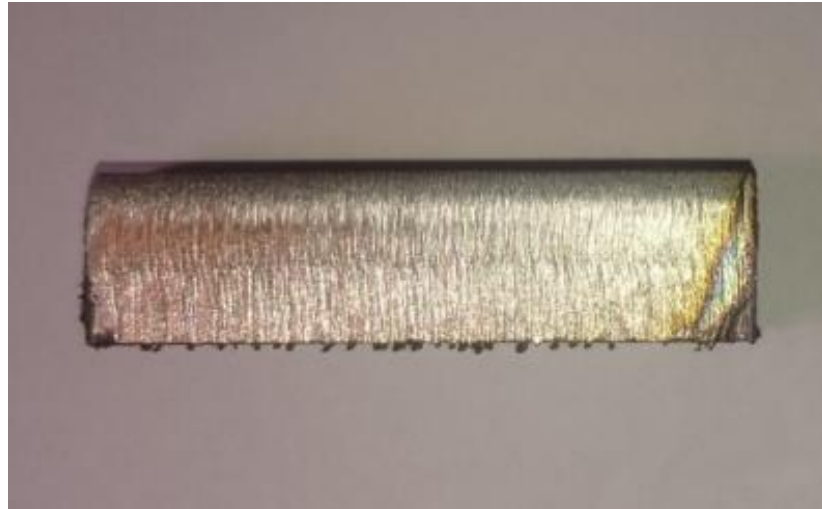


Figure 77: Stainless steel Taguchi table's parameter sets cutting edge.

Table 29: Better parameters for overall roughness.

	Modulus of the ring (Hz)	Assistant gas pressure (bar)	Feed rate (mm/s)	Nozzle diameter (mm)	Focal planes distance (mm)	Spot power (W)	Ring power (W)	Distance of the nozzle (mm)
First	CW	20	11	3	-12	1800	5900	0,5
Second	CW	22	10	3	-13	1800	6000	0,4
Third	CW	22	9	3	-13	2000	5800	0,5

Figure 78 shows the Table's 29 cutting edges from the left to right first, second and third parameter set.



Figure 78: Table's 29. parameter sets cutting edges.

7.9 Copper

The cutting of copper with high pressure oxygen was overall very clean and stable process, but some surface burning was shown with 6 mm and 10 mm thicknesses which gave bad surface roughness. The cutting process did need more power to achieve penetration than the mild steel cutting, because the copper does not absorb the laser light's wavelength as good as mild steel.

7.9.1 6 mm copper

The cutting of 6 mm thick copper plate was clean process, where the splatters was controlled with correct parameters. When the parameters were going to wrong direction it did show at the surface as burning and the splatters were not so controlled downwards. The fixed parameters for the cutting was the duty cycle 75% and the nozzle's distance 1 mm from the surface. The tested parameters are shown in the Table 30.

Table 30: The 6 mm copper's test parameters.**Test parameters**

	1	2	3
Assistant gas pressure (bar)	16	18	20
Feed rate (mm/s)	25	30	35
Nozzle's diameter (mm)	1,5	2	2,5
Focus spot's position (mm)	-4	-5	-6
Power of the spot (kW)	1,6	1,8	2
Power of the ring (kW)	5,2	5,6	6
Modulus of the spot (Hz)	CW	1000	5000
Modulus of the ring (Hz)	CW	1000	5000

The nozzle diameter was the most effecting parameter in this case. The nozzle diameter graph showed that when increasing the nozzle's diameter, it did give better surface roughness to the lower part of the cut edge. The best result for the upper edge gave diameter 2 mm nozzle and the middle and the lower edge 2,5 mm (shown in the Figure 74).

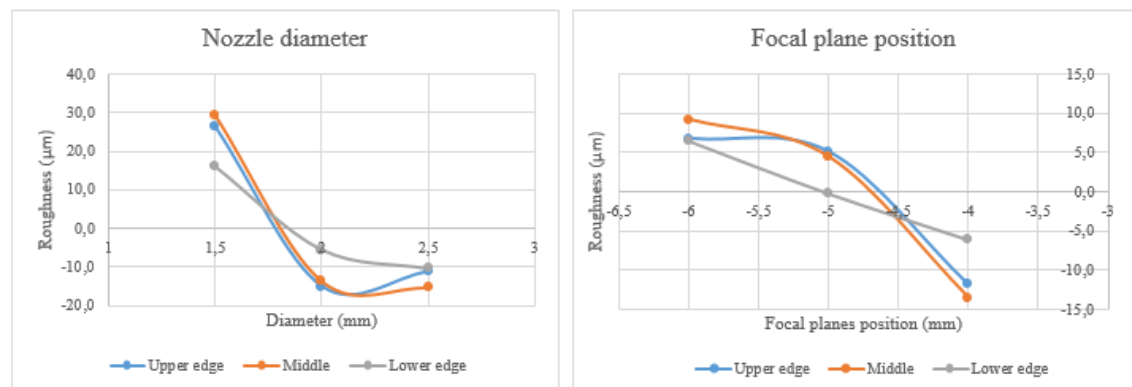


Figure 79: The nozzle's diameters and focal plane's positions effect on the average value of surface roughness.

The focal plane's position was second or third (upper edge) most effecting parameter to the surface roughness. This can be caused by that the smaller spot diameter and of the energy intensity on the surface. The highest value (- 4 mm) was best and when the focal plane did go lower the effect was negative due the increased spot size on the surface. It can be seen at Figure 79.

At the upper and the middle edges the assistant gas pressure did indicate that the lower gas pressure gives a better result (shown in the Figure 80), but in the lower part of the edge the highest pressure gave the best result. This might be caused by that the higher pressure can carry the molten material out of the lower edge more easily and this way

make smoother surface. The higher pressure did also influence the dross formation with nozzle diameter, that there was less formatted dross underside at the lower edge.

The continuous wave mode was better use than the modulation of 1000 Hz or 5000 Hz with the duty cycle of 75%. The modulation 5000 Hz did give better value than a 1000 Hz, shown in the Figure 81 (in the figure 0 means CW mode) to all parts. This was also noticeable in the middle and the lower part of the test pieces. This can be caused by that the fact, that there is not enough power coming from the laser, because the output is only 75% from the set power value. The burning of the surface was result from lack of the output power.

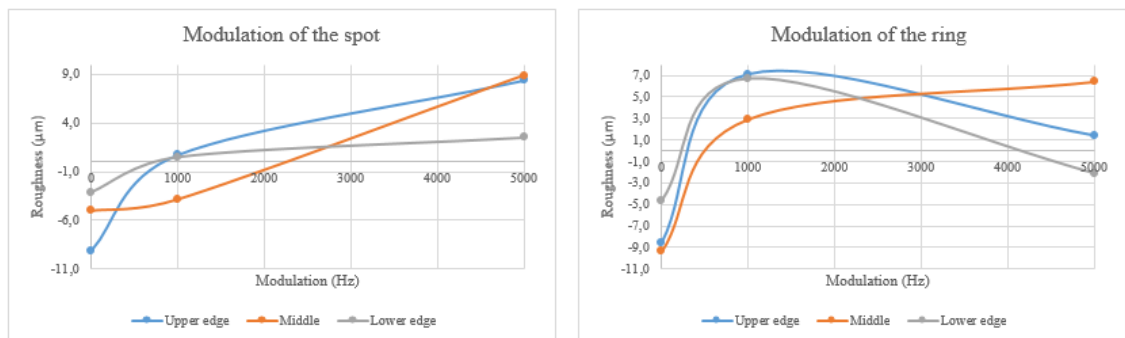


Figure 80: Modulations (spot and ring beams) effect on the surface roughness.

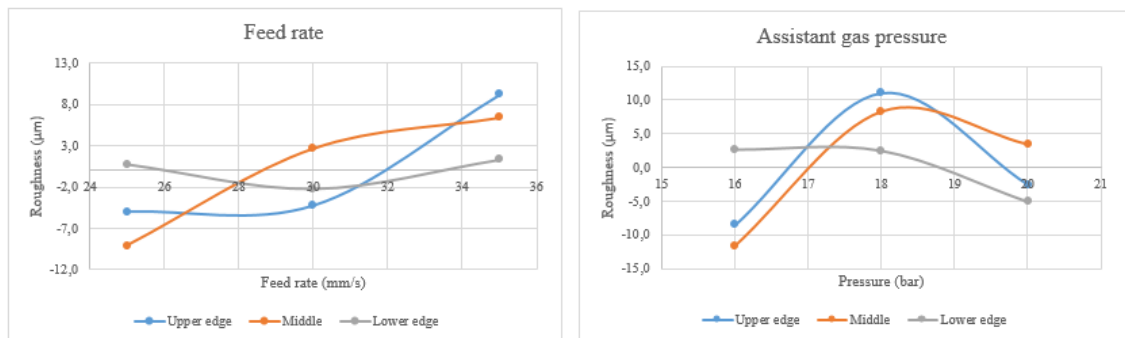


Figure 81: Assistant gas pressure and feed rate's effect.

The feed rate had most impact on upper and middle part of the piece, but not so significant in the lower part of the piece. The lowest feed rate gave the better surface in upper and middle part and the highest value in the lowest part of the piece (shown in the Figure 81).

The output power of the spot and ring beam's effect on the upper and the lower edge quality were similar, but when looking middle part, the spot beam had to be highest value 2 kW when the upper and the lower part needed only 1,6 kW when the ring power did not change at all from 5,6 kW. Figure 82 show the impact of the output powers to the average in the surface roughness.

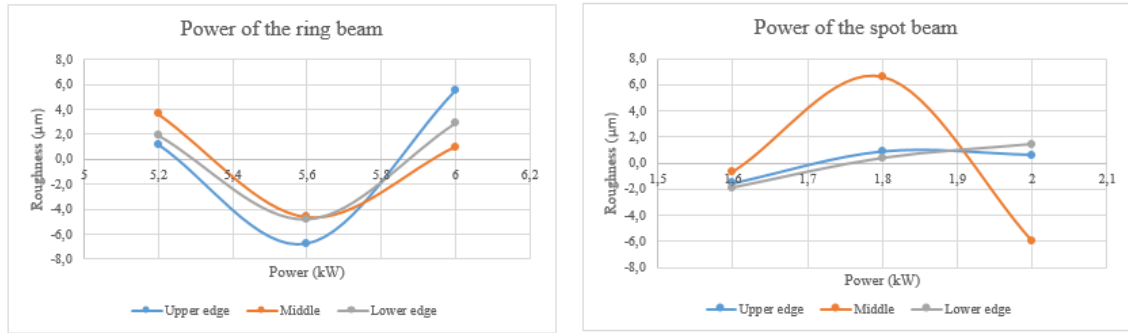


Figure 82: Output's power effect on the average value.

The Taguchi table's average response table calculations gave a good parameter's sets (shown in the Table 31) to all areas with them the overall surface roughness did get better and the individual edges values were better. With the best parameters set the surface roughness quality class of 2 was achieved. Anyhow, this value cannot be validated because the SFS-ISO EN 9013 is not taking into consideration of copper's cutting quality. The cutting edges are shown in Figure 83. The parameter sets did achieve the best overall surface roughness values with:

- the upper edge set 34,44 µm
- the middle set 35,84 µm
- the lower edge set 33,79 µm

Table 31: Taguchi's suggested parameter values for different areas.

	Assistant gas pressure (bar)	Feed rate (mm/s)	Nozzle diameter (mm)	Focal planes position (mm)	Power of the spot (kW)	Power of the ring (kW)	Modulation of the spot (Hz)	Modulation of the ring (Hz)
Upper edge	16	25	2	-4	1,6	5,6	CW	CW
Middle	16	25	2,5	-4	2	5,6	CW	CW
Lower edge	20	35	2,5	-4	1,6	5,6	CW	CW



Figure 83: 6 mm copper's cutting edges. From the left to right upper, middle and lower part of the edge.

7.9.2 10 mm copper

The cutting of 10 mm copper was interesting process, because we were on the limit at the output powers, so there was no room to adjust the powers and it also did give limitation to modulation to spot and ring beams. That's why we did fix the duty cycle to 75 % and the nozzle's distance from the surface to 1 mm. Also, the ring beam was not modulated. The spot beam was modulated. Also, the powers were in the highest value 2+6 kW. The modulation of the spot did have a negative effect on the surface quality as the surface burned badly (Figure 84). There was not enough power available to cut neatly through the whole thickness. The tested parameters are shown in the Table 32.



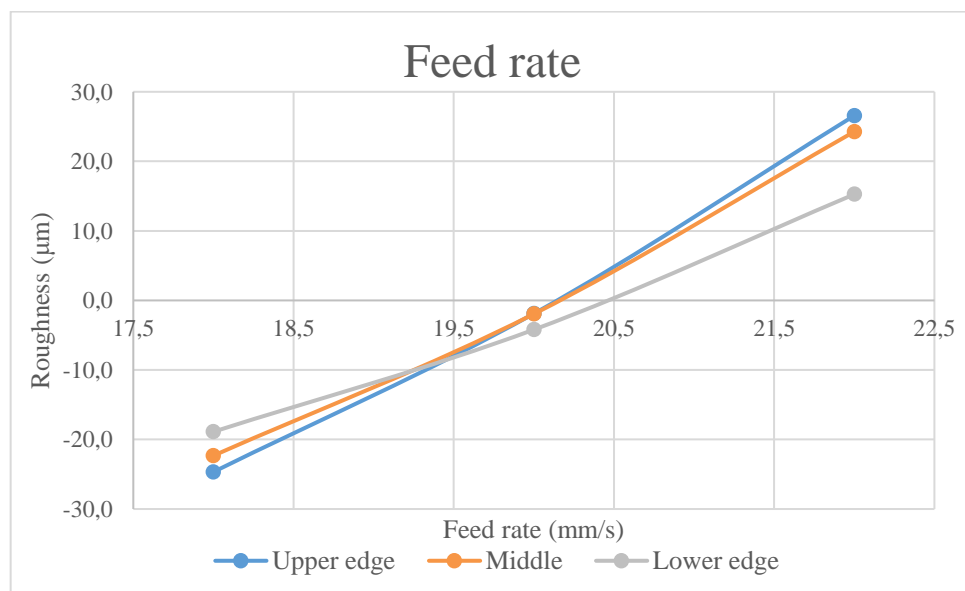
Figure 84: Coppers burned cut edge.

Table 32: The 10 mm copper's test parameters.**Test parameters**

	1	2	3
Assistant gas pressure (bar)	16	18	20
Feed rate (mm/s)	18	20	22
Nozzle's diameter (mm)	2	2,5	3
Focus spot's position (mm)	-8	-9	-10
Power of the spot (kW)	2	2	2
Power of the ring (kW)	6	6	6
Modulus of the spot (Hz)	CW	1000	5000

Because the power was on maximum, the feed rate did rise to the major effecting parameter. This is due to the fact that here is delicate balance between the power and the feed rate. The feed rate did settle in this case to 18 mm/s (1,08 m/min) value and with these power settings. It did show that when we increased the feed rate, the value of surface roughness rose in all the areas (shown in the Figure 85)

As mentioned earlier, the modulation of the spot beam did have effect on the surface roughness through the whole piece, by lowering the overall power value. The continuous wave mode was the best, because it does not have effect on the overall power, but when we did use the modulation 1000 Hz and 5000 Hz it increased the surface roughness in all edges and the most effected part was the upper edge (shown in the Figure 86). The figure shows similar behavior for all areas in the tests.

**Figure 85:** The feed rates effect on surface roughness average value.

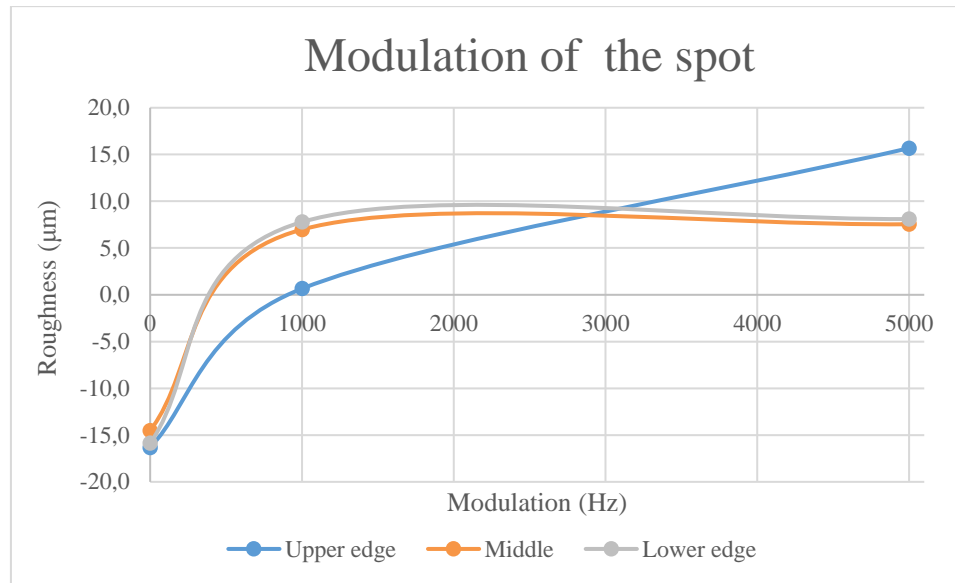


Figure 86: The spot's modulation effect on the surface roughness. The 0 means CW mode in the figure.

The focal plane's position had impact on the surface roughness, but it was not so significant as the feed rates change. It did show that if we did go deeper with the position we did get higher surface roughness value than with -8 mm position. This is in the last third of the material thickness. The change was almost linear from the value to value, (shown in the Figure 87).

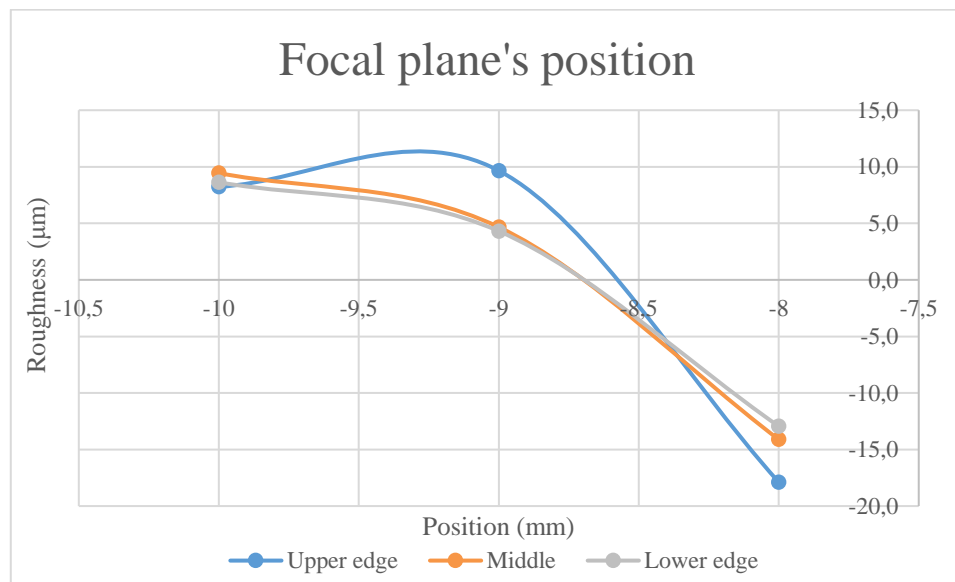


Figure 87: Focal plane's positions effect on the surface.

The nozzle's diameter change did show that, the larger diameter nozzle was better in the upper and the lower part of the edge. But the smallest and the largest nozzle in the middle part had very similar average roughness values. The assistant gas alternation did

show that the higher pressure gives better result for the measured areas, but the upper edge had higher average value with the highest pressure shown in Figure 88.

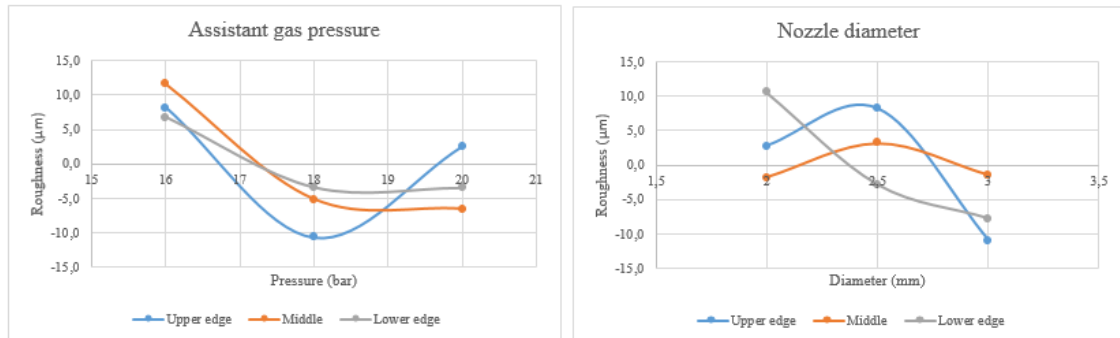


Figure 88: Assistant gas pressure and the nozzle's diameter change effect on the surface roughness.

The Taguchi table's average response table gave better parameter groups, which did lower the overall and the areas surface roughness average value. The parameter groups (shown in the Table 33) are almost identical through all areas, except the upper edges gas pressure is lower. With the best parameters set the surface roughness quality class of 2 was achieved. Anyhow, this value cannot be validated because the SFS-ISO EN 9013 is not taking into consideration of copper's cutting quality. The cutting edges of the 10 mm copper's are shown in Figure 89, where the right edge is for upper edge, the middle piece is for the middle and the left is for the lower edge parameter set.

Table 33: 10 mm response table suggested parameter values for different area.

	Assistant gas pressure (bar)	Feed rate (mm/s)	Nozzle diameter (mm)	Focal plane position (mm)	Power of the spot (kW)	Power of the ring (kW)	Modulation of the spot (Hz)	Modulation of the ring (Hz)
Upper edge	18	18	3	-8	2	6	CW	CW
Middle	20	18	3	-8	2	6	CW	CW
Lower edge	20	18	3	-8	2	6	CW	CW

The Taguchi tables did achieve overall surface roughness values with:

- the upper edge set 38,92 µm
- the middle set 46,34 µm
- the lower edge set 42,17 µm



Figure 89: The 10 mm copper's Taguchi table's edges.

7.9.3 15 mm copper

With the 10 mm thickness, we used the maximum output power of the laser source. So now we needed full output power to drive with CW mode both beams, because we did not achieve in preliminary test penetration through whole thickness of 15 mm. Also, it did decrease the feed rate for test parameters. The nozzle's distance from the surface was fixed into 1 mm. The tested parameters are shown in the Table 34.

Table 34: The 15 mm copper's test parameters.

Test parameters

	1	2	3
Feed rate (mm/s)	2	3	4
Nozzle's diameter (mm)	2	2,5	3
Focus spot's position (mm)	-8	-10	-12
Output power of the spot (kW)	2	2	2
Output power of the ring (kW)	6	6	6
Assistant gas pressure (bar)	16	18	20

The cutting process with high pressure oxygen was clean and stable through all test parameter groups. With this thickness, the feed rate did rise the most significant parameter to affect the surface roughness for all areas. This was caused by the output powers could not be raised and the oxygen did not bring any more energy to process by burning. So, the feed rate must come down. The test shows that the fastest speed (4 mm/s) did give the best result for the upper part, the middle value (3 mm/s) for the middle part and the

lowest value (2 mm/s) for the lower part (shown in the Figure 90). This effect from that the energy which is provided from the source and burning is more time to melt the solid copper better.

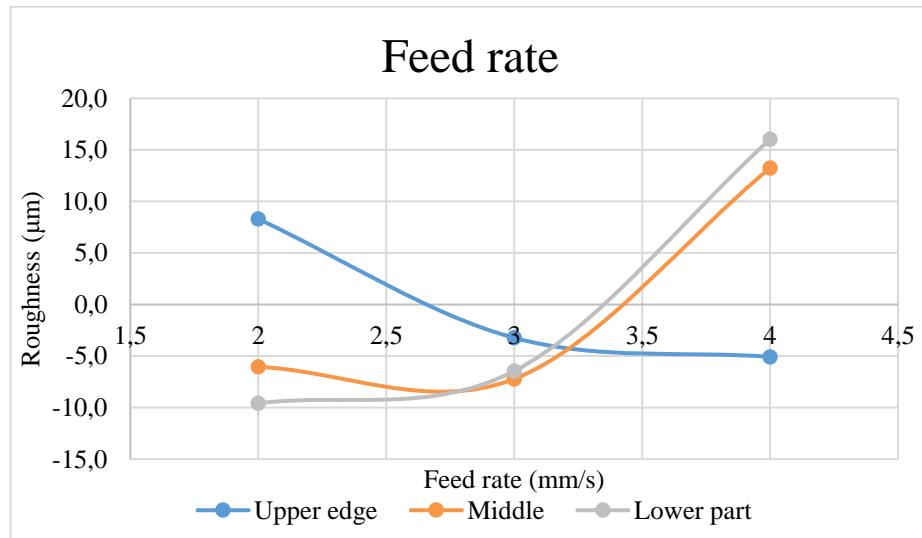


Figure 90: Feed rate's effect on different areas in 15 mm copper.

The oxygen gas pressure for the 15 mm thickness, showed that the lowest pressure give the best result (shown in the Figure 91), but it also increased the dross formation under the cut edge. But the effect is not so significant like the feed rates, so in general the usage of higher pressure could be recommended.

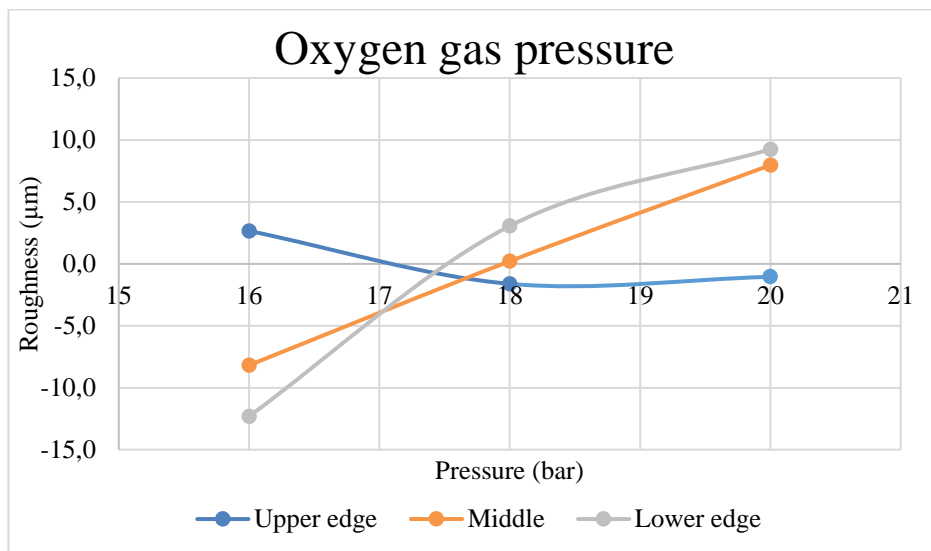


Figure 91: Oxygen gas pressure's impact to the surface roughness.

The change of the nozzle's diameter to bigger did not help to achieve better quality of cut edge, but it had big impact to the surface (shown in Figure 92).

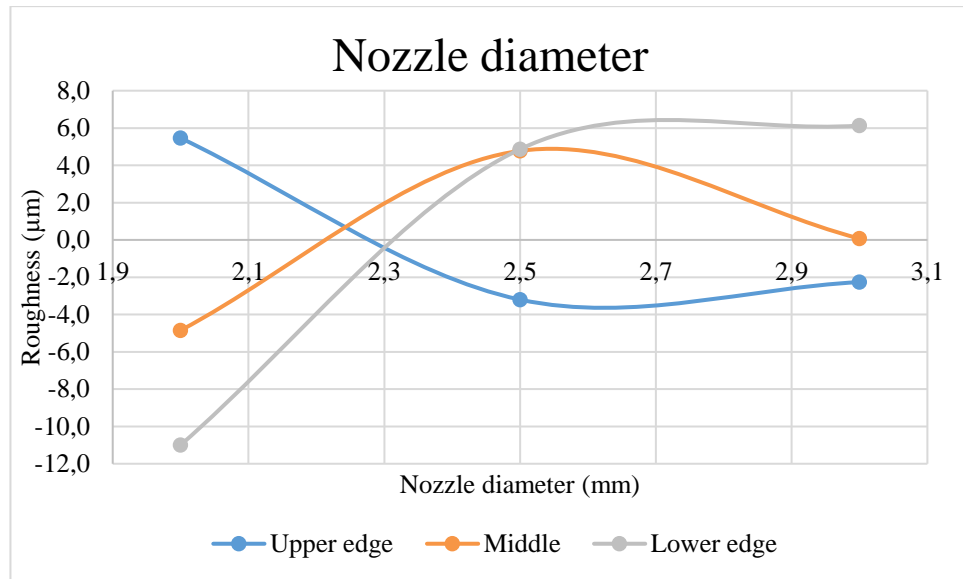


Figure 92: Nozzle's diameter impact to the surface quality.

The focal plane's position did effect when we changed it to deeper setting, the deeper areas surface roughness did get better (shown in Figure 93). In the middle and the lower parts average values have so little fluctuation that it can be solved by the uncertainty of measurement. The focal plane's position was the lowest effecting parameter in this case when comparing with other parameters in this case.

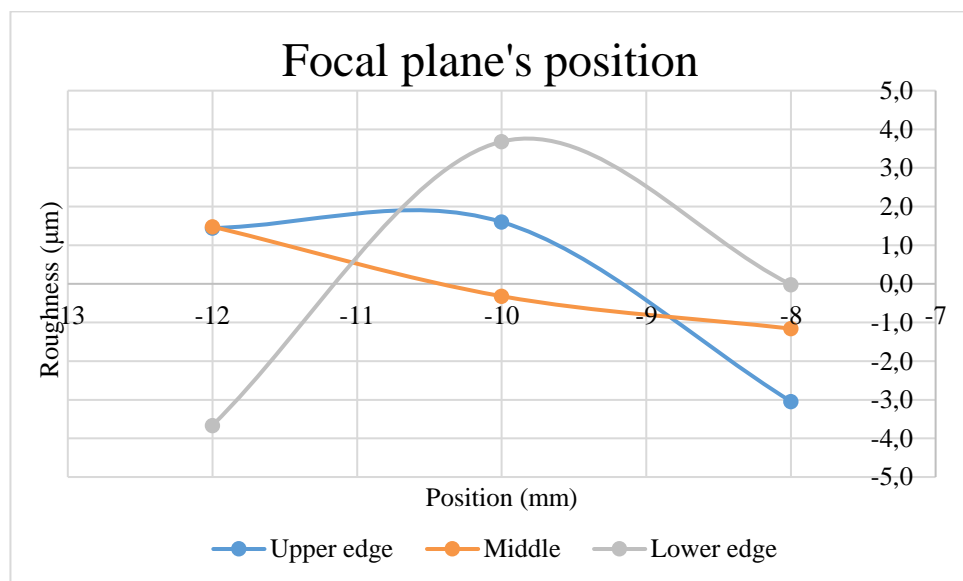


Figure 93: Focal plane's position effect.

The average response table did suggest parameter groups (Table 35), which did do similar overall surface roughness value, but there were seen the growth of dross formation under the cut edge due the low pressure and lack of gas flow. But they did perform better in their own areas than some of the test table's parameter groups. There were three parameters sets which did perform better in overall roughness (shown in the Table 36)

The difference between these two tables parameter sets were between 0 to 10 μm . With the best parameters set the surface roughness quality class of 2 was achieved. Anyhow, this value cannot be validated because the SFS-ISO EN 9013 is not taking into consideration of copper's cutting quality. Figures 94 and 95 shows the cutting edges for the different table's parameter sets.

Table 35: Suggested parameters for different areas.

	Pressure (bar)	Feed rate (m/s)	Nozzle diameter (mm)	Focal planes position (mm)	Spot power (kW)	Ring power (kW)	Modulation of the ring (Hz)	Modulation of the spot (Hz)	Surface roughness value (μm)
Upper edge	18	4	2,5	-8	2	6	CW	CW	56,72
Middle	16	3	2	-8	2	6	CW	CW	62,29
Lower edge	16	2	2	-12	2	6	CW	CW	65



Figure 94: Taguchi table's suggested cutting edges from the left to right.

Table 36: Three parameters set which did perform better than the Taguchi sets.

	Pressure (bar)	Feed rate (m/s)	Nozzle diameter (mm)	Focal planes position (mm)	Spot power (kW)	Ring power (kW)	Modulation of the ring (Hz)	Modulation of the spot (Hz)	Surface roughness value (μm)
First	18	4	2	-10	2	6	CW	CW	58,1
Second	18	3	3	-8	2	6	CW	CW	59
Third	16	3	2,5	-12	2	6	CW	CW	60,8



Figure 95: The table's 36. cutting edges from the left to right.

7.10 Aluminium

The aluminium cutting was very splattering process because of the use of high pressure of nitrogen. With correct parameters, a stable process was found. There was dross formation in both cases 15 mm and 20 mm and fully dross less cut was not achieved.

7.10.1 15 mm aluminium

With the 15 mm aluminium, the fixed parameters were nozzle's distance from the surface (2 mm), the output powers for the spot and the ring beams were at maximum (2+6 kW), the ring beam was not modulated and the duty cycle for the spot modulation was 50%. The tested parameters are shown in the Table 37.

Table 37: The 15 mm aluminium's test parameters.

Test parameters

	1	2	3
Assistant gas pressure (bar)	16	18	20
Feed rate (mm/s)	5	7	9
Nozzle's diameter (mm)	1,5	2	2,5
Focus spot's position (mm)	-9	-10	-11
Modulus of the spot (Hz)	CW	1000	2000

There was not dross free cut in these parameter groups, but the higher pressures did help to lower the formation of the dross. The assistant gas pressure's effect on the surface roughness was interesting, because the higher pressure did lower the middle part's and the lower edge's roughness, but did rise upper edge's roughness instead significantly

(shown Figure 96). The change between the pressure values did not show so major an impact to the middle and the lower parts of the piece.

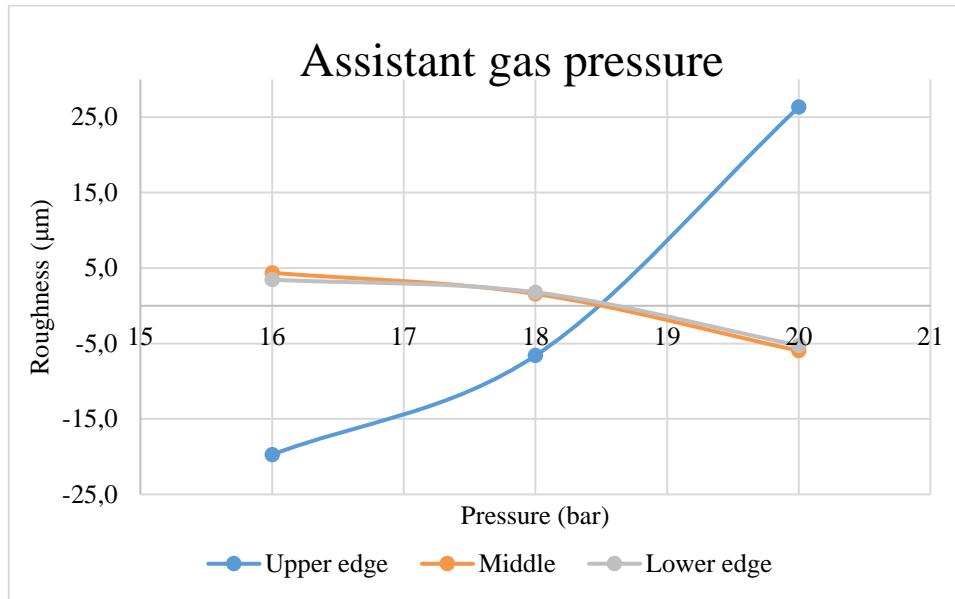


Figure 96: Assistant gas pressures effect on different parts.

The feed rate's impact on the surface roughness was almost linear, when increasing the feed rate, also the surface roughness did rise, but the middle part did show different kind behavior (shown in the Figure 97). This increasing of the roughness during increase of the speed indicates that there is needed more power to give smoother surface. This is shown in the modulation of spots graphs influence to the roughness (shown in Figure 98).

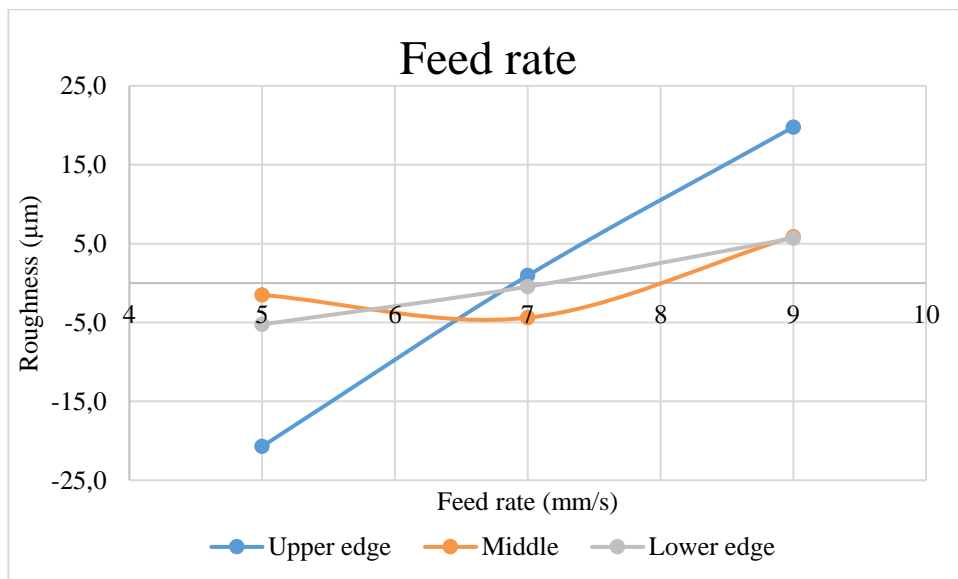


Figure 97: Feed rate's effect on the surface smoothness.

The nozzle's diameter change shows that usage of bigger diameter the nozzle is preferred if better surface roughness quality is (shown in Figure 99) needed. But here the upper edge gets the same kind of impact, like in the higher-pressure case that the roughness value increases. There is moderate change between values.

The focal plane's position had it best values when the plane was at -9 mm under the surface (shown in the Figure 100). When going deeper into the material the surface roughness value did get higher, but it also did get lower values with the deepest value to compare the middle value.

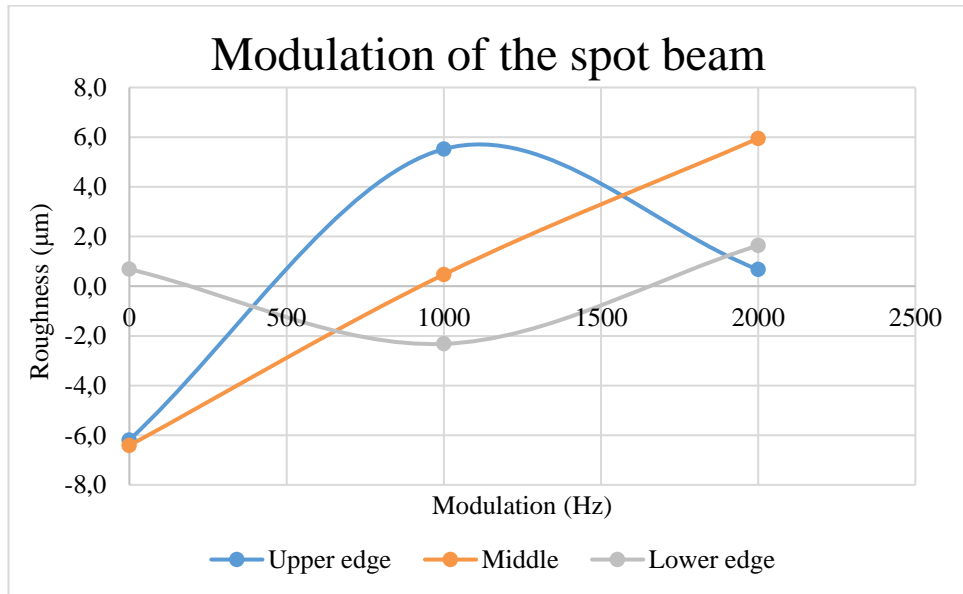


Figure 98: The spot beam's modulation. The 0 value indicate continuous wave mode.

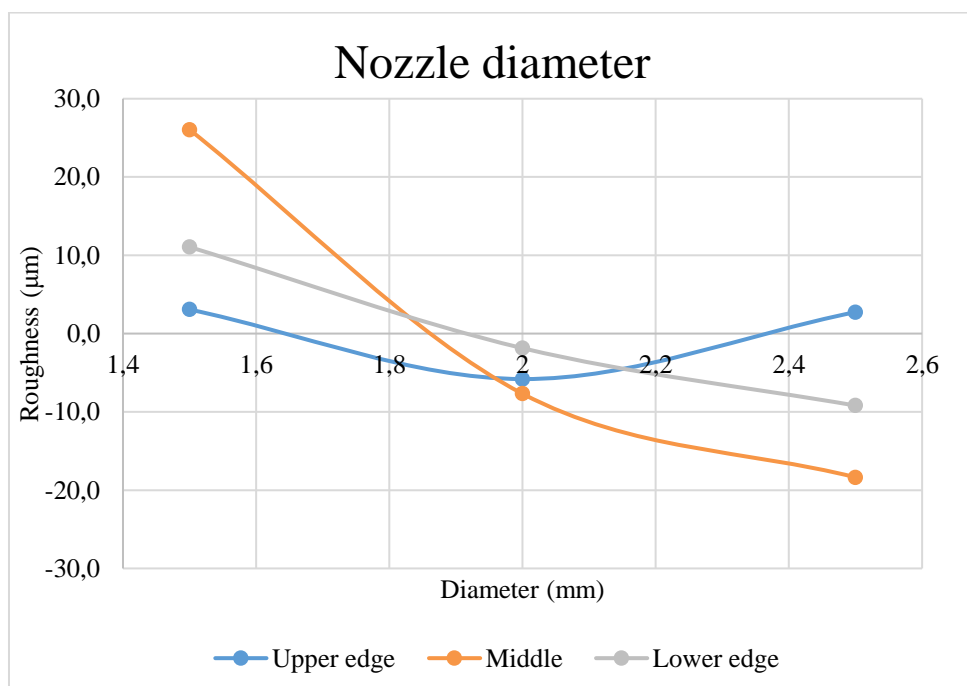


Figure 99: Nozzle's diameter changes impact to the surface roughness.

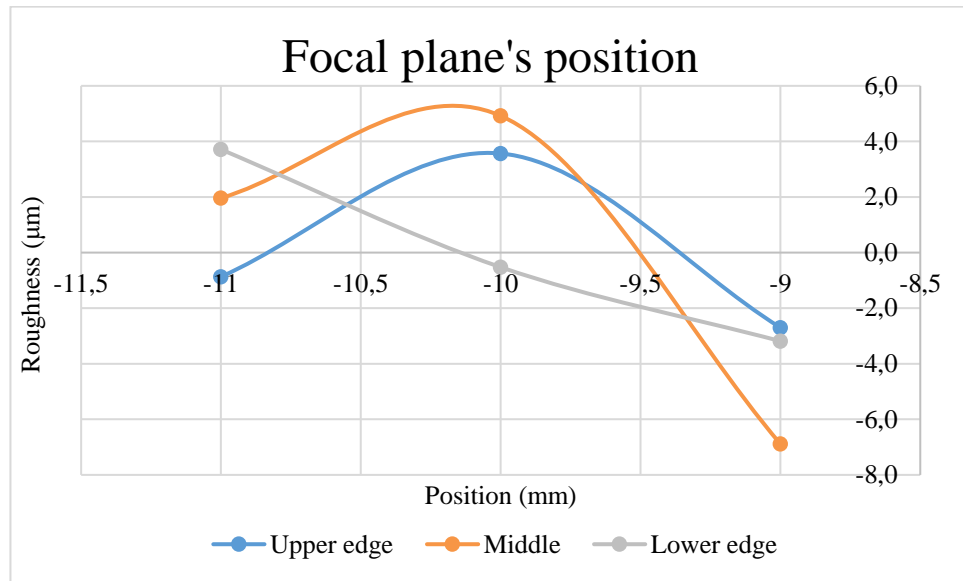


Figure 100: Focal plane positions chances effect.

The Taguchi response table (Table 38) gave parameters groups which gave to the overall and for the current area better surface roughness value. The 15 mm aluminium did achieve cutting class 3. Anyhow, this value cannot be validated because the SFS-ISO EN 9013 is not taking into consideration of aluminium cutting quality. The cut edges of the table are shown in Figure 101. In the figure, the table parameters are left to the right.

Table 38: Suggested parameters.

	Assistant gas pressure (bar)	Feed rate (mm/s)	Nozzle diameter (mm)	Focal planes position (mm)	Power of the spot (kW)	Power of the ring (kW)	Modulus of the spot (Hz)	Modulus of the ring (Hz)	Surface roughness value (µm)
Upper edge	16	5	2	-9	2	6	CW	CW	84,57
Middle	20	7	2,5	-9	2	6	CW	CW	83,44
Lower edge	20	5	2,5	-9	2	6	1000	CW	90,26

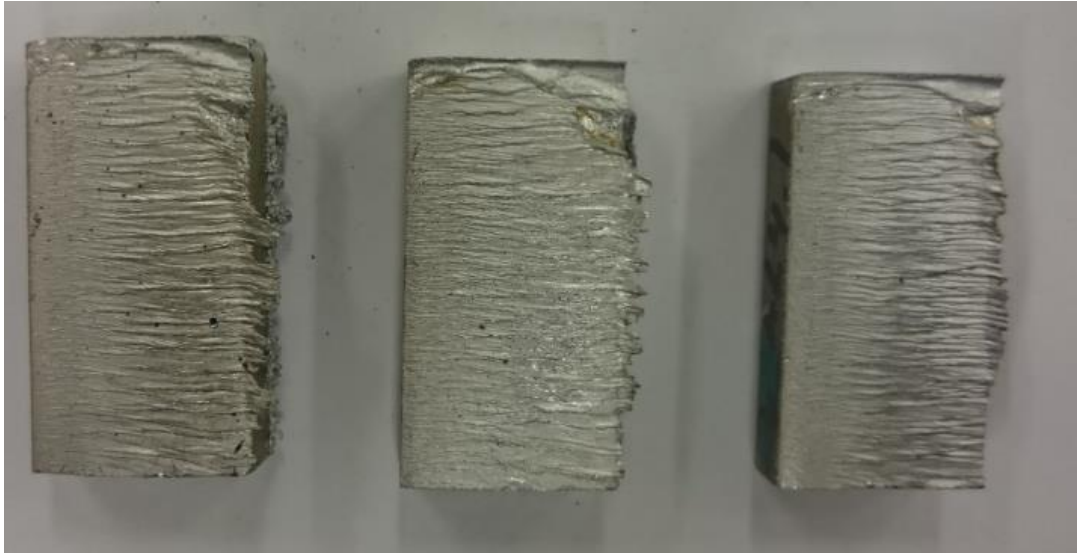


Figure 101: The Taguchi table's cut edges.

7.10.2 20 mm aluminium

For the 20 mm thick plate we did fix the nozzle's distance from the surface to 1 mm, the output powers were at maximum value (2+6 kW) and the modulation was not used, only CW mode. The process was stable through all parameter groups. The tested parameters for the 20 mm aluminium are shown in the Table 39.

Table 39: Test parameters for the 20 mm aluminium.

Test parameters

	1	2	3
Assistant gas pressure (bar)	18	20	22
Feed rate (mm/s)	2	3	4
Focus spot's position (mm)	-15	-16	-17
Nozzle's diameter (mm)	2	2,5	3

The focal plane's change did show that the highest level (-15 mm) could give the best value for the middle and lower part of the piece, because there the spot size is smaller. The middle value did give the best value for the upper edge, but the deepest value was near (shown in the Figure 102).

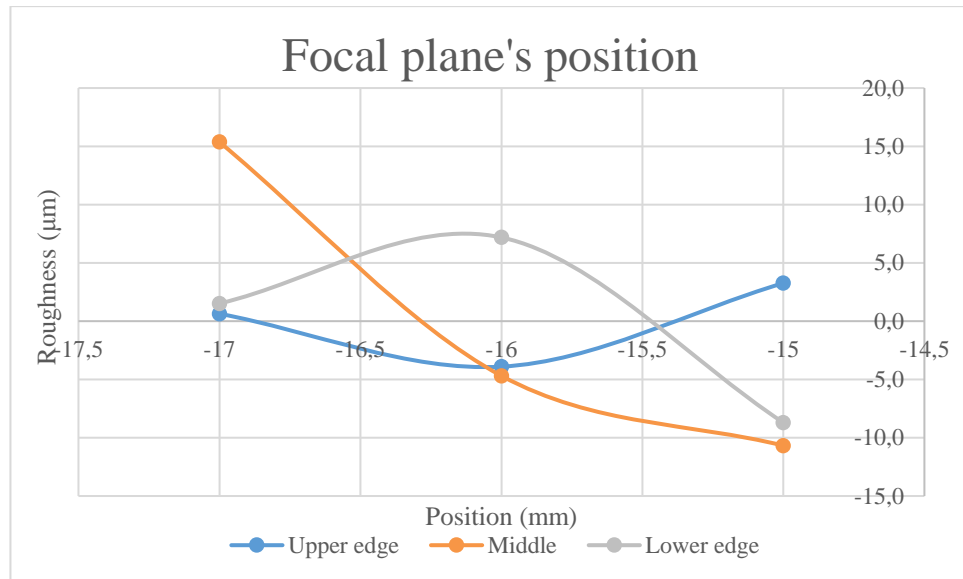


Figure 102: Focal plane's position.

The feed rate did indicate that with these output powers, we could use the smallest value (2 mm/s) (shown in the Figure 103) to achieve the best value for the surface roughness. There might be some room to speed up to 3 mm/s because the change is not so significant and the lower and middle part gets better values in there.

The assistant gas pressure shows that 18 bar pressure should use to get better surface roughness. The roughness did increase when was used higher pressure, but not so much. The observation of dross formation shows the same kind of behavior, but also the higher pressure did give moderate dross under the cut edge. The nozzle diameter 2,5 mm seems to be optimal choice for this thickness, because it gives the best values for each part of the cut edge (show in the Figure 104).

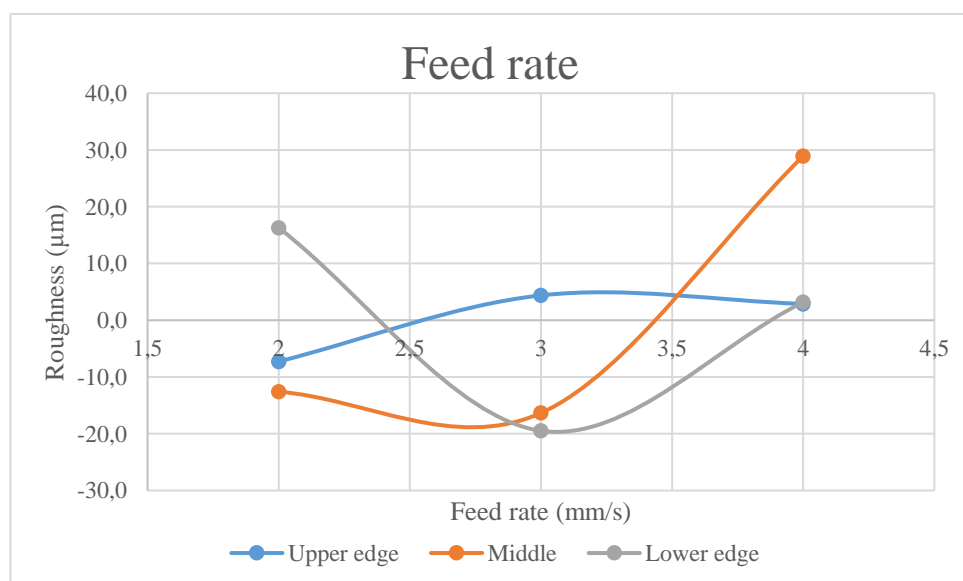


Figure 103: Feed rate's impact to roughness of surface.

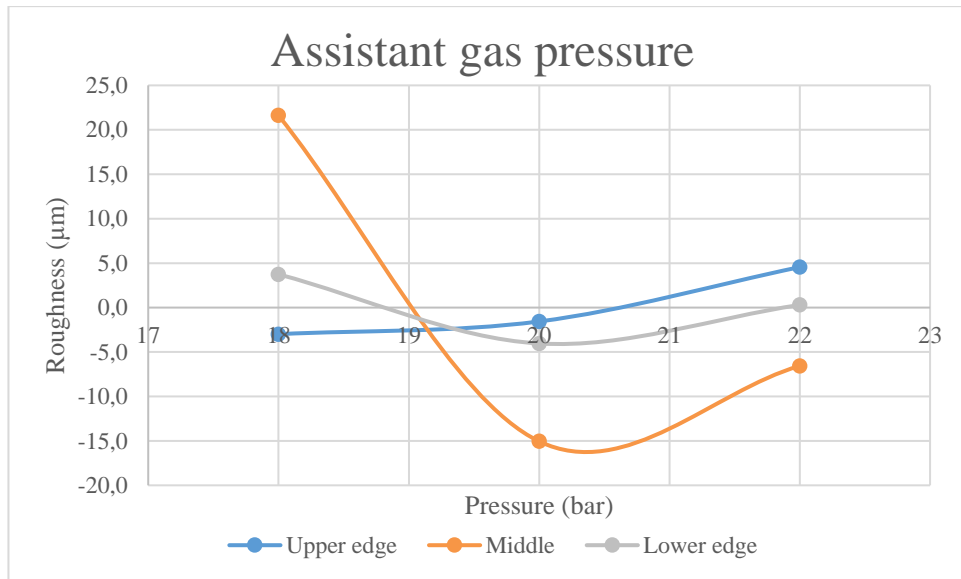


Figure 104: Assistant gas pressure's impact to the surface.

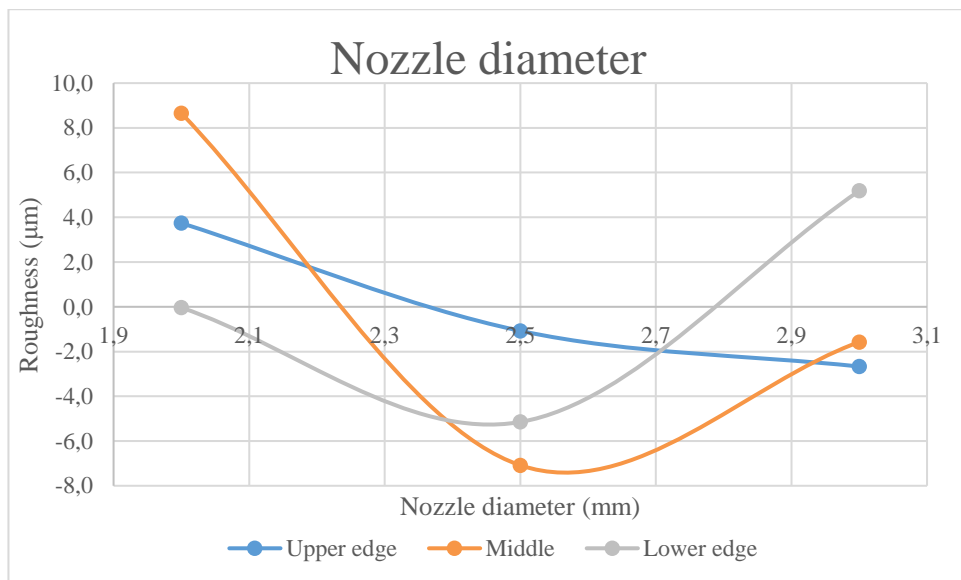


Figure 105: Nozzle diameters effect on 20 mm aluminums roughness.

The suggested parameter groups (Table 40) gave worse overall surface roughness than the three best Taguchi test tables parameter sets, but they did perform better in their own field. Better values were achieved with three parameters sets and they are shown in Table 41. With the best parameters set were achieved surface roughness quality class of 3. Anyhow, this value cannot be validated because the SFS-ISO EN 9013 is not taking into consideration of aluminium's cutting quality because of the high striation of lower part of cut edge.

Table 40: Suggested parameters.

	Assistant gas pressure (bar)	Feed rate (mm/s)	Nozzle diameter (mm)	Focal planes position (mm)	Power of the spot (kW)	Power of the ring (kW)	Modulation of the spot (Hz)	Modulation of the ring (Hz)	Surface roughness value (μm)
Upper edge	18	2	3	-16	2	6	CW	CW	108,9
Middle	20	3	2,5	-15	2	6	CW	CW	115,6
Lower edge	20	3	2,5	-15	2	6	CW	CW	115,6

*Figure 106: The Taguchi table's cut edges, from up to down.**Table 41: Three parameter sets which did give better overall roughness.*

	Assistant gas pressure (bar)	Feed rate (mm/s)	Nozzle diameter (mm)	Focal planes position (mm)	Power of the spot (kW)	Power of the ring (kW)	Modulation of the spot (Hz)	Modulation of the ring (Hz)	Surface roughness value (μm)
First	22	3	3	-15	2	6	CW	CW	91,9
Second	20	2	3	-16	2	6	CW	CW	99,8
Third	18	3	2,5	-17	2	6	CW	CW	100,1



Figure 107: The best table's cut edge from the left to right.

7.11 Cut edges angularity

The cut edges angularity was measured only for the three best surface roughness values for each 15 mm and 20 mm thickness pieces. The measurements were made with the coordinate measurement machine. The measured angle is for the one side of cut edge. Because of the similarity of the parameters for the material there were not very much fluctuation between parameter sets. There was seen the effect of spot size which depends on the focal planes position according to surface. The feed rates decrease or increase had small effect on the angle. All parameters and their angle can be seen in the Table 42.

With the middle steel 15 mm the angle did fluctuate between 0,88 to 2,21 degrees. The largest value was with the slower feed rate and the smaller nozzle when comparing with the smaller angle value. With 20 mm, the angle did fluctuate between 1,29 to 1,53 degrees. The minor fluctuation comes from the little change of the parameters.

Stainless steel had only one thickness 15 mm to measure the opening angle. The angle make change from 0,47 to 0,90 degrees, depending from the feed rate and the nitrogen pressure. The combined output power of the spot and the ring beams can explain this change, because there is 100 W more power in the best value.

The copper's opening angle for cut edge make change from 0,55 to 1,09 degrees. There can be seen the focal planes positions effect on angle, because when the focal plane did change to deeper the angle did also rise, not much but enough to see it in measurements.

The aluminums 15 mm thick plates angularity did range from 1,12 to 1,51 degrees. Here the explain is the powers change, because the smaller value is achieved with 1000 Hz with 75% duty cycle modulation to the spot and the highest value had no modulation at all when the other parameters were the same. With the 20 mm aluminium, the angle make change between 0,81 to 1,07 degrees and here the major parameter is the focal

plane's position, when going deeper to the material with plane it did grow cut kerfs opening angle.

Table 42: The cutting edges angle results for 15 mm and 20 mm thick plate

Material	Thickness (mm)	Feed rate(mm/s)	Feed rate (m/min)	Focal planes position (mm)	Assistant gas	Assistant gas pressure (bar)	Nozzles diameter (mm)	Nozzles distance (mm) from material	Power spot (kW)	Power ring (kW)	Modulation of the spot beam (Hz)	Modulation of the ring beam (Hz)	Duty cycle (%)	Angularity degrees
Aluminium	15	5	0,3	-9	N	16	2	2	2	6	CW	CW	-	1,29
Aluminium	15	5	0,3	-9	N	20	2,5	2	2	6	CW	CW	-	1,51
Aluminium	15	5	0,3	-9	N	20	2,5	2	2	6	1000	CW	75 %	1,12
Aluminium	20	3	0,18	-15	N	22	3	1	2	6	CW	CW	-	0,81
Aluminium	20	2	0,12	-16	N	20	3	1	2	6	CW	CW	-	0,92
Aluminium	20	3	0,18	-17	N	18	2,5	1	2	6	CW	CW	-	1,07
Copper	15	4	0,24	-10	O	18	2	1	2	6	CW	CW	-	1,09
Copper	15	3	0,18	-8	O	18	3	1	2	6	CW	CW	-	0,55
Copper	15	3	0,18	-12	O	16	2,5	1	2	6	CW	CW	-	0,86
Mild Steel	15	10	0,6	4	O	0,6	2,5	0,8	0,4	3,3	5000	CW	50 %	2,21
Mild Steel	15	12	0,72	5	O	0,6	3	1	0,4	3,3	5000	CW	50 %	0,88
Mild Steel	15	12	0,72	4	O	0,6	2,5	0,8	0	3,3	5000	CW	50 %	1,19
Mild Steel	20	10	0,6	4,5	O	0,6	3	1,7	0,8	2	5000	1000	50 %	1,53
Mild Steel	20	10	0,6	4,5	O	0,6	3	1,5	0,9	2,2	CW	5000	50 %	1,29
Mild Steel	20	10	0,6	4,5	O	0,6	3	1,7	1	1,8	1000	CW	50 %	1,50
Stainless Steel	15	11	0,66	-12	N	20	3	0,5	1,8	5,9	CW	CW	-	0,90
Stainless Steel	15	10	0,6	-13	N	22	3	0,4	1,8	6	CW	CW	-	0,58
Stainless Steel	15	9	0,54	-13	N	22	3	0,5	2	5,8	CW	CW	-	0,47

8 CONCLUSIONS

The laser cutting is used in various fields of industry to cut simple or complex 2D-shapes from plates or pipes. With the laser cutting can be achieved good and even excellent cutting surface roughness with high cutting speed which is achieved with optimal cutting parameters. The reflective materials have been challenging to cut with the laser, but the laser beams quality has been improved to cut these materials and different kinds of solutions have been also invented to help in this problem.

The laser cutting did turn out be very complex to master, because the parameters' have many connections between each other and this must be taken into consider. There were four main parameters which did rise most effecting parameters. The parameters were feed rate, focal plane's position, nozzle's diameter and assistant gas pressure. The focal plane's position was the major parameter from four of these which did affect most to the surface roughness. The feed rate did affect to the start of the cutting, because if we did use to high cutting speed the cutting did even penetrate the whole material. The nozzle's diameter and the cutting gas pressure did ensure that the molten material was carried away from the kerf and this how ensure the good cutting surface.

The other parameters had minor impact to surface roughness, but it was not so significant when compared to these major four parameters. But there were seen fluctuation between thicknesses and materials which were in there the major parameters. The formation of dross, the one major parameter was gas pressure and nozzle's diameter which did lower the growth of it.

With the mild steel cutting, we did achieve surface roughness quality class 2 for 5 mm and 15 mm thicknesses and for the 20 mm thick plate quality class of 3. For the stainless steel, we achieved surface roughness quality class 2 for the both thickness. The performance with copper, the quality class also were 2 through all thickness and for the aluminum we did achieve quality class 3 for both, but both metals do not belong under the SFS-ISO EN 9013 quality assessment. We did notice that there is some room to get better parameter sets and surface quality values when the optimization further from these parameters.

The cutting result did show that, with the ARM® laser source you can cut versatile materials and thicknesses with only one setup and achieve good surface roughness values with correct parameter sets. The ARM® laser source with this configuration can cut so thin material as thick materials and if the focus is changed even thicker than in these tests.

9 DISCUSSION AND FUTURE WORK

The objective of this Master of Science Thesis was to analyze and research the adjustable ring mode laser in cutting process and give data from its quality performance in this process. Also, it gives data from different materials cutting parameters which are affecting the cutting quality the most. This study should give more information for Corelase Oy, from cutting strengths and weaknesses and its capability to cut various thicknesses of materials.

The laser cutting sounds easy to execute, but what I did discover that it is very complex process to master, where many parameters which must be “correct” if wanted to achieve good cutting quality or even get started the cutting process. This leads to that you should know very well your used laser source, cutting heads parameters and how to adjust the cutting parameters if the cutting process is not giving you the wanted result.

These tests were made in the test laboratory conditions so it would be next step to test achieved value with a production machine. There also could test different focus optics to achieve better surface roughness for the thicker plates. Also there should be make a comparing test with this laser source and laser source which has only one laser beam to show what kind of benefits the ring beam have.

Because this study concentrates only cutting process and its quality, so the next study could be in field of welding were could be study what are the adjustable ring mode lasers benefits with different materials especially very reflective materials (example copper) and with different welding parameters. It could be compared to conventional welding like MIG welding and which are the key benefits in this area. Also in the future, this laser could be tested in coating or heat treatment applications.

REFERENCES

- [1] J.C. Ion, Laser processing of engineering materials: principles, procedure and industrial application, Boston, Oxford, 2005, 1 online resource (xviii, 556 pages) p.
- [2] F. Träger, Springer Handbook of Lasers and Optics, 2012, XXXII, 1694p. 1210 illus. in color p.
- [3] V. Kujanpää, A. Salminen, J. Vihinen, Lasertyöstö, Teknologiainfo Teknova, Helsinki, 2005, 373 sivua, 25 ilmoitussivua p.
- [4] J. Berkmanns, M. Faerber, Laser cutting. LASERLINE® Technical, BOC, 2008, Available: http://www.boconline.co.uk/internet.lg.lg.gbr/en/images/laser-cutting410_39553.pdf?v=2.0.
- [5] D. Petring, "Laser Cutting", LIA Handbook of Laser Materials Processing, Laser Institute America, 201,
- [6] C. Wandera, **Laser Cutting of Austenitic Stainless Steel with a High Quality Laser Beam**, Master's thesis, 2006, Available: <http://urn.fi/URN:NBN:fi-fe20061326>.
- [7] D. Bäuerle, Laser Processing and Chemistry, 4.th ed. 2011, XXII, 851p. 337 illus., 19 illus. in color p.
- [8] J. Canning, Fibre lasers and related technologies, Optics & Lasers in Engineering, Vol. 44, No. 7, 2006, pp. 647-676.
- [9] J. Wallace, **Lockheed Martin's 30 kW fiber-laser weapon disables truck from a mile away**, Laser Focus World, web page. Available (accessed 5/22): <http://www.laserfocusworld.com/articles/2015/03/lockheed-martin-s-30-kw-fiber-laser-weapon-disables-truck-from-a-mile-away.html>.
- [10] H. Hugel, New solid-state lasers and their application potentials, Optics And Lasers In Engineering, Vol. 34, No. 4-6, 2000, pp. 213-Dec,.
- [11] Laser Material Processing, in: Springer eBooks, 4th Edition. ed., Springer-Verlag London, Engineering.Structural control (Engineering)Surfaces (Physics)EngineeringOperating Procedures, Materials TreatmentLaser Technology, PhotonicsCharacterization and Evaluation of Materials, London, 2010, .
- [12] CO₂ lasers: The Industrial workhorse, Photonics Media, web page. Available (accessed 5/3): <http://www.photonics.com/EDU/Handbook.aspx?AID=25155>.
- [13] CO₂ lasers, RP-Photonics Encyclopedia, web page. Available (accessed 5/3): https://www.rp-photonics.com/co2_lasers.html.
- [14] A. Giesen, Thin Disk Lasers Power scalability and beam quality, Laser source, Vol. 2, No. June, 2005, pp. 42.

- [15] Solid-State Laser Engineering, in: Springer Series in Optical Sciences, ISSN 0342-4111 ; 1.; Springer eBooks, Springer, Physics.Particles (Nuclear physics)Laser physics.Microwaves.PhysicsLaser Technology and Physics, PhotonicsSolid State Physics and SpectroscopyMicrowaves, RF and Optical Engineering, New York, NY, 2006, .
- [16] R. Paschotta, Diode-pumped lasers, RP-Photonics Encyclopedia, web page. Available (accessed 5/4): https://www.rp-photonics.com/diode_pumped_lasers.html.
- [17] Lamp-pumped lasers, RP-Photonics Encyclopedia, web page. Available (accessed 5/4): https://www.rp-photonics.com/lamp_pumped_lasers.html.
- [18] D. Larcombe, Fiber versus CO2 laser cutting, Industrial laser solutions for manufacturing, web page. Available (accessed 5/23): <http://www.industrial-lasers.com/articles/2013/11/fiber-versus-co2-laser-cutting.html>.
- [19] D. Hoffman, **CO2 Versus Fiber Laser: Cost to Cut a Part**, FABSHOP Magazine direct, web page. Available (accessed 5/23): <http://www.fsmdirect.com/cutting/laser-cutting/75-co2-versus-fiber-laser-cost-to-cut-a-part>.
- [20] S. Stelzer, A. Mahrle, A. Wetzig, E. Beyer, Experimental investigations on fusion cutting stainless steel with fiber and CO2 laser beams, pp. 399-404.
- [21] What does the laser beam do to the material? Trumpf, web page. Available (accessed 4/27): <http://www.trumpf-machines.com/en/solutions/more-knowledge-for-the-best-production/laser-cutting/the-work-process.html>.
- [22] **Light and photosynthetic pigments** Properties of light. How chlorophylls and other pigments absorb light. web page. Available (accessed 1/15): <https://www.khanacademy.org/science/biology/photosynthesis-in-plants/the-light-dependent-reactions-of-photosynthesis/a/light-and-photosynthetic-pigments>.
- [23] V. Niziev, Influence of beam polarization on laser cutting efficiency, Journal Of Physics D-Applied Physics, Vol. 32, No. 13, 1999, pp. 1455-Applied.
- [24] J. Powell, LIA Guide to laser cutting, Laser Institute of America, United States of America, 2008, .
- [25] J.F. Ready, D.F. Farson, LIA HANDBOOK OF LASER MATERIALS PROCESSING, 1st ed. Laser Institute of America Magnolia Publishing, Inc, United State of America, 2001, 715 p.
- [26] **ProCutter – the cutting head for every task**, Precitec, web page. Available (accessed 5/10): <http://www.precitec.de/en/products/laser-cutting/solid-state-laser/procutter/#tab1>.
- [27] C.L. Caristan, Laser Cutting: Guide fo Manufacturing, 1.th ed. Society of Manufacturing Engineers (SCE), United States of America, 2004, 447 p.

- [28] SFS-ISO EN 9013, Thermal cutting. Classification of thermal cuts. Geometrical product specification and quality tolerances, Technology Industries of Finland, Standarts, Helsinki, 2003, 56 p.
- [29] Madić Miloš J., Analysis of the heat affected zone in CO₂ laser cutting of stainless steel, Thermal Science, Vol. 16, 2012, pp. 363-373.
- [30] O. Haupt, D. Müller, F. Gäbler, Shorter pulse widths improve micromachining, Photonics Media, web page. Available (accessed 5/11): <http://www.photonics.com/Article.aspx?AID=54123>.
- [31] G. Taguchi, System of experimental design : engineering methods to optimize quality and minimize costs, 3. pr. ed. UNIPUB, White Plains, NY, 1988, 2 osaa (1189 sivua) p.
- [32] R.H. Locher, Design For Quality, Chapman and Hall, Oxford University Press, 1990, .
- [33] E. Karjalainen, Teollinen koesuunnittelu : esimerkkejä Suomessa toteutetusta koekellisestä tuotteen ja prosessin suunnittelusta Taguchi-menetelmällä, Metalliteollisuuden kustannus, Helsinki, 1992, 162 sivua p.
- [34] E. Karjalainen, Tuotteen ja prosessin optimointi koesuunnittelulla - Taguchi-menetelmä, Metalliteollisuuden kustannus, Hki, 1990, 95 sivua p.
- [35] J. Heiska, Taguchi-menetelmä laadun suunnittelussa : diplomityö, Tampereen teknillinen korkeakoulu, Tampere, 1993, 97 lehteä p.
- [36] N. Logothetis, H.P. Wynn, Quality through design : experimental design, off-line quality control and Taguchi's contributions, Clarendon, Oxford, 1989, 464 sivua p.
- [37] **Study Interactions Using The Taguchi Method**, Taguchi Split Test, web page. Available (accessed 6/22): <http://www.taguchisplittest.com/user-contributions/study-interactions-using-the-taguchi-method/>.
- [38] G. Taguchi, Introduction to quality engineering : designing quality into products and processes, Asian Productivity Organization, Tokyo, 1986, 191 sivua p.
- [39] M. Milos, APPLICATION OF THE TAGUCHI METHOD FOR OPTIMIZATION OF LASER CUTTING: A REVIEW, Revista de tehnologii neconventionale = nonconventional technologies review, Vol. 17, No. 4, 2013, pp. 50.
- [40] Company History, Corelase Oy, web page. Available (accessed 4/20): <http://www.corelase.fi>.
- [41] Corelase Oy Company information, Taloussanommat, web page. Available (accessed 8/20): <http://yritys.taloussanommat.fi/y/corelase-oy/tampere/1780572-9/>.
- [42] **ARM™ – New possibilities in materials processing**, Corelase Oy, web page. Available (accessed 8/22): <http://www.corelase.fi/products/arm/>.

[43] **SFS-EN 10025-2 Kuumavalssatut rakenneteräkset. Osa 2: Seostamattomat rakenneteräkset. Tekniset toimitusehdot**, 1st ed., Suomen Standardisoimisliitto SFS, Standard, Helsinki, 2005, pp. 1-65.

[44] AK Steel Corporation, STAINLESS STEEL 304/304L, AK Steel Corporation, web page. Available (accessed 9/7):

http://www.aksteel.com/markets_products/stainless_austenitic.aspx.

[45] Datenblatt zu Aluminiumplatten EN AW-6082, klöckner&co, web page. Available (accessed 9/7):

<http://shop-msm.dkh.ch/productlist.cfm?CFID=41220433&CFTOKEN=4531f8592b4a4bd4-C9C63C08-BA46-CF87-9C49909ADFA4D6D7&ParentID=10>.

[46] Chemische und mechanische Eigenschaften / Chemical and mechanical properties CU-OF, MKM Mansfelder Kupfer und Messing GmbH, 2015.

[47] Taylor-Hobson surtronic 3+ surface measurement instrument, 1st ed., Pirkka Ulmanen, 2016/6, .

[48] Taylor Hobson Precision Surtronic 3+: Rapid on the floor Surface Texture Measurement, Taylor Hobson Limited,

<http://www.zimmerman.com.tw/uploads/sur3005-salesbrochure.pdf>, .